

Dissertation

**THE INFLUENCE OF HISTONE ORTHOLOGUES, HISTONE VARIANTS
AND POST-TRANSLATIONAL MODIFICATIONS ON THE STRUCTURE AND
FUNCTION OF CHROMATIN**

Submitted by

Michael George Resch

Department of Biochemistry and Molecular Biology

In partial fulfillment of the requirements
for the Degree of Doctor of Philosophy
Colorado State University
Fort Collins, Colorado
Fall 2008

UMI Number: 3346432

INFORMATION TO USERS

The quality of this reproduction is dependent upon the quality of the copy submitted. Broken or indistinct print, colored or poor quality illustrations and photographs, print bleed-through, substandard margins, and improper alignment can adversely affect reproduction.

In the unlikely event that the author did not send a complete manuscript and there are missing pages, these will be noted. Also, if unauthorized copyright material had to be removed, a note will indicate the deletion.

UMI[®]

UMI Microform 3346432

Copyright 2009 by ProQuest LLC.

All rights reserved. This microform edition is protected against unauthorized copying under Title 17, United States Code.

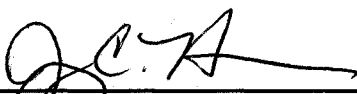
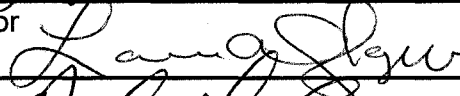
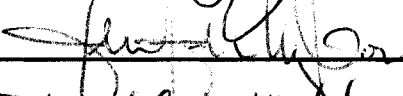
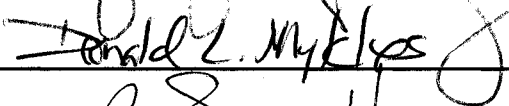
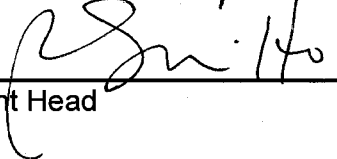
ProQuest LLC
789 E. Eisenhower Parkway
PO Box 1346
Ann Arbor, MI 48106-1346

COLORADO STATE UNIVERSITY

August 21, 2008

WE HEREBY RECOMMEND THAT THE DISSERTATION PREPARED UNDER OUR SUPERVISION BY MICHAEL GEORGE RESCH ENTITLED "THE INFLUENCE OF HISTONE ORTHOLOGS, HISTONE VARIANTS AND POST-TRANSLATIONAL MODIFICATIONS ON THE STRUCTURE AND FUNCTION OF CHROMATIN" BE ACCEPTED AS FULFILLING IN PART REQUIREMENTS FOR THE DEGREE OF DOCTOR OF PHILOSOPHY.

Committee on Graduate Work

	(Jeffrey C. Hansen)
Advisor	
	(Karolin Luger)
Co-Advisor	
	(Laurie A. Stargell)
	(Paul J Laybourn)
	(Jennifer K Nyborg)
	(Don Mykles)
	(P. Shing Ho)
Department Head	

Abstract of Thesis

“The influence of histone orthologs, histone variants and post-translational modifications on the structure and function of chromatin”

Two meters of DNA is packaged into the nucleus of each eukaryotic cell in the form of chromatin. DNA wraps around a protein histone octamer to form a nucleosome, the fundamental repeating unit of chromatin. The highly basic histone octamer contains two copies each of H2A, H2B, H3 and H4 to form the protein core of the nucleosome. There is a dynamic interplay of accessibility which compacts DNA yet allows access for fundamental cellular processes like transcription and DNA replication. This thesis investigates how histone variants and post-translational modifications contribute to the level of chromatin compaction.

I demonstrated that defined nucleosomal arrays made with histones from multiple species oligomerize at different concentrations of $MgCl_2$. A comparison of endogenous and recombinant *Drosophila melanogaster* histone octamers showed that this is unlikely due to posttranslational histone modifications, but likely a result of subtle changes in the sequences constituting the histone tails and structured surface of the histone octamer.

I investigated the effect of incorporation of the centromere specific H3 histone variant centromere protein – A (CENP-A) into nucleosomes and nucleosomal arrays. Despite the fact that CENP-A shares only 60% sequence homology within the structured domain of major-type H3 (15% in the N-terminal domain), CENP-A (together with the other three core histones) forms nucleosomes and condensed nucleosomal arrays comparable to major-type H3.

Post-translational modifications (PTM) contribute to the regulation of chromatin structure. I have analyzed the effect of H3 lysine 56 acetylation on nucleosome structure and chromatin condensation. This modification was previously thought to disrupt nucleosome structure. I developed methods to enzymatically acetylate large amounts of H3 specifically at Lys 56, and demonstrated that histone octamers containing H3-K56Ac form canonical nucleosomes. However, nucleosomal array condensation is compromised by this particular PTM.

Together, these studies suggest that even subtle variations in histone sequence or posttranslational modifications result in differences in chromatin higher order structure.

Michael George Resch
Department of Biochemistry and Molecular Biology
Colorado State University
Fort Collins, Colorado 80523
Fall 2008

TABLE OF CONTENTS

Title Page	i
Signature Page	ii
Abstract of Dissertation	iii
Acknowledgments	iv
Table of Contents	v
Acknowledgments	x
Chapter 1: Review of Literature	1
1.1 Introduction	2
1.2 The nucleosome	2
1.3 In Vitro chromatin self-association (oligomerization) and its relevance to genome architecture	4
1.3.1 In vitro chromatin self-association: a historical perspective	5
1.3.2 Chromatin self-association: recent advances	9
1.3.3 Chromatin self-association: physiological relevance	11
1.4 Folding of the chromatin fiber; the '30 nm' chromatin fiber	14
1.5 Post-translational modifications	18
1.6 The centromere and CENP-A associated proteins	22
Chapter 2: The Influence of histone orthologues in nucleosomal array oligomerization	26
2.1 Introduction	27
2.2 Methods and Materials	29
2.3.1 Gel Electrophoresis	29
2.3.2 DNA purification	29
2.3.3 Histone Purification	29

2.3.4 Salt Dialysis Reconstitution	30
2.3.5 Analytical Ultracentrifugation	30
2.2.6 Agarose Multigels	30
2.2.7 EcoR1 template saturation analysis	31
2.2.8 Folding of nucleosomal arrays	31
2.2.9 Oligomerization of nucleosomal arrays	31
2.3 Results	32
2.3.1 Endogenous <i>Drosophila</i> histone octamers have a low but detectable level of PTM or histone isoforms	32
2.3.2 Reconstitution and saturation analysis of <i>Drosophila</i> nucleosomal Arrays	34
2.3.3 Reconstituted endogenous and recombinant nucleosomal arrays have similar sedimentation coefficient distributions	34
2.3.4 Reconstituted nucleosomal arrays have similar surface charge density indicating similar octamer saturation	36
2.3.5 Analytical EcoR1 restriction digestion indicates similar template loading	38
2.3.6 Nucleosomal array oligomerization is similar with endogenous and recombinant histone octamers	39
2.3.7 Folding of recombinant and endogenous <i>Drosophila melanogaster</i> nucleosomal arrays is similar	42
2.3.8 Nucleosomal array reconstitution and analysis using histone orthologues	43
2.3.9 Oligomerization of nucleosomal arrays containing histone orthologues	45
2.4 Discussion	46
2.4.1 Endogenous and recombinant histone octamers have similar chromatin oligomerization characteristics	46
2.4.2 Nucleosomal arrays reconstituted with histone octamers from different species require different amounts of MgCl ₂ to oligomerize	47
2.5 Future Directions and alternative hypotheses	49
Chapter 3: Structural and functional investigation of the histone H3 variant CENP-A	55
3.1 Introduction	56
3.2 Methods and materials	62
3.2.1 Protein Expression and Purification	62
3.2.2 DNA purification	62
3.2.3 Binding affinity measurements	62
3.2.4 Stoichiometry	63
3.2.5 Salt Dialysis Reconstitution	63

3.2.6	EcoR1 template saturation analysis	64
3.2.7	Nucleosome Crystallization	64
3.2.8	Analytical Ultracentrifugation	65
3.2.9	Folding of nucleosomal arrays	65
3.2.10	Atomic force microscopy	65
3.2.11	Oligomerization of nucleosomal arrays	65
3.3	Results	66
3.3.1	CENP-A/H4 interaction with nucleosome assembly protein – 1 (Nap-1)	66
3.3.1.1	Histone complexes retain their tertiary structures at low salt	66
3.3.1.2	CENP-A/H4-Nap1 complex has a different gel mobility than the H3/H4-Nap1 complex	68
3.3.1.3	Hydrodynamic analysis of purified histone:Nap1 complexes	71
3.3.1.4	CENP-A/H4 binds Nap-1 as a dimer	73
3.3.2	CENP-A mononucleosomes have similar nucleosome stability	76
3.3.3	Reconstitution of fully saturated nucleosomal arrays contain a histone octamer with CENP-A	80
3.3.4	Nucleosomal arrays containing CENP-A have similar folding characteristics as MT H3 arrays	84
3.3.5	CENP – A and major type H3 containing nucleosomal arrays make similar inter-nucleosomal interactions	86
3.4	Discussion	88
3.4.1	The histone chaperone Nap-1 has a unique binding to the CENP-A/H4 complex	88
3.4.2	CENP-A nucleosomes have similar ionic strength stability	90
3.4.3	Nucleosomal arrays containing CENP-A have the similar ability to oligomerize nucleosomal arrays as arrays containing major type mouse H3.	90
3.5	Future Directions	93
3.5.1	Crystallization attempts of nucleosomes containing CENP-A	93
Chapter 4: The effect of histone H3-K56 acetylation on the nucleosome and chromatin structure		96
4.1	Introduction	97
4.2	Methods and Materials	99
4.2.1	Histone mutagenesis	99
4.2.2	Protein expression and purification	99
4.2.3	DNA purification	100

4.2.4	Gel Electrophoresis	100
4.2.5	Acetylation Reactions	100
4.2.6	Mass Spectrometry	101
4.2.7	Reconstitution of Nucleosomes and Nucleosomal Arrays	101
4.2.8	EcoR1 template saturation analysis	102
4.2.9	Nucleosome Crystallization	102
4.2.10	Analytical Ultracentrifugation	103
4.2.11	Folding of nucleosomal arrays	103
4.2.12	Oligomerization of nucleosomal arrays	103
4.3	Results	104
4.3.1	Optimization of large scale specific acetylation of histone H3 at lysine 56 <i>in vitro</i>	104
4.3.2	Histone octamers containing H3-K56Ac and point mutants H3-K56E and H3-K56Q are able to reconstitute canonical-like nucleosomes	110
4.3.3	Analysis to whether H3-K56Ac affects the nucleosomes crystal structure	113
4.3.4	H3-K56 contributes to nucleosome stability	115
4.3.5	H3-K56Ac disrupts chromatin condensation	118
4.4	Discussion	123
4.4.1	Large scale <i>in vitro</i> acetylation of H3-K56	124
4.4.2	H3-K56 contributes to the stability of the nucleosome	124
4.4.3	Acetylation to the nucleosome core disrupts nucleosomal array condensation	126
4.5	Future Directions	128
	References	131

Acknowledgments

First of all I would like to thank my “bosses” Dr. Jeffrey Hansen and Dr. Karolin Luger. Their dedication to detail, the lab, their family and my education is admirable. My interaction with them has given me a foundation to work in any field of biochemistry and molecular biology. Second, it is important to thank my love Laura Baker for putting up with me through my tenure at Colorado State in good times and bad. Also, the basis of my life and strong work ethic comes from my mother Beverly Resch whom raised and supported me as a single mother. This dissertation is dedicated to my late father William A. Resch I felt like he has been with me all of my life.

CHAPTER 1

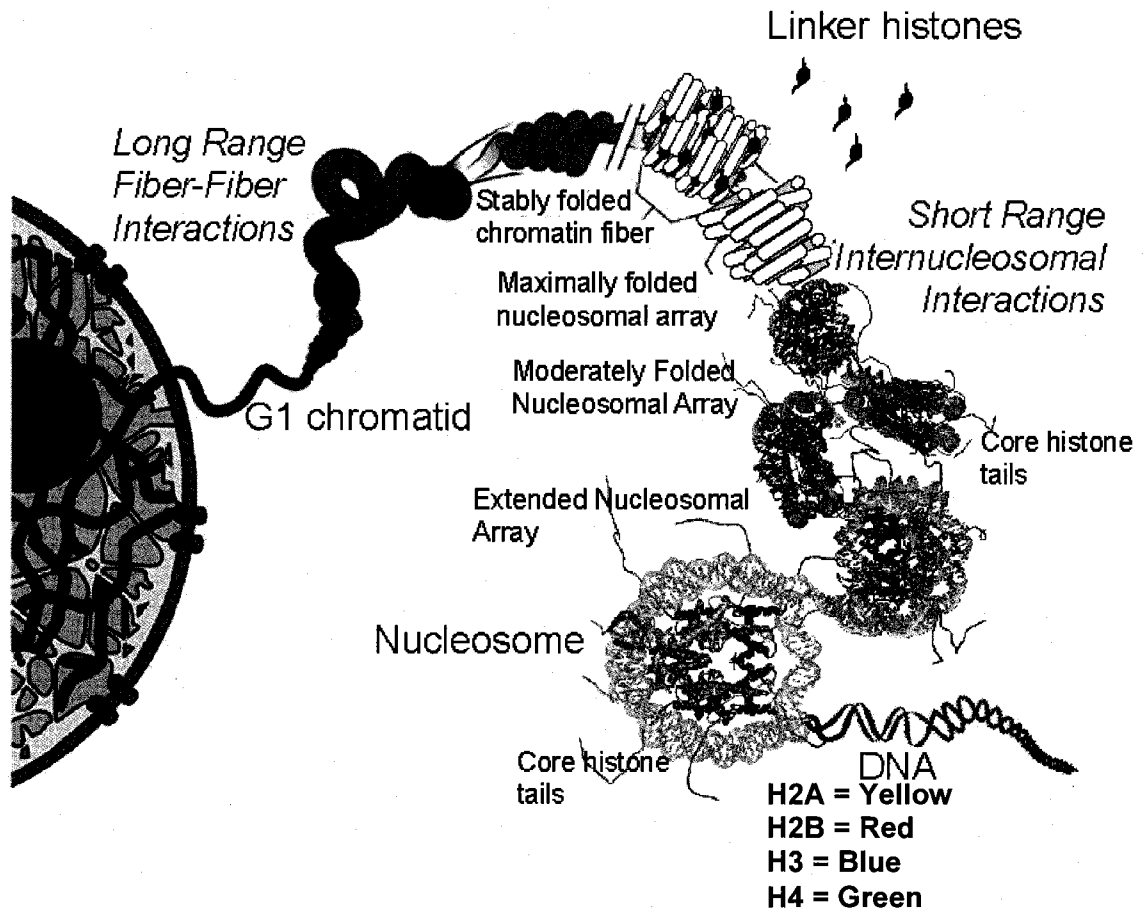
Review of literature

1.1 Introduction

In a eukaryotic multi-cellular organism each healthy cell has an identical composition of double stranded DNA. End to end the genome would be about two meters in length, and chromatin is the compact form of DNA in the nucleus. In chromatin, DNA is in complex with histones and other nuclear proteins, as the basic fundamental repeating unit of chromatin, the nucleosome. Nucleosome polymers, known as nucleosomal arrays, have the dynamic ability to compact and regulate, chromatin structure. Condensation aids in managing cellular and, ultimately, organism function in regulating transcription. This chapter focuses on the properties that affect nucleosome and chromatin structure: understanding these processes will ultimately lead to an increased knowledge of the regulation of cellular functions.

1.2 The Nucleosome

One hundred and forty seven base pairs of double stranded DNA wraps around each histone protein octamer in 1.65 superhelical turns to form a canonical nucleosome core particle (NCP) (Luger et al., 1997). The histone octamer contains two copies each of the histone proteins H2A, H2B, H3 and H4 small (11-14 kDa) highly basic proteins. The C – terminal structured domain, which makes protein – protein and protein – DNA interactions, is referred to as the histone fold domain and contains a center long α -helix flanked by two smaller α -helices and connected by two loop regions (figure 1.1 and 2.7) (Arents et al., 1991; Arents and Moudrianakis, 1995; Luger et al., 1997). At physiological ionic strength, histones H2A and H2B form a (H2A/H2B) hetero-dimer and H3 and H4 form a (H3/H4)₂ tetramer. Reconstitution of the nucleosome is propagated



1.1 The levels of Chromatin Architecture A schematic diagram of how DNA is packaged into the chromosome in eukaryotic cells. Adapted from Hansen (2002)

1.3 In vitro chromatin self-association (oligomerization) and its relevance to genome architecture

Xu Lu, Joshua M. Klonoski, **Michael G. Resch**, and Jeffrey C. Hansen

Section 1.3 has been published in 2006 in the journal *Biochem. Cell Biol.* as a mini-review. This article reviews one of the main techniques that I use to study chromatin condensation and describes the physical relevance of this technique. At the time this review was written we referred to nucleosomal array polymerization as self-association, although since then we have used the term 'oligomerization' because the term self-association is often confused with non-physiologically relevant aggregation. This self-association process has been proposed to mimic processes involved in the assembly and maintenance of tertiary chromatin structures in vivo. In this article, we review thirty years of studies of chromatin self-association, with an emphasis on the evidence suggesting that this in vitro process is physiologically relevant.

1.3.1 In vitro chromatin self-association: a historical perspective

Chromatin self-association was first observed and called precipitation over 30 years ago. At that time, researchers isolated chromatin fragments extracted from the nuclei of various cell types in different ionic conditions. Under certain salt conditions researchers frequently observed chromatin "precipitants", i.e., high molecular weight material which pelleted rapidly upon centrifugation (van Holde 1988). While "insoluble"

materials were discarded, the “soluble” fractions were used for the first studies of chromatin dynamics (Olins and Olins 1974; Van Holde et al. 1974; Lewis et al. 1975; Renz et al. 1977; Stratling 1979; Thoma et al. 1979). Interestingly, Davie and coworkers digested chromatin from trout testis, calf thymus and chicken erythrocytes with DNase I, II and micrococcal nuclease (MNase) and found that, compared to the insoluble fractions, the soluble fractions generally contain lower amounts of linker histones and higher amount of acetylated H4 histones, which were generally associated with active transcription (Davie and Candido 1978; Davie and Saunders 1981). In retrospect, this was the first time chromatin self-association was linked to *in vivo* chromatin function. In 1984, it was also found that endogenous chromatin fibers containing inactive genes could form a discrete “supranucleosome particle” on agarose gels, probably through a process similar to chromatin self-association (Weintraub 1984). This work also suggested that linker histones played a role in the stability of the particle.

In two separate papers, Eisenberg and coworkers fully characterized the influence of divalent cations on oligomerization of endogenous nucleosomal and chromatin arrays and determined the minimum concentration at which oligomerization was induced by Mg^{2+} and Na^+ (Ausio et al. 1984; Borochoy et al. 1984). Hypotheses quickly arose to explain the salt-dependence of oligomerization, but the one most widely adopted was that salt simply neutralizes the negative charge on DNA backbone, eliminating electrostatic repulsive forces, and allowing array-array interactions during oligomerization (Manning 1977; Widom 1986; Clark and Kimura 1990).

The reversibility of oligomerization was subsequently demonstrated (Jin and Cole 1986), and work from the same group showed that anions and pH also affected the oligomerization process (Guo and Cole 1989a; Guo and Cole 1989b). Specifically, they found enhanced chromatin self-association at lower pH. These researchers

pointed out that there was a corresponding pH change in the cell cycle and discussed possible physiological significance of this observation.

Before the mid 1980s, all studies of chromatin self-association used heterogeneous, endogenous nucleosomal and chromatin arrays. In 1985, a model system developed by Robert Simpson and coworkers totally changed the field (Simpson et al. 1985). Currently, the most common version of this model system, the 208-12 DNA, contains 12 tandem repeats of DNA of the *Lytechinus* 5S rRNA gene. Each repeat of this model system possesses a nucleosome positioning sequence. Homogenous nucleosomal arrays were generated using the 208-12 DNA template and purified chicken histone octamers (Hansen et al. 1989). This model system was shown to behave very similarly to extensively purified endogenous chicken nucleosomal arrays in sedimentation velocity experiments, MNase digestion experiments and electron microscopy imaging experiments (Garcia-Ramirez et al. 1992; Carruthers et al. 1998). Since then, many laboratories have utilized this model system and made significant contributions to the understanding of chromatin dynamics (Fletcher and Hansen 1996; Hansen 2002).

Using the 208-12 model system, Hansen and Schwarz found that the self-association of 208-12 nucleosomal arrays was induced by low divalent salt concentration (~ 2 mM MgCl_2), and inhibited at high divalent salt concentration, i.e., >90 mM of MgCl_2 (Schwarz and Hansen 1994). This was in agreement with an earlier observation that native chromatin “disaggregated” over the range of 50-100 mM MgCl_2 (Jin and Cole 1986). While the first study by Schwarz and Hansen established that 208-12 nucleosomal arrays could reversibly self-associate, their subsequent paper more closely investigated the reversibility of oligomerization, and in addition characterized the effects of a wide range of monovalent and divalent salts (Schwarz et al. 1996). Sedimentation velocity and differential centrifugation experiments showed

that self-association was reversed by dialysis back into low salt buffers. In contrast to divalent cations, monovalent salts were incapable of oligomerizing nucleosomal arrays. The divalent cations differed in the minimal concentrations able to induce oligomerization in the following fashion: $Mn^{2+}=Zn^{2+}>Ba^{2+}>Mg^{2+}>Co^{2+}>>Cd^{2+}$. Anions, in contrast, were found to only weakly affect oligomerization and displayed differences in the order of acetate $>Cl^->Br^->NO_3^->>SO_4^{2-}$. In stark contrast to nucleosomal arrays, naked 208-12 DNA did not self-associate at any salt concentration observed in the study (Schwarz et al. 1996). These investigators also utilized low speed sedimentation velocity experiments to show that during oligomerization, nucleosomal arrays existed in solution as either monomers or very large oligomers (in excess of several hundred S). No dimers, trimers or other small oligomers were observed. This study indicated that oligomerization occurs via a 2-step mechanism: The first step involves a highly cooperative process that creates defined *soluble* oligomers, and the second step involves "open-ended" monomer addition to these oligomers to form even larger particles (once known as precipitants) with increasing Mg^{2+} concentration. This study also showed that chromatin folding and self-association were separate processes. Neither arrays of H3/H4 tetramers nor highly subsaturated arrays containing many nucleosome-free gaps could fold, yet each could oligomerize in divalent salts (Hansen and Wolffe 1994; Schwarz et al. 1996). Therefore, formation of folded secondary chromatin structures is not a pre-requisite for self-association into tertiary chromatin structures in vitro.

What are the core histone determinants of oligomerization? Selective removal of the histone NTDs using trypsin abolished the ability of nucleosomal arrays to oligomerize (Allan et al. 1982; Harborne and Allan 1983; Ausio et al. 1989; Perry and Annunziato 1991; Garcia-Ramirez et al. 1992). These studies identified the unstructured histone NTDs as the key mediators of array self-association. Importantly,

these results also showed that the core histone NTDs do not function as simple cations, because divalent cations cannot replace their function in chromatin self-association.

Tse and Hansen (1997) addressed roles of the different core histone NTDs by creating hybrid tailless arrays that lacked the H3/H4 or H2A/H2B NTDs. They found that although both H3/H4 and H2A/H2B NTDs contributed to the self-association process, H3/H4 appeared to play a more important role. Similar results were independently reported by Moore and Ausio (Moore and Ausio 1997).

As discussed above, acetylation was first found to be associated with the “soluble” fractions of endogenous chromatin (Davie and Candido 1978; Davie and Saunders 1981). Using the 208-12 model system, Hansen and coworkers (Tse et al. 1998) found self-association decreased in proportion to the extent of NTD acetylation. Also using the 208-12 model system, Jason and coworkers found out that nucleosomal arrays containing ubiquitinated histone H2A had higher ability to self-associate than arrays with unmodified histone (Jason et al. 2001). The effects of histone modifications other than acetylation and ubiquitination remain to be established.

Meanwhile, polyamines were found to be able to induce chromatin self-association (Pollard et al. 1999). These researchers also found that polyamine-induced chromatin self-association could be partially inhibited by core histone NTD acetylation in vitro. Importantly, the same study also found that depletion of polyamine in vivo could partially alleviate the defects caused by the inactivation of histone acetyltransferase GCN5.

Linker histones also influence chromatin self-association (Hansen 2002). Early studies showed that linker histones were associated with “Mg²⁺-insoluble” chromatin fractions, and that linker histones reduced the amount of MgCl₂ needed to induce

oligomerization in vitro (Olins et al. 1976; Ausio et al. 1984; Rocha et al. 1984). Using the 208-12 chromatin model system and chicken linker histone H5, Hansen and coworkers confirmed that chromatin arrays with H5 self-associated at a significantly lower Mg^{2+} concentration than their parent nucleosomal arrays (Carruthers et al. 1998). Furthermore, these researchers found that chromatin arrays with linker histone H5 could oligomerize in NaCl, an ability that nucleosomal arrays without linker histones do not possess (Fletcher and Hansen 1996; Hansen 2002). Subsequently, Carruthers and Hansen (Carruthers and Hansen 2000) demonstrated that chromatin arrays containing tailless core histone and full-length linker histone could not self-associate. This finding further confirmed that the core histone NTDs are required for self-association, while linker histones had additive stabilization effects.

1.3.2 Chromatin self-association: recent advances

All of the chromatin self-association experiments discussed previously were performed using endogenous core and linker histone proteins. However, due to the limits imposed by selective trypsin digestion of endogenous histones, characterization of the role of each individual tail domain was not possible. More recently, studies using recombinant proteins have increased our understanding of self-association and its mechanism. The first study using recombinant core histones compared the abilities of nucleosomal array containing histone H2A variant, H2A.Z to “major” type H2A. H2A.Z itself is highly conserved from yeast to humans and is essential in *Drosophila*, *Tetrahymena* and mouse (van Daal and Elgin 1992; Liu et al. 1996; Jackson and Gorovsky 2000; Faast et al. 2001). Interestingly, Tremethick and coworkers observed that H2A.Z-containing nucleosomal arrays oligomerized at higher Mg^{2+} concentrations than native nucleosomal arrays (Fan et al. 2002). This was the first time an essential

histone variant was shown to affect chromatin self-association. This observation is also consistent with the *in vivo* functions of H2A.Z in gene activation and antagonizing gene-silencing (Raisner and Madhani 2006).

The functions of the core histone NTDs were further studied by two laboratories. Using recombinant wild type and tailless core histone proteins, Richmond and coworkers found out that H4 NTD made the single biggest contribution to chromatin self-association (Dorigo et al. 2003). On the other hand, Gordon and Hansen used recombinant core histone to construct all 16 possible octamer combinations of full length and tailless H2A, H2B, H3 and H4. They confirmed the importance of the H4 NTD but also found that all four tails contributed additive and independent functions to array oligomerization (Gordon et al. 2005). This result indicates that all core histone NTDs contribute to the assembly and maintenance of chromatin structures.

How do core histone NTDs function in chromatin self-association? A study by Hayes and coworkers provided some hint to this question. Using recombinant core histone proteins and a novel crosslinking technique, Hayes and coworkers (Zheng et al. 2005) showed that the H3 tail domain rearranged from a nucleosomal to non-nucleosomal location during oligomerization, consistent with a role of the NTDs in mediating nucleosome-nucleosome interactions (Gordon et al. 2005).

Using recombinant protein technology, together with protein ligation strategy, Peterson and coworkers were able to create homogenous nucleosomal arrays containing H4 acetylated on lysine 16 (Shogren-Knaak et al. 2006). Interestingly, they found that this single specific acetylation event could disrupt chromatin self-association to the same degree as deleting the entire H4 NTD. This study strongly suggests that the H4 NTD mediates self-association through a specific protein-protein interaction that can be disrupted by a specific acetylation.

The highly basic C-terminal domains (CTDs) of linker histones are responsible for linker histone function in chromatin condensation (Allan et al. 1980a). To further dissect the functions of linker histone CTDs, gradual CTD truncation mutants of linker histone H1° were created and their abilities to facilitate chromatin self-association were determined (Lu and Hansen 2003; Lu and Hansen 2004). Lu and Hansen found out that only the first quarter of the H1° CTD and the globular domain were important for chromatin self-association. Because the positive charges essentially are evenly distributed throughout the linker histone CTDs, this finding ruled out the prevailing hypothesis that the linker histone CTD functioned by a simple charge neutralizing mechanism. Instead, Lu and Hansen proposed that the linker histone CTD functions as an intrinsically disordered protein (Lu and Hansen 2003; Lu and Hansen 2004; Hansen et al. 2006).

1.3.3 Chromatin self-association: physiological relevance

The finding that chromatin self-association is reversible and highly cooperative suggests that it has physiological significance. Although chromatin self-association has often been referred to as chromatin precipitation, it is very different from protein precipitation in the following aspects. Very high concentrations of salts are usually required to precipitate proteins (Arakawa and Timasheff 1984; Arakawa and Timasheff 1985). High concentrations of salts significantly decrease the solvating power of water, and proteins in the solutions precipitate out. In contrast, the salt concentrations required to induce self-association are very low (e.g., several mM Mg^{2+}) (Hansen 2002), compared to those required to precipitate proteins. At these salt concentrations, the solvating power of water is almost unchanged. Chromatin self-association is also very ion-selective. Specifically, only divalent cations can induce self-association of nucleosomal arrays, while both monovalent and divalent cations can induce that of

chromatin arrays containing linker histones. Even different cations of the same valency have very different abilities to induce self-association, however, their abilities to induce chromatin self-association do not follow the Hofmeister series, in contrast to protein precipitation. Another difference between protein precipitation and chromatin self-association is the extreme cooperativity of the self-association process. In retrospect, chromatin self-association has been confused with precipitation simply because the soluble chromatin oligomers are so huge and pellet so easily.

Effects of cations and pH on chromosome condensation and decondensation during the cell cycle. Both monovalent and divalent cation concentrations have been long found to fluctuate throughout the cell cycle (Cameron et al., 1979; Poenie et al., 1986; Warley et al., 1983). Importantly, a recent study found that the transition from interphase to metaphase correlated with a roughly 4-fold increase in the concentration of Mg^{2+} and Ca^{2+} (Strick et al. 2001). Metaphase chromosomes in cells depleted of these two cations were partially decondensed (Strick et al. 2001). Therefore, it seems that divalent cations are essential for the complete condensation of metaphase chromosomes. The ion dependence of metaphase chromosome condensation is similar to that of in vitro chromatin self-association. Therefore, in vitro chromatin self-association may be related to chromosome condensation during mitosis.

The mitotic cycle is also correlated with changes in intracellular pH. Specially, intracellular pH increases in S phase and decreases again when cells go into mitosis (Gerson and Kiefer 1982; Gerson et al. 1982; Gerson and Kiefer 1983). As discussed above, pH affects chromatin self-association, and higher pH condition favors a lesser degree of self-association. As previously pointed out (Guo and Cole 1989a), the increased pH in S phase in vivo might help partially decondense chromosomes and this decondensation may be required for DNA replication.

Chromatin self-association and genome functions. Chromatin fibers that have nucleosome-free gaps have a reduced ability to self-associate (Fletcher and Hansen 1996; Hansen 2002). Correspondingly, actively transcribed chromatin in vivo tends to have nucleosome-free gaps and is less condensed (Ercan et al. 2004). Histone acetylation has been found to impair chromatin self-association. Endogenous chromatin fragments that are hyperacetylated self-associate at higher salt concentrations. These chromatin fragments also are enriched in active genes (Davie and Candido 1978; Davie and Saunders 1981). It seems likely that this results from that fact that transcriptionally active chromatin is hyperacetylated and less likely to self-associate. The recent work by Peterson and coworker (Shogren-Knaak et al. 2006) demonstrate that in vitro chromatin self-association, specific acetylation and in vivo chromatin functions are tightly linked. They found that specific acetylation on H4 NTD K16 totally disrupted the activity of the H4 NTD to mediate chromatin self-association, and that this modification is enriched in "Mg²⁺-soluble" chromatin. Importantly, H4 K16 acetylation is associated with transcriptional activation in vivo (Akhtar and Becker 2000).

Ubiquitination of H2A facilitates chromatin self-association (Jason et al. 2001), which argues that ubiquitination of H2A can help organization more compacted chromatin in vivo. Interestingly, H2A ubiquitination was shown to be enriched in the transcriptionally inactive, heterochromatic X and Y chromosomes in meiotic prophase in male mammals (Baarends et al., 1999; Baarends et al., 2005), and in the heterochromatic inactive X chromosome in female mammalian cells (Smith et al., 2004; Baarends et al., 2005). Although a direct link between H2A ubiquitination and chromatin organization in vivo remains elusive, the aforementioned studies strongly argue that H2A ubiquitination is involved in organizing more compacted chromatin structure in vivo, consistent with its effect on in vitro chromatin self-association.

The reduced ability of H2A.Z-containing arrays to self-associate in vitro (Fan et al. 2002) is consistent with its in vivo functions of facilitating gene activation and antagonizing gene silencing (Raisner and Madhani 2006). Both the in vitro and in vivo functions of H2A.Z suggest that chromatin containing H2A.Z forms relatively decondensed structure.

Polyamines induced chromatin self-association and depletion of cellular polyamines could partially alleviate the defect caused by inactivation of GCN5 (Pollard et al. 1999). This work highly suggests that polyamines also are involved in organizing chromosomes in vivo, probably through a process similar to their actions in chromatin self-association. Meanwhile, this work suggests that polyamines are transcription repressors and the repressing activity can be counteracted by histone acetylation, which actually in turn can decondense the compacted chromatin organized by polyamine.

1.4 Folding of the chromatin fiber; the '30 nm' chromatin fiber

At $MgCl_2$ concentrations from 0.0-2.0 mM nucleosomal arrays transition from a make short range intra-nucleosomal array interactions through protein-DNA and protein-protein interactions mediated by the histone NTDs (Kan et al., 2007; Schwarz and Hansen, 1994). The nucleosomal array transition to the moderately folded and fully folded structures is evident by changes in the sedimentation coefficients from 30S to 40S and 55S, respectively (Schwarz and Hansen, 1994). This process reproduces physiological relevant reversible transitions that are seen when endogenous chromatin purified from living cells is similarly treated (Fletcher and Hansen, 1996). For over 30 years, the structure of the condensed chromatin fiber has been disputed; however, most of the studies agreed that the diameter of the compacted chromatin fiber is ~30

nm and the condensed nucleosomal arrays make nucleosome-nucleosome interactions via the nucleosome protein surface (Robinson et al., 2006; Schalch et al., 2005; Van Holde, 1989) (figure 1.2). In the following section I will discuss the two main models of how intra-nucleosomal interactions condense chromatin into the '30 nm fiber': the one start helix and the two start helix (figure 1.2). At the heart of these two theories is the path of the DNA in the folded '30 nm fiber'.

One start helix – This usually involves tight packaging of nucleosomes in a helix or solenoid structure. Each nucleosome (N) and adjacent nucleosome (N+1) lies face-to-face along the helical path (figure 1.2). The linker DNA is contained in the center of the helix. In this model the linker DNA must bend to enter the next nucleosome.

Two start helix – In this model nucleosomes N and N+2 lie face-to-face along the helix. Nucleosomes N and N+1 are separated by straight linker DNA (figure 1.2). In this model the length of the linker DNA would determine the diameter of the chromatin fiber.

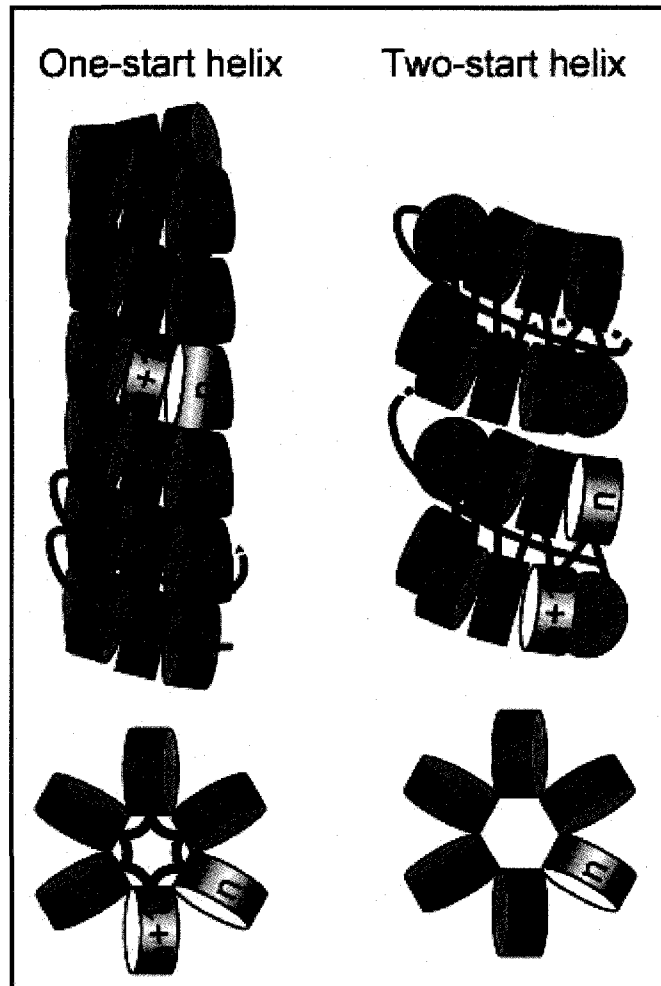


Figure 1.2 Two models for chromatin fiber condensation. The illustration above depicts the organization of nucleosomes (discs) within the '30 nm fiber'. (Left) the one-start helix and (right) the two-start helix, with top and side view. Different color is used to indicate nucleosomes that neighbor each other in the extended chromatin fiber (designated n and $n + 1$); these nucleosomes have different spatial location (and different neighbors) in the 30 nm fiber, depending on the type of model.

Figure adapted from van Holde, K. (2007)

The main argument to be tested between these two models is how the linker length affects the chromatin fiber diameter. In the one start helix, the diameter of the fiber is independent of linker length. Dimensional calculations obtained from the 9.0 Å X-ray crystal tetranucleosome structure with 167 bp nucleosome repeat lengths suggest a two start helical model with a diameter of 24-25 nm (Schalch et al., 2005). The linker DNA is nearly straight in this model. However, *in vivo* the nucleosome repeat length is rarely regular and this short. The addition of as little as 3 bp would cause a 108° twist of the next nucleosome along the strand, and the authors attempt to account for this by discussing variable nucleosome packaging (Schalch et al., 2005). Schalch et al discuss two molecular mechanisms that could account for this variability i) variations up to ±5 bp of DNA could be absorbed by adjusting the DNA length on adjacent nucleosome cores and ii) variations up to ± 10 bp of DNA could be accommodated by polymorphic packaging within each nucleosome stack. In contrast to the conclusions by the Richmond group, Rhodes *et al* have presented evidence to support the one start helix model. Using variable nucleosome repeat length (167-212 bp) reconstituted nucleosomal arrays under varying ionic conditions to induce folding, these researchers produced the same measured fiber diameter of 33-34 nm (Robinson et al., 2006). This group concluded that the fibers were indeed the solenoidal, one start helix model, because of the consistent diameter of the fibers with variable linker length, not expected from a two start helix.

Both of the above observations were made using a defined template DNA with a strong positioning sequence and periodic 10 bp linker length. *In vivo*, however, imaging of native chromatin does not indicate homogeneously folded fibers with uniformly positioned nucleosomes (Woodcock and Horowitz, 1998). If both models exist, linker length would determine the diameter of the fiber and path of the DNA. Such a proposed mechanism would involve both the two start helix and the solenoid

model and involve a dynamic packaging of DNA in the chromatin fiber and leave room for influence of variable linker length. Changes in the nucleosome packaging could lead to perturbations in the chromatin fiber with could assist in nucleosome accessibility. The work outlined in chapters II-IV of this thesis addresses how histones from multiple species, histone variants, and post translationally modified histones influence the processes described above.

1.5 Histone post-translational modifications

The level of complexity in gene expression, which exists during the development from a single cell to a multi-cellular organism, is based on gene accessibility and chromatin structure. Chromatin condensation can be influenced by covalent post-translational modifications (PTM) of histones. The term epigenetics refers to the heritable patterns of gene expression that do not involve changes in DNA sequence but are influenced by the post-translational modification pattern of histones (Cheung and Lau, 2005; Van Holde, 1989). Histones are PTM on the nucleosome surface and more notably on the N-terminal tail. Covalent histone modifications include lysine acetylation, lysine and arginine methylations, serine phosphorylation, lysine ubiquitylation, ADP-ribosylation and sumoylation. These modifications are thought to affect chromatin through two mechanisms. First, most of the PTMs change the amino acid side chain physio-chemical properties, which could affect histone structure, nucleosome-nucleosome interactions and DNA binding. Second, PTMs could influence the binding of chromatin associated proteins and/or histone chaperone complexes (Kouzarides, 2007). That a specific combination of covalent modifications would have specific functional consequences established the 'histone code' hypothesis (Strahl and Allis, 2000). However, because of the complexity of

understanding how non-modified and major type (MT) histones contribute to chromatin function; it is difficult to make conclusions on how PTMs affect these fundamental processes.

Specific modifications have been associated with heterochromatin and euchromatin. Heterochromatin has been defined as condensed chromatin that does not decondense during interphase (Van Holde, 1989). Heterochromatin structure is less accessible to enzymes such as nucleases (Weintraub and Groudine, 1976) and contains few actively transcribed genes (Mizzen and Allis, 1998). In contrast, euchromatin is more accessible to nucleases and contains actively transcribed genes (Mizzen and Allis, 1998)

Here I will give a brief description of some of the known PTMs and how they affect the nucleosome structure, nucleosomal array condensation and transcription.

Acetylation – Histone acetyltransferase (HAT) enzymes acetylate histones by transferring an acetyl group from acetyl CoA to lysine to form ϵ -N-acetyl lysine. HAT enzymes can be associated with transcriptional co-activators such as the SAGA complex (Sterner and Berger, 2000) suggests the role of acetylation in euchromatin and actively transcribed genes (Pollard et al., 1999; Ridsdale and Davie, 1987). Within the nucleosome core, H3-K56 acetylation has been shown to enhance gene expression (Xu et al., 2005), DNA repair, and is found on newly synthesized histones (Masumoto et al., 2005). The structural consequence of H3-K56Ac is analyzed in chapter four. To regulate heterochromatin foci such as telomeres, acetyl groups are removed by histone deacetylases (HDACs), which results in transcriptional repression (Williams et al., 2008; Xu et al., 2007).

Histone methylation – Histones are methylated by histone methyltransferases (HMTs) on arginine and lysine side chains. Arginine can be mono- or dimethylated whereas lysine can be mon-, di-, or trimethylated (Margueron et al., 2005). Different

states of methylation are associated with euchromatin or heterochromatin. For instance, trimethylation of H3-K4 is specific to actively transcribed regions, whereas dimethylation of the same amino acid is associated with both transcriptionally active and silent chromatin (Santos-Rosa et al., 2002). Therefore, the number of methyl groups, not just the amino acid modified, determines the functional consequences of the modification. The first enzyme discovered to remove lysine mono- and dimethylation was the histone lysine demethylase LSD1 (Shi et al., 2004). The reversibility of methylation, much like acetylation, highlights another level of complexity to the 'histone code' (Lan et al., 2008).

Histone Phosphorylation – Histones are phosphorylated by kinases and these groups are reversed by phosphatases. Phosphorylation of H3-S10 has a dual role in transcription activation and chromatin condensation during mitosis (Cheung et al., 2000). This dual role of phosphorylation supports the hypothesis that histone modifications can be protein binding surfaces rather than directly modifying chromatin architecture (Kouzarides, 2007).

Histone Ubiquitination – Ubiquitin is a 76 amino acid peptide that is conjugated to proteins by a multi-protein ubiquitin ligase complex (Weake and Workman, 2008). Ubiquitin can be removed by thiol-proteases known as ubiquitin specific proteases (Nijman et al., 2005). The substrates can either be monoubiquitinated or polyubiquitinated. Mono-Ub usually tags proteins to signal a particular function, whereas poly-Ub marks proteins to be degraded by the 26S proteasome (Weake and Workman, 2008). Mono-Ub is found on histones H2A and H2B. Studies have shown that Mono-Ub acts as a cross-talk between H2B and other histone modifications such as H3 methylation at K79 and K4 (Osley, 2006); although, the consequences of histone ubiquitination is not yet fully understood.

Histone sumoylation – Sumoylation consists of a ubiquitin-like protein that contains ~100 amino acids. It shares the three-dimensional structure of ubiquitin and also requires similar multi-subunit enzymes to target lysine side-chains (Johnson, 2004). Histones H2A, H2B, H3 and H4 have been shown to be sumoylated, and has been associated with transcriptional repression (Nathan et al., 2006). Much like mono-Ub, there have been suggestions of cross-talk between SUMO and other modifications suggesting that this PTM might also serve as a protein binding motif.

Histone ribosylation – The addition of mono-ADP-ribose or poly-ADP-ribose is catalyzed by mono ADP-ribosyltransferase (MART) or poly ADP-ribosyltransferase (PARP) enzymes. Histones H1, H2A, H2B, H3 and H4 are mono-ADP-ribosylated on glutamate and arginine sidechains (Hassa et al., 2006). The role of ribosylation is not fully understood. However, the PARP-1 enzyme is localized to sites of DNA double strand breaks (Ju et al., 2006) and the level of mono-ADP-ribosylation of H2A and H1 increased in the presence of DNA damaging agents (Kreimeyer et al., 1984). Suggesting ribosylation might aid in DNA accessibility.

The PTMs listed above seen both individually and in combination on the N-, C-terminal, and within the nucleosome core. To date we not fully understand how each un-modified histone affects chromatin structure and function, nor do we know the affects each individual type of modification. The amount of different combinations of PTM adds to the complexity of the biological significance of the 'code'. This makes clarifying and understanding the histone code a daunting task. In chapter four of this dissertation I examine the affect acetylation of H3-K56 has on the nucleosome structure and nucleosomal array condensation.

1.6 The centromere and CENP-A associated proteins

Chromosomes accomplish chromosome segregation via the centromere locus (Sullivan et al., 2001). On each chromosome the centromere is the location of kinetochore formation and microtubule capture during mitotic segregation, which mediates proper distribution of DNA to dividing daughter cells (Vos et al., 2006). The centromere exists as a multi-domain locus; containing many highly conserved protein components (Sullivan, 2001). The centromere coordinates chromosome movement in mitosis and meiosis and synchronizes aspects of chromatin structure and function. This section presents an overview of some of the centromere (CEN) specific proteins required for centromere function.

Centromeric chromatin is distinguished by the presence of the H3 variant, centromere protein-A (CENP-A) (Palmer et al., 1991). CENP-A proteins are present from yeast to humans and have conserved function, even though CEN DNA is widely divergent (Saffery et al., 2000). Nucleosomes can be assembled in vitro containing CENP-A, H4, H2B and H2A, indicating that CENP-A can replace both copies of H3 in the nucleosome (Yoda et al., 2000). However, a comparison of the structure and function of CENP-A containing chromatin has yet to be directly compared to chromatin containing H3.

Blocks of heterochromatin flank both sides of the centromeric chromatin, indicated by differences in the PTMs compared to CENP-A containing chromatin (Sullivan and Karpen, 2004). The only PTM associated with CENP-A is phosphorylation of serine-7 by aurora-B kinase (Zeitlin et al., 2001), whereas the surrounding heterochromatin contains H3-K9 tri-methylation (Sullivan and Karpen, 2004). However, Ser-7 is not conserved among CENP-A orthologs, so it may not have a conserved regulatory

function. Perhaps a unique set of PTM may play a role in the deposition and maintenance of CENP-A at the centromere.

Unlike MT H3, CENP-A nucleosomes are not removed or replaced, but are inherited semi-conservatively, so that pre-existing CENP-A is equally divided between daughter strands (Sullivan and Karpen, 2001). This indicates that CENP-A could be the epigenetic mark that maintains centromeric chromatin through generations of cell divisions.

CENP-A, and -B form the pre-kinetochore chromatin complex, which is central to the developing kinetochore (Ohzeki et al., 2002). One CENP-B dimer (Kitagawa et al., 1995) binds to the 17 bp CENP-B box, that is present every-other 171 bp monomer (Ohzeki et al., 2002). CENP-A and core histones are assembled into nucleosomes between the CENP-B binding regions: the position of CENP-B at either end of the nucleosome is thought to establish nucleosome positioning within the 171 bp repeat (Tanaka et al., 2005).

Assembly of the prekinetochore containing CENP-A, core histones (H2A, H2B and H4) and CENP-B is completed by the addition of other CEN proteins. This distinct group of CEN proteins (CENP-C, -H, -I and -K) associate with CENP-A throughout the cell cycle (Foltz et al., 2006; Okada et al., 2006). Two independent groups discovered CEN proteins and categorized them in reference to CENP-A nucleosomes, one being CENP-A distal (CAD) (not purified with CENP-A nucleosomes) and the other CENP-A nucleosome associated complex (NAC). Components of the NAC and CAD were found to be constitutively associated with centromeric chromatin, suggesting that they may play a role in kinetochore association and/or CENP-A deposition and maintenance (see table 1.1). In general, NAC components recruit CAD proteins, which are required for recruitment of a subset of kinetochore proteins. The overall organization of the centromere is coordinated by the assembly of CEN

Vertebrate protein name	Role in Mitosis	Depletion or loss-of-function	Localization dependency	NAC or CAD
CENP-A	Histone H3 variant that forms a centromere-specific nucleosome; separate assembly pathway from Mis2, required for localization of all centromere proteins except Mis 12	Kinetochores –null phenotype; embryonic lethal; inability to localize CENP-C, CENP-H, CENP-I, Ndc80 complex, CENP-E and Mad2	RbAp46 and RbAp48 in human cells and numerous proteins identified in yeast	NAC
CENP-B	Not essential; may assist in centromere site determination	No Mitotic defects	17 bp DNA sequence: CENP-B box	NAC
CENP-C	Specifies localization of kinetochores assembly proteins	Kinetochores-null phenotype; cell death	Requires CENP-A	NAC
CENP-G	Unknown	Unknown	Unknown	
CENP-H	Specifies localization of Ndc80 complex and CENP-U; required for CENP-C localization	CENP-H: inability to localize CENP-C in chicken DT40 cell line; metaphase arrest	Requires CENP-A	NAC
CENP-I		CENP-I: cell cycle delay in G2; inability to localize Ndc80 complex, CENP-F, Mad1, Mad2 to kinetochores		
CENP-U	Unknown	Unknown	Requires CENP-H and CENP-I	NAC
CENP-E	Kinetochores kinesin motor required for reliable bi-oriented spindle microtubule-kinetochores attachment; interacts with and activates mitotic checkpoint mechano-sensory complex	Delayed mitosis due to unaligned chromosomes	Required Bub1 and BubR1	
CENP-F	Stabilizes kinetochores microtubule interactions	Decreased stability of kinetochores microtubule interactions	Requires Zwint-1 and Bub1	
CENP-M,N,T			Requires CENP-A	NAC
CENP-K,L,O,P,Q,R,S		Errors in chromosome alignment and segregation		CAD

Table 1.1 CEN proteins adapted from (Vos et al., 2006)

chromatin and heterochromatin. Stacks of CENP-A nucleosomes are positioned toward the outward face of the chromosome, facing the kinetochore. This recruits other CEN proteins and orients sister kinetochores towards opposite spindle poles. Conversely, H3 containing chromatin is located interiorly in heterochromatin. Most centromeres are located near heterochromatin, suggesting that some unique aspect of centromere chromatin structure may distinguish the centromere from the flanking heterochromatic material.

Studies outlined in chapter three of this dissertation aim to investigate the contribution of CENP-A to the structure and function of centromeric chromatin. Based on the amount of centromere specific proteins with unknown function it is plausible that one function of CENP-A is to form a recognition site for other centromeric proteins to bind.

Chapter 2

The Influence of histone orthologs on nucleosomal array oligomerization

Abstract

In this chapter I demonstrate that defined nucleosomal arrays made with histones from multiple species oligomerize at different concentrations of $MgCl_2$. A comparison of endogenous and recombinant *Drosophila melanogaster* histone octamers showed that this is unlikely due to posttranslational histone modifications, but likely a result of subtle changes in the sequences constituting the histone tails and structured surface of the histone octamer.

2.1 Introduction

Genomes of different species vary in many fundamental aspects, for example in the amount transcribed genes per base pair, nucleosome repeat length, amount of histone H1 per nucleosome, and ionic environments.(www.genomesize.com;(Cameron et al., 1988; Fernandez-Segura and Warley, 2008; Woodcock et al., 2006) However, all higher eukaryotes have nucleosomes containing a histone octamer of H2A, H2B, H3, H4 and ~146 bp of DNA. This is due to the high sequence conservation between histone orthologs between species. I am interested in determining if the differences in histone ortholog composition from different species affect the formation higher order chromatin structures.

Historically, in order to study chromatin, researchers purified chromatin fragments and histones from endogenous sources (i.e. blood, larvae and cultured cells). Endogenously purified histone octamers are combined with defined length DNA to reconstitute nucleosomes and nucleosomal arrays (Lusser and Kadonaga, 2004). These nucleosomal arrays were used to biophysically characterize the formation of salt-mediated chromatin condensation (Hansen, 2002). However, the use of endogenous histone octamers limited study how specific histone modifications and histone variants affect higher order chromatin formation.

The Hansen and Luger labs are interested in studying histone variants, post-translationally modified histones and the role of histone amino acid composition in chromatin structure and function. These *in vitro* studies require milligram quantities of homogenous histones. Therefore, it is practical to use histones from recombinant sources. Using recombinant proteins will also allow us to mix and match various histones in order to dissect the effect of PTM and histone variants. Recombinant histones have been used in the reconstitution of highly pure homogenous mono-

nucleosomes to obtain high resolution x-ray crystallographic structures (Luger, 2006). Interestingly, crystal contacts of the H4 tail with the acidic patch of the adjacent nucleosome surface suggest a mode of nucleosome packing (Chodaparambil et al., 2007). Also, the crystal lattice packing of the yeast nucleosome structure indicated a difference in the nucleosome-nucleosome interactions within the unit cell (White et al., 2001). Obtaining structural information about the histone N-terminal tails has been difficult as these residues are highly unstructured and intrinsically disordered.

Preliminary experiments indicated that arrays containing recombinant *Xenopus* octamers require approximately half the $MgCl_2$ concentration to oligomerize as arrays reconstituted with endogenous chicken histone octamers. To determine if these differences are the result of histone PTM or organism source, I began by comparing nucleosomal array condensation using endogenous and recombinant histones from the same species. For this comparison I used purified histones from *Drosophila melanogaster* embryos and recombinant *D. melanogaster* histones from *E. coli*. Due to possible differences in reconstitution of histone octamers from recombinant and endogenous sources I have carefully analyzed the extent of template saturation using sedimentation velocity, nuclease digestion and agarose multigel analysis. I found that nucleosomal arrays reconstituted with endogenous and recombinant *Drosophila* histone octamers have similar but not identical ability to condense nucleosomal arrays. Our *Drosophila* studies were done as a control for our ultimate goal of evaluating the differences in chromatin condensation between species.

I compared the formation of higher order chromatin structures using equally saturated arrays reconstituted with endogenous chicken, endogenous *Drosophila*, recombinant yeast, recombinant *Xenopus* and recombinant mouse histone octamers. I have demonstrated that the amount of $MgCl_2$ required to oligomerize nucleosomal arrays varies between species. I hypothesize that these differences in nucleosomal

array oligomerization are due to the differences in the primary amino acid composition of the N-terminal domain and the nucleosome surface.

2.2 Methods and Materials

2.2.1 Gel electrophoresis Triton-X-100, Acetic Acid, Urea, 15% polyacrylamide gel electrophoresis (TAU-PAGE) was performed by Katherine Dunn in Dr. Jim Davie's lab (University of Manitoba, Canada) as previously described (Davie, 1982). 18% SDS-PAGE was performed by combining the samples with 4X SDS-PAGE loading dye and boiling for 10 min. Samples were loaded and electrophoresed for 1.5 hours at 150V.

2.2.2 DNA purification – The 208x12 DNA used to reconstitute nucleosomal arrays was purified as previously described (Georgel et al., 1993; Schwarz and Hansen, 1994).

2.2.3 Histone Purification – Chicken histone octamers were purified from chicken erythrocyte nuclei as described in (Hansen et al., 1989). Briefly, chromatin fibers were purified from chicken erythrocyte by nuclease digestion followed by lysis of the nuclei. Linker histones were separated from chromatin fibers using CM-sephadex C-25 resin (Garcia-Ramirez et al., 1990). After linker histones were removed, oligonucleosomes were subject to more extensive micrococcal nuclease digestion and then loaded onto a hydroxyapatite affinity column and core histone octamers were eluted with buffer containing 2 M NaCl (Hansen et al., 1989). The concentration of histone octamers were measured by A_{230} and by BCA protein assay kit. Endogenous *Drosophila* octamers were purified as described in (Butler and Thomas, 1980; Kerrigan and Kadonaga, 1992; Laybourn and Kadonaga, 1991). Briefly, *Drosophila* embryos (collected <12 hours after fertilization) were prepared by purification of oligonucleosomes by sucrose gradient centrifugation followed by hydroxylapatite

chromatography and elution with buffer containing 2 M NaCl to yield fractions containing histone octamers. (Laybourn and Kadonaga, 1991). Recombinant histones H2A, H2B, H3 and H4 were purified as described (Dyer et al., 2004). The quality of the histone octamers was observed by SDS-PAGE.

2.2.4 Salt Dialysis Reconstitution - Nucleosomal arrays were reconstituted as described (Hansen et al., 1991). Briefly, equal molar ratios of histone octamers were mixed with the 208-12 DNA template in TE buffer (10 mM Tris-HCl, 0.25 mM EDTA, pH 7.8) containing 2.0 M NaCl₂, followed by extensive salt gradient dialysis to low salt TEN buffer (2.5 mM NaCl₂-TE) (Hansen et al., 1991).

2.2.5 Analytical Ultracentrifugation – Sedimentation velocity studies were carried out using a Beckman XL-I/XL-A analytical ultracentrifuge with absorbance optics. Samples were mixed to a final A₂₆₀ of 0.6 - 0.8 and equilibrated at 20⁰ C. for one hour prior to sedimentation. Nucleosomal arrays were sedimented at 18-25,000 rpm with scanning radial increments of 0.001 cm. Data was analyzed using the method of van Holde and Weischet (Demeler and van Holde, 2004) to obtain an integral distribution of sedimentation coefficients (G(s)) using UltraScan v9.4 for windows. V-bar and ρ were calculated using Ultrascan.

2.2.6 Agarose Multigels - Electrophoretic mobility (μ) of nucleosomal arrays was determined using 0.2 – 1.0% agarose multigels as described (Fletcher et al., 1994). Briefly, 9 lane running gels encased in a 1.5% agarose frame were cast in 40 mM Tris-HCl, 0.25 mM EDTA, pH 7.8. Samples were mixed with T3 phage and electrophoresed at 1 V/cm. For direct comparison endogenous and recombinant *Drosophila* arrays were electrophoresed and analyzed on the same gel. Endogenous *Drosophila* arrays were loaded first and electrophoresed for 2 hours, and then recombinant *Drosophila* arrays were loaded in the same wells and run for an additional 8 h. The gels were visualized by UV illumination after ethidium bromide staining. The electrophoretic

mobility (μ) was calculated as the distance from the well to the front of the band. The gel-free μ (μ_0) of the nucleosomal arrays were obtained from the experimentally measured electrophoretic mobility μ as described (Fletcher et al., 1994)

2.2.7 EcoR1 template saturation analysis - Assays were performed as described (Tse and Hansen, 1997). Briefly, 1 μ g of reconstituted nucleosomal arrays was digested with 10 units of EcoR1 for 2 hours at 21^o C. Digested arrays were separated on a 1% agarose gel, stained with ethidium bromide and imaged using a Gel Logic 200 imager. The gel image was used for densitometry analysis of bands to determine the percentage of naked DNA using Scion software and calculated with the equation below.

$$\% \text{ Free DNA} = \frac{\text{Free DNA}}{((\text{Free DNA}) + (\text{NCP} \bullet 2.5))} \quad \text{eq. 2}$$

2.2.8 Folding of nucleosomal arrays- Nucleosomal arrays were diluted with TEN buffer to a final concentration of 2.0 mM MgCl₂ and a final A₂₆₀ of 0.6 – 0.8. Sedimentation velocity experiments were carried out at 18,000 RPM for 2 hours with radial increments of 0.001cm. Data was analyzed using the improved method of van Holde and Weischet (Demeler and van Holde, 2004) to obtain the integral distribution of sedimentation coefficients (G(s)) using UltraScan v9.4 for windows.

2.2.9 Oligomerization of nucleosomal arrays- Differential centrifugation was used as previously described (Gordon et al., 2005; Lu et al., 2006). Briefly, nucleosome arrays were diluted to an A₂₆₀ = 1.2 with TEN buffer. Arrays were mixed with MgCl₂-TEN buffer, incubated for five min. at room temperature then centrifuged in a bench-top microfuge at 13,000 RPM (~16,000 x g) for 5 min. The A₂₆₀ of the supernatant was then measured in a Beckman DU 800 Spectrophotometer. Data are expressed as a percentage of the total sample that remained in the supernatant as a function of MgCl₂. Results shown are the average of 3 independent assays.

2.3 Results

2.3.1 Endogenous *Drosophila* histone octamers have a low but detectable level of PTM or histone isoforms

Post-translational modifications (PTMs) (Shogren-Knaak et al., 2006; Tse et al., 1998b) and template saturation (Fletcher et al., 1994) can influence the concentration of $MgCl_2$ needed to oligomerize nucleosomal arrays and ultimately chromatin structure. While there is a low level of post-translational modifications in undifferentiated cells I was interested in determining the degree of PTM and histone variants found in histone octamers purified from *Drosophila* larvae. Triton-X, acetic acid, urea, polyacrylamide gel electrophoresis (TAU-PAGE) can separate post-translational modification states and protein isoforms based on differing charge and hydrophobicity. In collaboration with Katherine Dunn of the Davie lab (University of Manitoba) we have compared the electrophoretic mobility of endogenous *Drosophila* histone octamers to recombinant histone octamers using TAU-PAGE and SDS-PAGE (figure 2.1). As a histone migration control I loaded acid extracted mouse histone octamers (figure 2.1.A. lane 1) that have been probed with histone antibodies to determine relative mobility (data not shown) (Dunn and Davie, 2005). I observed a decreased mobility in the endogenous *Drosophila* histones H4 and H3 (figure 2.1.B lane 2) compared to the recombinant octamers (figure 2.1.B lane 3). This may be an indication of histone modifications and/or histone variants present in octamers purified from *Drosophila* larvae. To confirm that the sizes of the histones are similar I analyzed the histone octamers by SDS-PAGE (figure 2.1.B.). The denaturing gel did not show a difference in the histone mobility. Therefore, I attribute the difference of TAU-PAGE mobility to

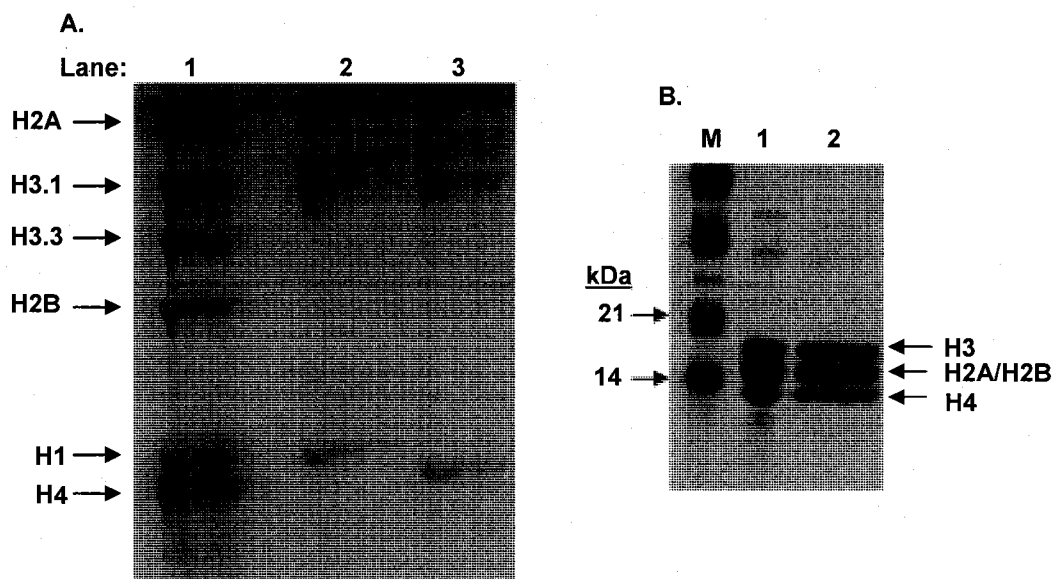


Figure 2.1 Endogenous *Drosophila* histone octamers have a low level of PTMs and/or histone isoforms. A. TAU-PAGE of Acid-extracted *Mus Musculus* histones (lane 1), endogenous *Drosophila* (lane 2) and recombinant *Drosophila* (lane 3) electrophoresed on an AUT-PAGE stained with coomassie blue. Histones are indicated left of gel. **B.** Protein analysis of histone octamers. 5 ug of endogenous (lane 1), recombinant (lane 2) *Drosophila* histone octamers electrophoresed on a 15% SDS-PAGE and stained with coomassie blue.

changes in charge and/or hydrophobicity due to PTMs or a difference in histone isoforms. I used these two types of *Drosophila* histone octamers to reconstitute nucleosomal arrays in order to compare the chromatin condensation of endogenous and recombinant nucleosomal arrays.

2.3.2 Reconstitution and saturation analysis of *Drosophila* nucleosomal arrays.

I was interested in determining if the low level of PTM or histone variants in the endogenous octamers affects nucleosomal array condensation. To do this I added a slight molar excess (r-value = 1.1) of histone octamers to the 208-12 DNA template and dialyzed from 2 M NaCl, TE buffer to 2.5 mM NaCl TE (TEN) buffer by step-wise dialysis. Because MgCl₂ dependent nucleosomal array condensation assays can be influenced by the amount of histone octamer saturation of the DNA template, I carefully determined the extent of histone octamer saturation on the 208-12 DNA template by three complementary assays: i) sedimentation velocity analysis in low salt buffer, to measure the degree of heterogeneity and saturation of the nucleosomal array, (ii) digestion with EcoR1 to determine the percentage of the histone-bound and histone-free DNA template, and (iii) agarose multigel electrophoreses in low salt buffer to determine the surface charge density.

2.3.3 Reconstituted endogenous and recombinant nucleosomal arrays have similar sedimentation coefficient distributions

Using the Beckman XL-A analytical ultracentrifuge (AUC) I performed sedimentation velocity experiments and analyzed the data using an improved van Holde and Weischet method (Demeler and van Holde, 2004) to obtain the integral distribution of

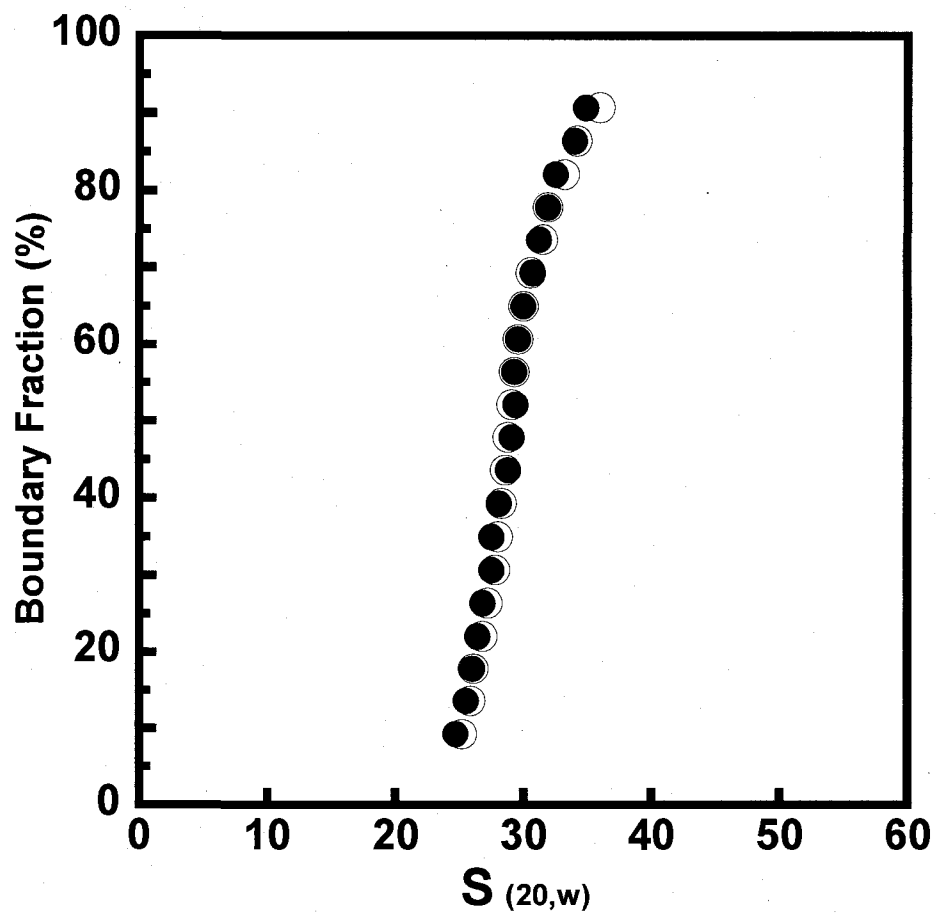


Figure 2.2 Sedimentation velocity analysis of nucleosomal arrays. Reconstituted endogenous (○) and recombinant (●) 208-12 nucleosomal arrays in TEN buffer. Dotted lines indicate the amount of arrays which are over saturated (% >30S). Sedimentation velocity experiments were carried out at 20,000 RPM, 20° C. and analyzed as described in M&M. Shown is the diffusion corrected integral distribution of S corrected for water at 20° C. ($S_{20,w}$).

sedimentation coefficients ($G(s)$) of reconstituted nucleosome arrays (Carruthers et al., 2000; Demeler and van Holde, 2004). This is a quantitative tool for determining the heterogeneity and histone octamer saturation of nucleosomal arrays (Demeler et al., 1997; Fletcher et al., 1994; Hansen et al., 1997; Hansen and Lohr, 1993; Hansen et al., 1991). Sedimentation coefficient distributions of the reconstituted arrays closely overlapped (figure 2.2) that is the first indication that there are similar amounts of histone octamers reconstituted on each DNA template. Sedimentation distributions in TEN buffer indicated that about 30% of the sample sedimented over 30S indicating this fraction of the arrays are over-saturated with histone proteins (12 nucleosomes per DNA template plus extra bound histone dimers and tetramers). Ten percent of the sample sedimented less than 27S indicating that there is a small population of arrays, which contain less than 12 nucleosomes per template. Fifty percent of the sample sedimented between 27 and 30S, which indicates full saturation with 12 nucleosomes per DNA template (Hansen et al., 1989).

2.3.4 Reconstituted nucleosomal arrays have similar surface charge density indicating similar octamer saturation

Quantitative agarose gel electrophoresis has been used extensively to determine the effective radius (P_E) and surface charge density (μ'_o) of nucleosome arrays (Fletcher et al., 1994; Hansen et al., 1997). In agarose multigel experiments the electrophoretic mobility (μ) of the sample is reduced by the interaction of the nucleosome array with the pores formed in the agarose gel matrix (Hansen et al., 1997). To obtain gel free mobility (μ_o), the logarithmic plot of μ verses agarose concentration (Ferguson plot) is extrapolated to 0% agarose using standard least-squares linear regression (figure 2.3.B). The mobility of the nucleosomal arrays is dependent on the size, shape, conformational flexibility and surface electrostatic properties. The amount of octamer

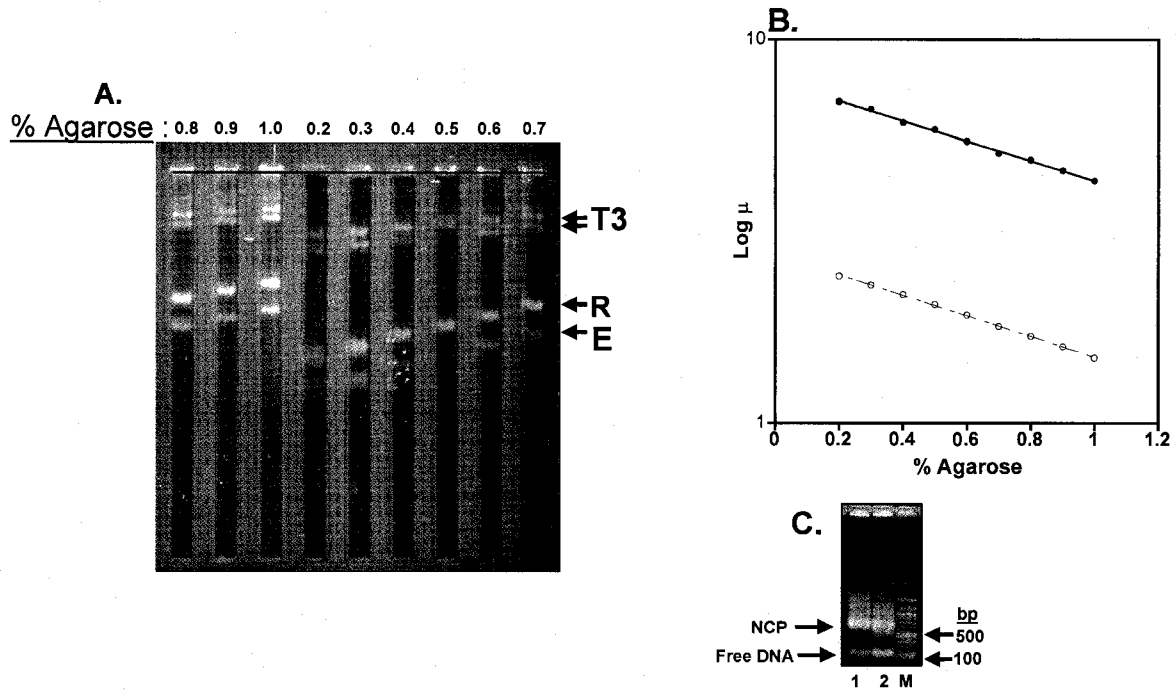


Figure 2.3 Measurement of surface charge density by agarose multigel electrophoresis. A. Endogenous (E) and recombinant (R) *Drosophila* nucleosomal arrays electrophoresed on a nine lane agarose multigel. The gel was loaded with T3 and Endogenous N.A. (E) ran for 1 V/cm then loaded again with T3 and Recombinant N.A. (R) and ran for an additional 5 hours at 1 V/cm. T3 indicates bacteriophage T3. **B. Representative Ferguson plot** of nucleosomal arrays (●) and T3 bacteriophage (○). Results were calculated as described in methods and materials section. Ferguson plots were generated from the results of multigels with agarose concentration ranging from 0.2 – 1.0 % agarose in 1XTAE. **C. EcoR1 Digestion Assay of nucleosomal arrays.** 1 μ g of digested endogenous (lane 1) and recombinant (lane 2) *drosophila* nucleosomal arrays were electrophoresed on a 1% agarose gel, stained with EtBr and visualized as described in methods and materials. The positions of the λ BstE-II marker indicated on right (lane 3).

saturation of the DNA template determines the surface electrostatic charge density (μ'_o). As DNA templates are loaded with histones the negative charge decreases, thus, the gel free mobility μ_o also decreases. The μ'_o of 208-12 DNA was found to be $-2.42 (\pm 0.02) \text{ e-4 cm}^2\text{V}^{-1}\text{sec}^{-1}$, and a fully saturated nucleosomal array to be $1.95 \text{ e-4 } (\pm 0.03) \text{ cm}^2\text{V}^{-1}\text{sec}^{-1}$ (Fletcher et al., 1994).

I electrophoresed endogenous and recombinant nucleosomal arrays on a 9 well agarose gel with agarose percentages from 0.2 – 1.0 % agarose (as described in methods and materials). After electrophoresis, DNA was observed by staining with ethidium bromide and imaged under UV light (figure 2.3.A). The mobility of the arrays and T3 phage is decreased as the percentage of agarose increases (figure 2.3.A). I plotted the measured motilities in log scale (μ) as a function of agarose percentage on a ferguson style plot (figure 2.3.B) to extrapolate the gel free mobility μ'_o (as described above and in methods and materials). Endogenous and recombinant arrays had μ'_o of $-1.97\text{e-4 cm}^2\text{V}^{-1}\text{sec}^{-1}$ and $-2.02 \text{ e-4 cm}^2\text{V}^{-1}\text{sec}^{-1}$, respectively. These results indicate that the endogenous and recombinant *Drosophila* 208-12 nucleosomal arrays were loaded with an average of 11.5 nucleosomes per 208-12 DNA template.

2.3.5 Analytical *EcoR1* restriction digestion indicates similar template loading

EcoR1 digestion assays were performed as previously published (Hansen et al., 1989). This method is used to determine the average number of nucleosomes per 208-12 DNA template. There are two *EcoR1* restriction sites at each 208 bp junction within the tandemly repeated DNA template. Digestion of a fully saturated template yields a single band corresponding to nucleosome monomers (~600 bp). Repeats unbound by histone octamers migrate as free ~200 bp DNA. If nucleosomes span or

block the EcoR1 site due to over-saturation of histone octamers, nucleosome multimers bands will be observed.

I measured a slight loading difference between endogenous and recombinant N.A. with 9.4% and 7.3% unoccupied repeats for arrays containing recombinant and endogenous histones, respectively (figure 2.3.C). These results indicated that recombinant *Drosophila* 208-12 nucleosomal arrays had an average of 0.5 nucleosomes less per DNA template than endogenous N.A.

Together, sedimentation velocity, agarose multigels and EcoRI nuclease assays indicated that the *Drosophila* arrays were nearly equally saturated with an average of $11(\pm 2)$ nucleosomes per template, which allowed me to directly compare the folding and oligomerization of arrays reconstituted with endogenous and recombinant histone octamers.

2.3.6 Nucleosomal array oligomerization is similar with endogenous and recombinant histone octamers

At low salt, arrays exist in a 'beads on a string' conformation (Woodcock, 2006). As the divalent cation concentration is increased, nucleosomal arrays transition to a folded conformation (30 nm fiber, based on the measured diameter of the compact fiber) (Ausio et al., 1984a; Bednar et al., 1995; Felsenfeld and McGhee, 1986; Luger and Hansen, 2005; Thoma et al., 1979; Woodcock et al., 1984; Woodcock and Horowitz, 1998). By further increasing the salt concentration nucleosomal arrays form large oligomeric structures thought to mimic the long range fiber – fiber interactions in compact chromatin fiber (Gordon et al., 2005; Hansen, 2002; Luger and Hansen, 2005; Schwarz and Hansen, 1994). Nucleosome array oligomerization is a reversible and cooperative process, which mimics transitions seen with purified chromatin from

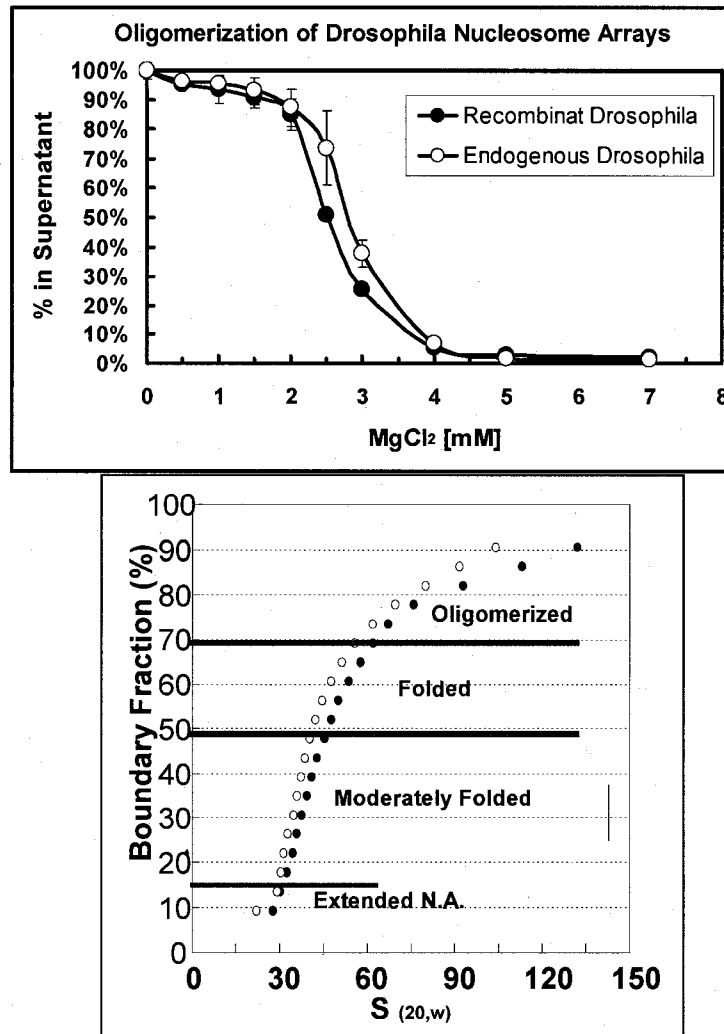


Figure 2.4.A. Endogenous and recombinant nucleosomal arrays have similar Mg^{+2} -dependent oligomerization. Equally saturated endogenous (○) and recombinant (●) *Drosophila* nucleosomal arrays were incubated with the indicated concentration of $MgCl_2$ and assayed for oligomerization (see methods and materials). Shown is the % total A_{260} that remained in the supernatant after micro-centrifugation as a function of $MgCl_2$. **B. Endogenous and recombinant *drosophila* nucleosomal arrays have similar chromatin condensation in 1.8 mM $MgCl_2$.** Reconstituted endogenous (○) and recombinant (●) 208-12 nucleosomal arrays in TEN buffer. Sedimentation velocity experiments were carried out at 18,000 RPM, 20° C. and analyzed as described in M&M. The diffusion corrected integral distribution of S corrected for water at 20° C. ($S_{20,w}$) is shown. Red lines indicate the percentage of arrays folded and oligomerized.

live cells (Lu et al., 2006; Schwarz and Hansen, 1994). Characterization of nucleosomal array oligomerization was first observed under low speed sedimentation velocity experiments (Schwarz et al., 1996) and has subsequently been assayed by differential centrifugation (Fan et al., 2002; Hansen, 2002; Hansen and Lohr, 1993; Hansen et al., 1991; Pollard et al., 1999; Schwarz et al., 1996; Schwarz and Hansen, 1994; Tse et al., 1998b). After the addition of $MgCl_2$, differential centrifugation separates oligomerized arrays from soluble non-oligomerized arrays. I used this oligomerization assay to investigate if the endogenous histone octamers influence nucleosomal array oligomerization.

Nucleosomal arrays were incubated with TE buffer containing 0.0 – 7.0 mM $MgCl_2$ and subject to differential centrifugation; the amount of monomeric arrays was plotted as a function of $MgCl_2$ concentration (figure 2.4.A). From 0-1.8 mM $MgCl_2$ the arrays are soluble (figure 2.4.A), which is consistent with previously published results from native chromatin where arrays transition from an unfolded to the folded conformation (Hansen, 2002). Both arrays begin to form large oligomers at 1.8 mM $MgCl_2$ and undergo cooperative oligomerization as observed by the sigmoidal curve from 1.8 - 5 mM (figure 2.4.A). At 2.5 mM I observed a small difference in the amount of intra-nucleosomal interactions between arrays with 50% of the recombinant arrays oligomerized compared to 20% of the endogenous arrays (figure 2.4). This assay shows that endogenous and recombinant *Drosophila* arrays oligomerize under nearly identical concentration of divalent cations. However, the difference that I observed at 2.5 mM may be due to small differences in saturation and/or histone PTMs.

2.3.7 Folding of recombinant and endogenous *Drosophila melanogaster* nucleosomal arrays is similar

Upon titration of $MgCl_2$, nucleosomal arrays transition from a “beads-on-a-string” array to folded arrays in which nucleosomes make short range intra – nucleosomal array interactions through protein-DNA and protein-protein interactions mediated by the histones (Hansen, 2002; Kan et al., 2007; Schwarz and Hansen, 1994). During nucleosomal array folding, arrays transition from moderately folded (40S) to maximally folded (55S) structures (Hansen, 2002; Schwarz and Hansen, 1994). This folding assay reproduces reversible transitions that are seen when endogenous chromatin purified from living cells is similarly treated (Fletcher and Hansen, 1996).

In order to study intra-nucleosomal array folding I incubated arrays with 1.8 mM $MgCl_2$ (the concentration arrays begin to oligomerize) (figure 2.4.A). I used sedimentation velocity to analyze the folding of endogenous and recombinant arrays. I observed a sedimentation coefficient distribution from 30 – 120S. The sedimentation coefficient distribution correlates to the degree of template saturation. At 1.8 mM $MgCl_2$ 30% of the arrays sedimented over 55S, which is equivalent to the amount of oversaturated arrays I observed using sedimentation velocity in TEN buffer (figure 2.2). 10% of the arrays did not sediment above 30S in 1.8 mM $MgCl_2$ that is equivalent to the amount of sub-saturated material. 50% of the arrays sediment from 30-55 S, which is a mixture of moderately folded (40S) and maximally folded (55S) nucleosomal arrays. I did observe a slight difference in the folding of endogenous and recombinant nucleosomal arrays. At 1.8 mM $MgCl_2$ endogenous octamer arrays had a slightly smaller S-value indicating that the folding was reduced at this salt concentration. These differences, which I observed between endogenous and

recombinant *Drosophila* arrays, may be due to a population of histone isoforms or modified histones.

At the time this study was accomplished it was unknown which species of histones could be used to optimally study recombinant nucleosomal array condensation. This led me to compare nucleosomal array oligomerization with histones from multiple species in order to investigate how the changes in histone tails and nucleosome surface effect nucleosomal array oligomerization.

2.3.8 Nucleosomal array reconstitution and analysis using histone octamers from multiple species

There are noticeable differences in the histone amino acid composition of the N-terminal tails and the histone structure region. To test the hypothesis that these amino acid differences will effect the inter-nucleosomal array interactions; I reconstituted 208-12 DNA with purified *Gallus gallus* (chicken) histone octamers from erythrocytes, *Drosophila melanogaster* (fruit fly) octamers from larvae, and renatured recombinant *Mus musculus* (mouse), *Xenopus laevis* (African tree frog) and *Saccharomyces Cerevisiae* (budding yeast) histone octamers. To assay the degree of 208-12 template saturation I used two complementary assays, sedimentation velocity and EcoRI nuclease digestion.

The sedimentation coefficient distribution is an accurate measurement of histone octamer saturation and homogeneity on the 208-12 DNA template (Fletcher and Hansen, 1996; Fletcher et al., 1994; Hansen, 2002; Hansen et al., 1989; Hansen and Turgeon, 1999; Hansen et al., 1991; Simpson et al., 1985; Tse and Hansen, 1997). All of the reconstituted nucleosomal arrays from multiple species sedimented between 22 - 32 S with midpoints ranging from 24 – 26 S (figure 2.5.B and C). These values

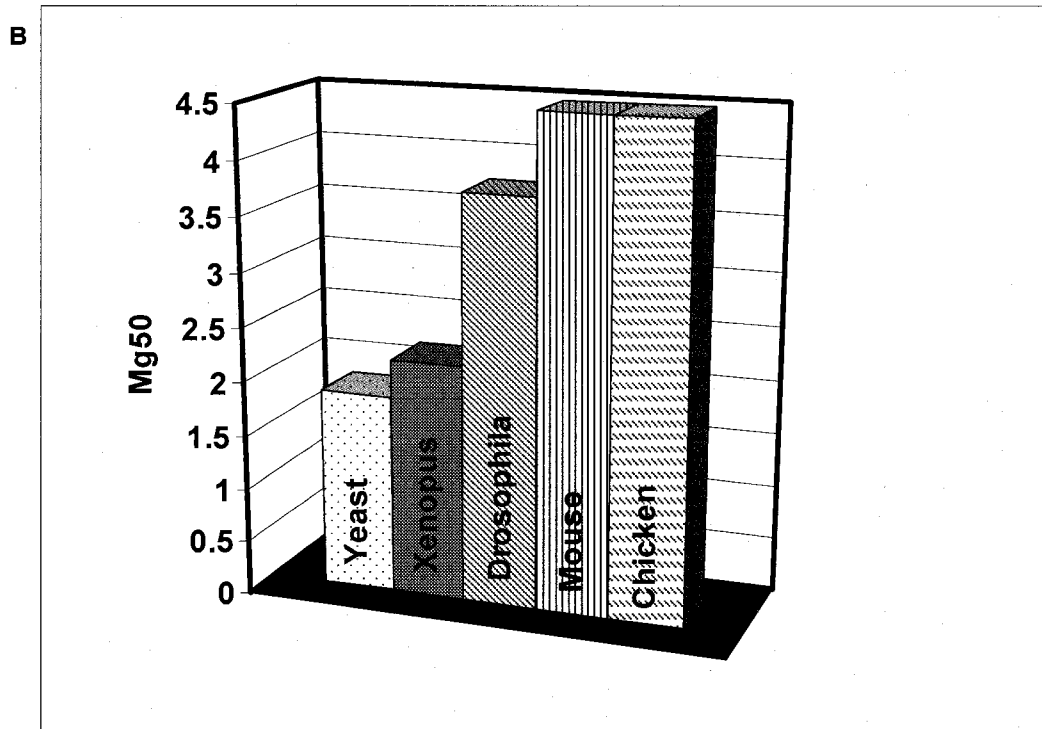
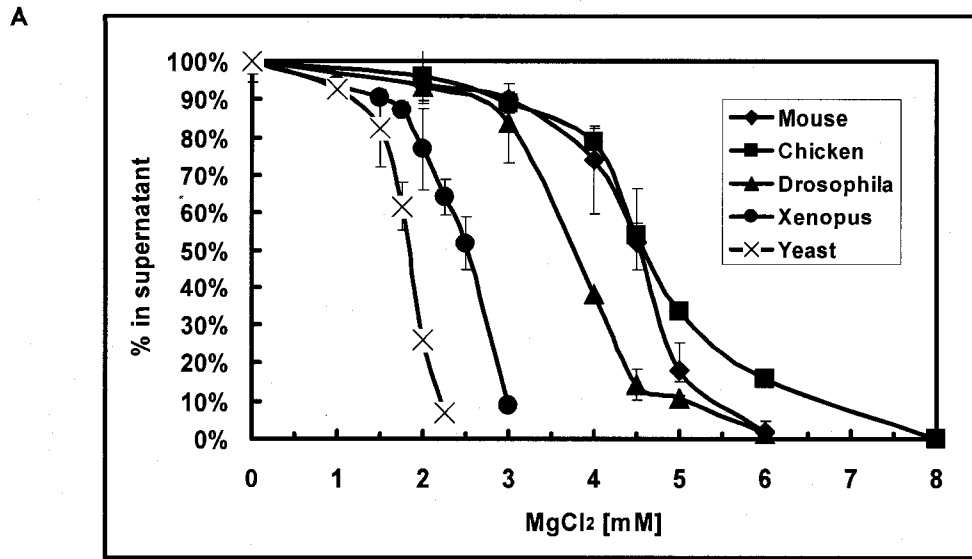


Figure 2.6 Species differences in nucleosomal arrays Mg^{+2} -dependent oligomerization. Equally saturated nucleosomal arrays reconstituted with histone octamers from various species were incubated with the indicated concentration of $MgCl_2$ and assayed for oligomerization (see methods and materials). (A) is the % total A_{260} that remained in the supernatant after microcentrifugation as a function of $MgCl_2$. (B) is the concentration of $MgCl_2$ mM at which half of the nucleosomal arrays are oligomerized (Mg^{50}).

are equivalent to 9-11 nucleosomes per DNA template with an average of 10.5 nucleosomes per template (Fletcher et al., 1994). About 10% of *Drosophila* and mouse arrays sedimented over 30S and are oversaturated (> 12 nucleosomes per 208x12 template).

To determine the amount of histone octamer saturation I digested the nucleosomal arrays from each species with EcoRI and analyzed the digest by electrophoresis on a 1% agarose gel. Figure 2.5 shows the results of the analyzed EcoRI digestion which confirmed a nearly equal amount of unoccupied templates with a range from 6.3 – 9.7% free DNA, suggesting ~11 nucleosomes per DNA template.

Together these assays have confirmed that the template saturations are similar between all of the nucleosomal arrays reconstituted. Therefore I can use these matched arrays to investigate the chromatin condensation properties from each species.

2.3.9 Oligomerization of nucleosomal arrays containing histone octamer from multiple species

I titrated MgCl₂ into nucleosomal arrays from multiple species to investigate if the differences in the amino acids between the species affect the inter-nucleosomal array oligomerization. Arrays containing yeast histone octamers required the least amount of MgCl₂ to oligomerize: the concentration of MgCl₂ at which 50% of the arrays are oligomerized (Mg⁵⁰) was 1.75 mM (figure 2.6). Arrays containing mouse and chicken histone octamers had the highest Mg⁵⁰ of 4.5 mM. *Xenopus* and *Drosophila* had Mg⁵⁰ of 2.25 and 3.75 mM MgCl₂, respectively.

There was no correlation between Mg⁵⁰ and template saturation. Mouse arrays had the highest level of template saturation with a midpoint S_(20, w) of 26 and the highest

Mg⁵⁰ of 4.5 mM. Also, Yeast had the lowest Mg⁵⁰ of 1.75 mM and an S_(20,w) of 24.5S. These data demonstrate that histone octamer orthologs significantly different ability to condense chromatin, with Mg⁵⁰ values ranging from 1.75-4.5 mM MgCl₂.

2.4 Discussion

2.4.1 Endogenous and recombinant histone octamers have similar chromatin oligomerization characteristics

In the 1970's salt fractionation techniques were developed to purify endogenous chromatin from whole cells (Sanders, 1978; Sanders and Hsu, 1977) Using this technique Davie and Saunders observed that chromatin which is accessible to micrococcal nuclease digestion in high Mg⁺² concentrations was highly enriched in transcriptionally active genes and hyper-acetylated histones (Davie and Saunders, 1981). This study is one link between the salt induced oligomerization of chromatin *in vitro* to the *in vivo* chromatin function. Chicken erythroid nuclei have been shown to be transcriptionally silent and hypoacetylated (Zhang and Nelson, 1988). The level of acetylation in immature *drosophila* larvae is also low, but there has never been a direct comparison fo the chromatin condensation ability between endogenous and recombinant histones. The comparison of nucleosomal array oligomerization using histone octamers from recombinant and endogenous sources was necessary in order move on to comparing multiple species.

There was a small difference observed in the oligomerization and folding between arrays of endogenous and recombinant *Drosophila* octamers reconstituted on the 208x12 DNA template (figure 2.4). I demonstrated that the octamer saturation level was similar using sedimentation velocity, agarose multigel and EcoRI digestion, they

contained an average of 11.5 NCP per 208-12 DNA template. Therefore the chromatin condensation differences that I observed are not attributed to template saturation.

Acetylation of the histone tails have been shown to affect chromatin condensation (Annunziato and Hansen, 2000; Peterson and Laniel, 2004). Analysis of the endogenous and recombinant histone octamers revealed the presence of histone PTMs and/or histone isoforms in the endogenous octamer sample. I attribute the increased amount of $MgCl_2$ required for oligomerization and the decreased amount of folding observed in the endogenous arrays to be caused by this population of histone variants and/or PTMs. However these small differences in endogenous and recombinant *Drosophila* arrays do not account for the large differences I observed between species.

2.4.2 Nucleosomal arrays reconstituted with histone octamers from different species require different amounts of $MgCl_2$ to oligomerize

It was surprising that that nucleosomal arrays reconstituted with histone octamers from different species oligomerize at such markedly different concentrations of $MgCl_2$. These results imply that there may be a difference in the chromatin compaction and/or nucleosome organization between organisms or divalent cation concentration in the nucleus. Nucleosomal arrays reconstituted with *Saccharomyces cerevisiae* histone octamers require the lowest concentration of $MgCl_2$ and chicken required the highest concentration to oligomerize.

The largest amino acid difference between species is found in the yeast and chicken histones H2A and H2B (figure 2.7). The primary amino acid differences may change the nucleosome surface and NTD physiochemical properties which may account for

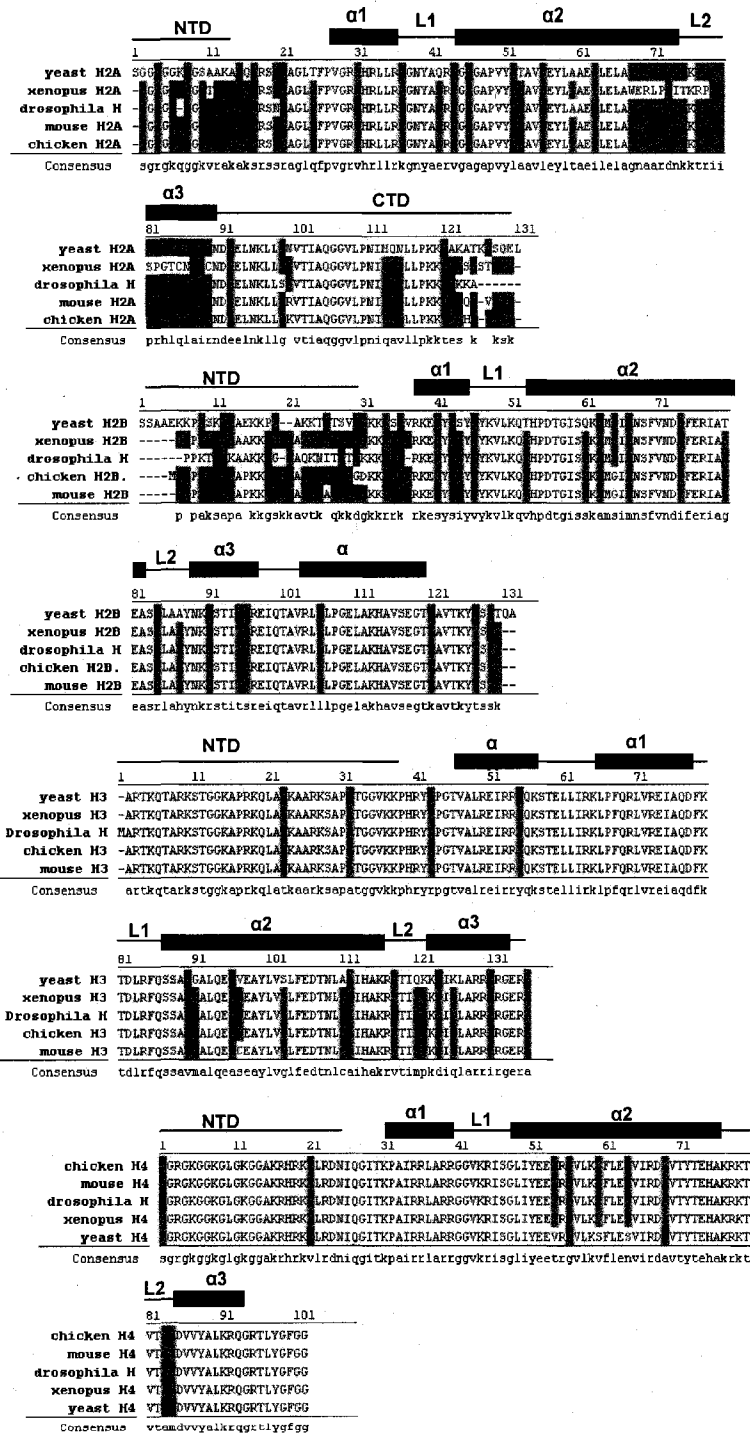


Figure 2.7 Primary sequence alignment of histones from multiple species. Indicated by colors of foreground and background for non-homologous (black/white), identical (red/yellow), frequent (blue/blue), strong similarity (black/green) and weak similarity (green/white). Structural histone fold features are marked by thick lines, loops, N-terminal tails (NTD) and C-terminal tails (CTD) are indicated by thin lines.

the difference in Mg^{50} . These differences may also account for the unique packing in the crystal lattice of the yeast nucleosome core particle (White et al., 2001), which is distinct from other species NCP crystal packing (Chakravarthy et al., 2005; Davey et al., 2002; Luger et al., 1997; Suto et al., 2000; White et al., 2001) This crystal packing could reflect a difference in yeast chromatin condensation although the crystal packaging is not consistent with current '30 nm' fiber models (Schalch et al., 2005; van Holde and Yager, 2003).

The differences we observed in nucleosomal array oligomerization between species can only be the result of amino acid differences. Although how the difference in histone composition change histone function has yet to be resolved. These differences may include, but are not restricted to, differences in exit trajectory of the histone NTD and possibly differences in the physiochemical properties of the surface of the nucleosome. Both of these theories could lead to a difference in histone-histone and/or histone-DNA interactions. Although, these hypotheses need to be directly tested.

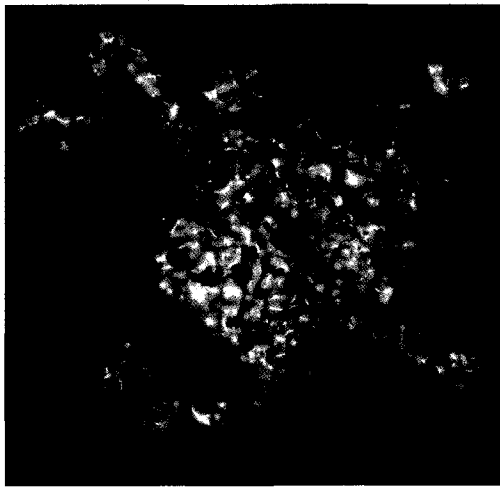
2.5 Future Directions and alternative hypotheses

An alternative rationalization to these differences may be explained by an electrostatic charge balance between the DNA and histones. The amount of DNA per nucleosome is known as the nucleosome repeat length (NRL). The average NRL varies between species and cell types. The amount of linker histone H1 (known to stabilize chromatin higher order structures (Hansen, 2002)) also varies between species and tissues. Yeast requires the least amount of $MgCl_2$ to oligomerize arrays (figure 2.6) and also have the shortest nucleosome repeat length (~165 bp) and least amount of H1 per nucleosome (~.03) (Freidkin and Katcoff, 2001) measured *in vivo* (figure 2.8). Among the species tested, chicken require the most $MgCl_2$ (4.5mM) to

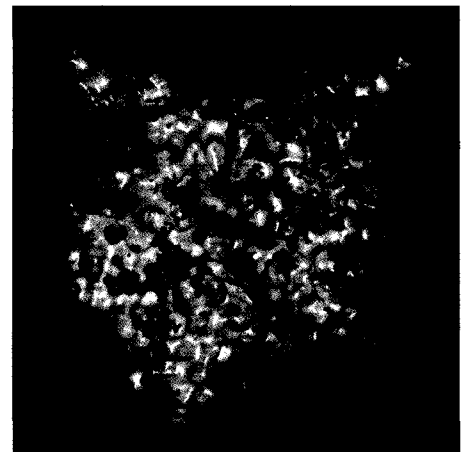
oligomerize arrays (figure 2.6) and also contains the longest NRL (~ 212) and the most H1 per nucleosome 1.3 *in vivo* (figure 2.8) (Woodcock et al., 2006).

These relationships may be an alternative explanation to the differences I have demonstrated in nucleosomal array oligomerization between species. An absence of linker histone could have allowed yeast core histone function to compensate intrinsically for the lack of H1 to stabilize higher order chromatin formation. There may be an unseen relationship between electrostatic masking of DNA charge by H1 and nucleosome repeat length. Although, the positive charge of H1 only accounts for neutralizing the charge of 8 bp of DNA. However, Xu *et al* found that the function of the H1 CTD was not solely DNA charge neutralization (Lu and Hansen, 2004). It is therefore possible that such mechanisms like histone modifications or an elevation of inter-nuclear cations or polyamines which may vary between species.

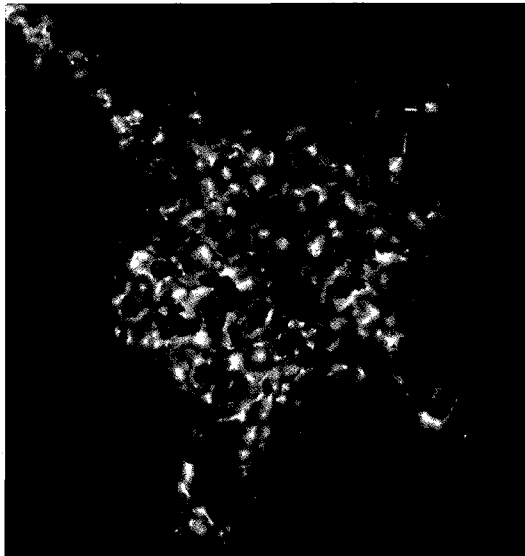
The contribution of the N-terminal histone tails to nucleosomal array oligomerization is independent and additive, in that each histone tail contributes to the oligomerization (Gordon et al., 2005). It has also been noted that the nucleosome surface is important to the oligomerization of nucleosomal arrays (Chodaparambil et al., 2007). The differences in oligomerization between species may also be explained through interactions between the histone NTDs and the amino acids on the surface of the nucleosome. I have calculated the surface electrostatic potential from nucleosomes structures which have been solved by x-ray crystallography (figure 2.9). Visually it is difficult to see a specific pattern which would correlate with the difference in the surfaces with nucleosomal array oligomerization. These generated surface electrostatic images can be influenced by the orientation of the highly dynamic surface side chains in the published structures. However, this illustrates the complexity of the surface and the large amount of surface area of which the histones could bind during chromatin condensation. Between species slight differences in the acid-patch and



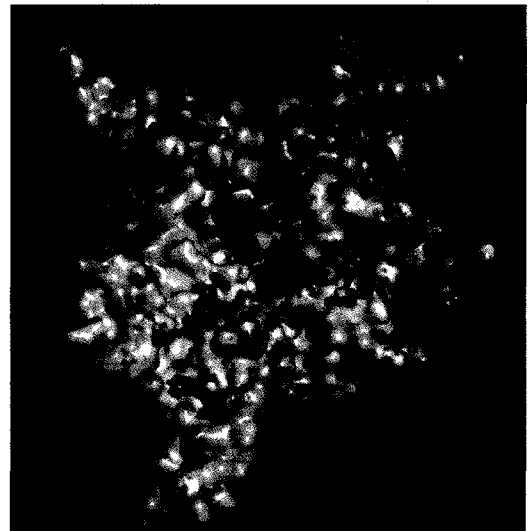
Chicken



Drosophila



Xenopus



Yeast

Figure 2.9 Surface charge potential of nucleosomes. Electrostatic charge potential of nucleosomes calculated with APBS within PYMOL with scale of -10,0,40 (Baker (2001)). PDB entries used chicken (1EQZ), xenopus (1KX5), yeast (1ID3) and *Drosophila* (2NQB) with ions and DNA deleted from the input files

A.

Organism	Genome Size (Mbp)	Estimated # of Genes	Base pairs per gene
Humans	3,300	20-32,000	132000
Mouse	3,000	30,000	100000
<i>Gallus gallus</i>	1,200	10-20,000	60000
<i>Drosophila Melanogaster</i>	120	13,370	10500
<i>Xenopus</i>	1,700	?	
<i>Saccharomyces cerevisiae</i>	10-15	5,770	2100

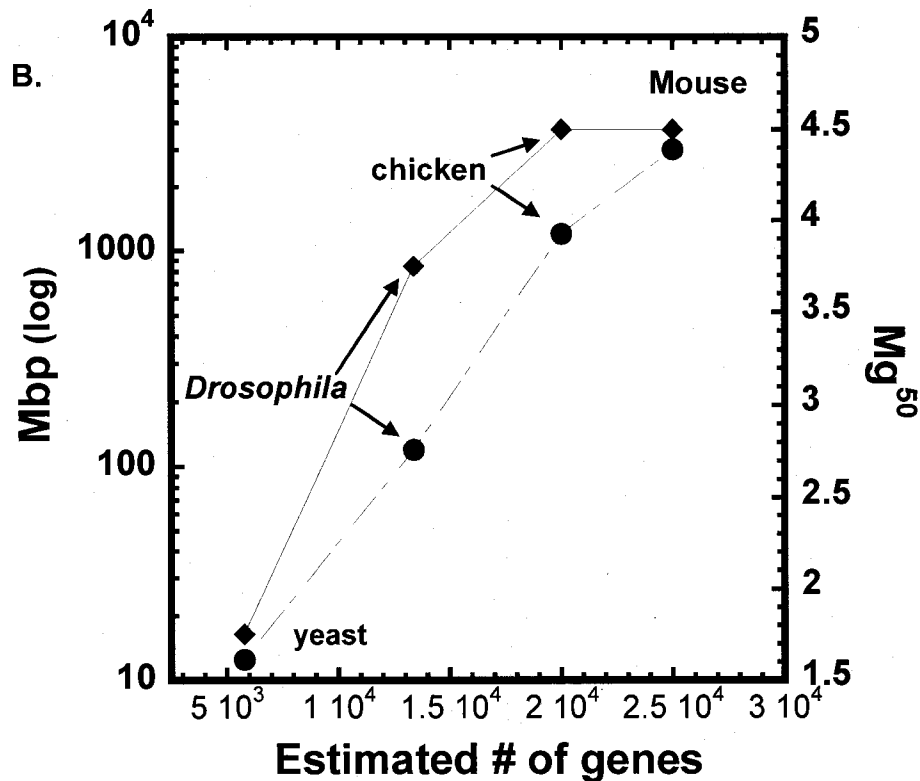


Figure 2.10 Relationship between the size of the genome and estimated number of genes. A. Estimated number of genes and genome size based on data obtained from genome sequencing results to date (www.genomesize.com). B. Plotted is the amount of DNA in mega-base pairs (Mbp) in log scale as a function of the estimated number of genes in each organism (●) and correlation to Mg^{50} values (◆).

other binding surfaces may account for differences between species in nucleosomal array oligomerization.

I found a potentially striking correlation of the Mg^{50} and the level of genome complexity. The size of the genome and the amount of genes increases from single cell to multi-cellular organisms. Here I refer to genome complexity as the number of genes per base pair of DNA. The amount of genes correlates with a range of features at the cell and organism levels, including cell size, cell division rate, and, depending on the species, body size, metabolic rate, developmental rate, organ complexity, geographical distribution, and/or extinction risk (Bennett and Leitch 2005; Gregory 2005). It has long been known that along with an increased genome size higher eukaryotes also contain larger amounts of intergenic spacers and introns (Thomas, 1971). Gene sequencing and genome mapping techniques have been able to determine the size of the genome and estimate the amount of genes in many organisms (see www.genomesize.com for an updated list). Table 2.10.A contains the size of the genome (Mbp), the estimated number of genes and the amount of Mbp per gene (genome complexity) of the species which I examined the nucleosomal array oligomerization. Based on this information I plotted the genome size (Mbp in log scale) as a function of the estimated number of genes and found a correlation to the amount of $MgCl_2$ required to oligomerize nucleosomal arrays reconstituted with histone octamers from multiple species (figure 2.10.B). Although, it is hard to simplify such a complicated correlation, I can not ignore this finding. Histones may have evolved to adapt to the nuclear environment and genome complexity to organize the chromatin in an optimal way to protect yet enable genome accessibility.

An in depth analysis of the differences in the nucleosome surface and the relationship between genome complexity and chromatin structure is necessary to come to a conclusion on why there is a difference between species in histone function.

Further experiments could include analysis of more species nucleosomal array condensation and *in vivo* chromatin conformations and functions.

Chapter 3
Structural and functional investigation of the histone H3
variant CENP-A

Abstract

The centromere is a multi-factorial chromatin epicenter controlled and modulated by multiple trans and cis acting elements. The role of CENP-A in forming and /or maintaining centromeric chromatin is poorly understood. Here I have compared the functions of CENP-A to major type H3 in vitro, using biochemical and biophysical approaches.

3.1 Introduction

The centromere is the locus on the eukaryotic chromosome of kinetochore formation and microtubule attachment for sister chromatid separation during mitosis and meiosis. This region is unique in that its nucleosomes contain the H3 histone variant CENtromere Protein – A (CENP–A) (Earnshaw and Migeon, 1985; Song et al., 2008). CENP–A was first recognized (along with other major type histones) by using antibodies derived from humans with unusual autoimmune disorders (Palmer et al., 1987). Chromatin containing arrays of CENP-A nucleosomes distinguish active centromeres, which participate in the equal separation of sister chromatids during cell division (Regnier et al., 2003; Sullivan et al., 2001; Zinkowski et al., 1991). CENP-A knock out cells exhibit aberrant chromosome segregation suggesting that this histone variant has specific functions at active centromeres (Blower and Karpen, 2001). Incorporation of newly translated CENP-A into chromatin is distinct from that of major type histones in that it occurs independent of DNA replication, during late mitosis/ G1 phase of cell cycle (Jansen et al., 2007). This implies that the presence of CENP – A at an existing centromere could serve as an epigenetic signal for the incorporation of newly synthesized CENP–A deposition into centromeric DNA. It is unknown whether it is the presence of CENP – A and/or other centromere (CEN) proteins binding to CENP – A and/or centromeric DNA which maintain centromeric chromatin. Important questions are whether the presence of CENP – A maintains the active centromere, and whether and how CENP – A influences the structure of centromeric chromatin.

In living cells, histones are deposited onto DNA by histone chaperones as replication-coupled (during S-phase) or replication-independent (any time) (De Koning et al., 2007; Eitoku et al., 2008). CENP-A is deposited into centromeric DNA as replication-independent during late mitosis and early G1 phase (Jansen et al., 2007).

However, it is unclear how CENP-A/H4 histone complexes are deposited onto the newly replicated DNA. Tagged CENP-A^{CID}/H4 has been purified along with a member of the CAF-1 complex (RbAp48-48-p55-Mis16) in *Drosophila* S2 cultured cells (Furuyama et al., 2006). RbAp48 is prevalent in *Drosophila* cells (~ 220,000/ cell) and has been associated with HDACs, HATs (CBP/p300) and the CAF-1 family chromatin remodelers. However, the RbAp48 ortholog, p55, has not been purified along with CENP-A in humans. This suggests that CENP-A could bind to more than one type of chaperone.

147 bp of double stranded DNA wraps around each protein octamer in 1.65 superhelical turns to form a canonical nucleosome core particle (NCP), the fundamental repeating unit of chromatin (Luger et al., 1997). The histone octamer contains two copies of each of the histone proteins H2A, H2B, H3 and H4. The histone C – terminal structured domain is involved in protein – protein and protein – DNA interactions (Luger et al., 1997). The histone N-terminal “tail” domains (NTDs) extend outside of the nucleosome core and are required for the formation of chromatin higher order structures (Carruthers and Hansen, 2000; Fletcher and Hansen, 1995; Garcia-Ramirez et al., 1992; Gordon et al., 2005; Hansen, 2002; Luger and Hansen, 2005).

Nucleosomes repetitively spaced by variable length linker DNA are referred to as nucleosomal arrays (Van Holde, 1989; Wolffe, 1998). These have been used to study the intrinsic and dynamic properties of the chromatin fiber. To package DNA in the nucleus, nucleosomes make “*trans*” inter – nucleosomal array and “*cis*” intra – nucleosomal array fiber-fiber interactions which are responsible for the formation of condensed chromatin (Van Holde, 1989; Wolffe, 1998). Nucleosomal arrays, along with non – histone proteins, are referred to as chromatin fibers. Chromatin fibers are

fully condensed during mitosis and meiosis in the form of chromosomes (Daban, 2003).

Yoda et al. have shown *in vitro* that human CENP – A forms mono-nucleosomes with similar ability to reconstitute chromatin as those containing major type H3 (Yoda et al., 2000). In fruit flies and yeast however, there is evidence that centromeric nucleosomes are non-canonical and contain a non-canonical combination of proteins and DNA that are unlike major type H3 containing nucleosomes. Since these discoveries, there has been a great deal of uncertainty regarding the composition of the centromeric nucleosome from various model organisms (Carroll and Straight, 2007).

Drosophila centromeres contain the H3 variant CenH3 In *Drosophila*. The CENP-A^{CID} NTD is 125 amino acids longer than the 37 amino acid *Drosophila* major type (MT) H3 NTD. Dalal et al. arrested *Drosophila* cells in early mitosis, cross-linked and purified the *Drosophila* CENP-A^{CID} containing nucleosomes by immuno-precipitation (Dalal et al., 2007). Some of these nucleosomes contained one copy of H2A, H2B, H4 and CENP-A^{CID} and protected only 120 bp of DNA. It has been proposed that this “half nucleosome” (‘hemisome’) contributes to the recognition of centromeric chromatin by forming a non-canonical CENP-A^{CID} containing nucleosome (Dalal et al., 2007).

Budding yeast are thought to contain “point” centromeres with a single nucleosome containing the yeast H3 variant, Cse4 (CENP-A^{Cse4}) (Stoler et al., 1995). Recently, the non-histone protein Scm3 has been shown to replace H2A/H2B dimers in CENP-A^{Cse4} nucleosomes at the yeast centromere. It appears that Scm3 monomers associate with one (CENP-A^{Cse4}-H4)₂ tetramer, forming a hexamer-type nucleosome on centromeric DNA. Interestingly, nucleosomes at the yeast centromere package 250 bp at the point centromere (Mizuguchi et al., 2007), much more than the yeast MT nucleosomes which protects ~ 147 bp (White et al., 2001). Mizuguchi et al. have shown that the

binding of Scm3 is exclusive to (CENP-A^{Cse4} - H4)₂ tetramers indicating that Scm3 might also serve to assemble and maintain CENP-A^{Cse4} - H4 at the centromeres.

CENP-As are quite divergent among species, suggesting that the evolution of the highly divergent centromeres could have been in parallel. The aforementioned studies have discovered novel nucleosome structures but do not rule out the existence of nucleosomes containing an octamer of H2A, H2B, CENP - A and H4.

Human CENP-A and MT H3 have 60% sequence homology within the histone fold domain. These similarities in the core domain allow CENP-A to form folded (CENP-A/H4)₂ hetero-tetramers. However, CENP-A is unable to form octamers consisting of H2A, H2B, CENP-A and H4 in 2 M NaCl as do MT (H2A, H2B, H3, H4)₂ histones (Black et al., 2004). Further work showed that CENP - A reconstituted nucleosomes have less solvent accessibility within the histone fold region of the CENP-A/H4 tetramer compared to nucleosomes containing MT H3 (Black et al., 2007). The areas most affected were the α 2 and α 3 helices of H4, which are thought to make direct contact with CENP-A (Black et al., 2007; Black et al., 2004) (figure 3.1). These results suggest that the incorporation of CENP-A results in unique structural features within the nucleosome (Black et al., 2004) This difference in structure could contribute to the distinction of CENP - A/ H4 from MT H3/H4 histone complexes *in vivo*.

Nucleosome core particles are soluble over a wide range of NaCl concentrations and undergo conformational changes between 0 - 700 mM NaCl (Ausio et al., 1984b; McGhee et al., 1980; Park et al., 2004; Wilhelm and Wilhelm, 1980; Yager and van Holde, 1984). Above 750 mM NaCl histones begins to disassociate from the DNA (Yager et al., 1989; Yager and van Holde, 1984). I have reconstituted octameric nucleosomes containing (H2A, H2B, CENP - A, H4)₂ and (H2A, H2B, H3, H4)₂ with 147 bp DNA to study the hydrodynamic properties using sedimentation velocity in increasing ionic strength.

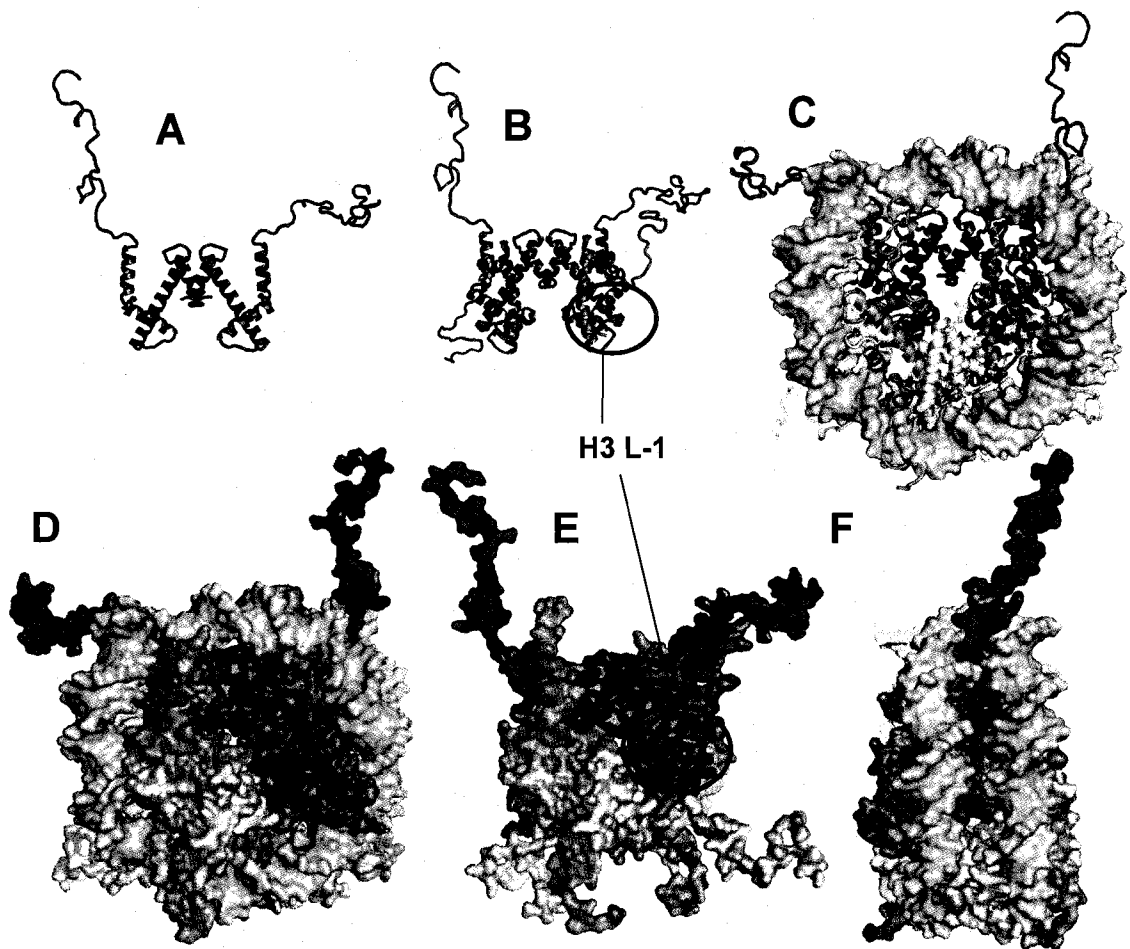


Figure 3.1 secondary and tertiary structure comparison between Cenp-A and major type (MT) H3. X-ray crystal structure of MT *X. laevis* nucleosome core particle (*reference*) with H2A (yellow), H2B (red), H4 (green), H3 (blue), Cenp-A residues that are different from H3 (pink), 147 bp DNA (grey) all structures are adapted from pdb entry 1KX5. CENP-A residues (pink) A. ribbon representation in the H3-H3 interface. B. CENP-A/H4 tetramer C. CENP-A nucleosome with 147 bp DNA (grey) D-F surface representation showing solvent exposed residues. L-1 loop highlighted in red circle.

Nucleosomal arrays purified from endogenous sources have been studied for the past three decades (Hansen, 2002; Woodcock, 2006). At low salt, arrays exist in a 'beads on a string' conformation. As the divalent cation concentration is increased, nucleosomal arrays transition to a folded conformation (30 nm fiber, based on the measured diameter of the compact fiber) (Ausio et al., 1984a; Bednar et al., 1995; Felsenfeld and McGhee, 1986; Luger and Hansen, 2005; Thoma et al., 1979; Woodcock et al., 1984; Woodcock and Horowitz, 1998). By further increasing the salt concentration, nucleosomal arrays form large oligomeric structures thought to mimic long range fiber – fiber interactions (Gordon et al., 2005; Hansen, 2002; Luger and Hansen, 2005; Schwarz and Hansen, 1994). These chromatin condensation transitions are mediated by the N-terminal tails (Carruthers and Hansen, 2000; Fletcher and Hansen, 1995; Garcia-Ramirez et al., 1992; Gordon et al., 2005; Hansen, 2002; Luger and Hansen, 2005). Using defined DNA templates with tandemly repeated positioning sequences and recombinant proteins (Dyer et al., 2004; Gordon et al., 2005; Lowary and Widom, 1998; Simpson et al., 1985), researchers have been able to reconstitute highly homogenous nucleosomal array model systems to study chromatin dynamics.

In this study I compared the properties of CENP-A to major type H3 in the context of its complex with H4, and studied its interaction with the histone chaperone Nucleosome Assembly Protein-1 (Nap1). I analyzed the hydrodynamic properties of CENP-A containing nucleosomes to characterize the role of CENP-A in the nucleosome structure and stability. Finally, reconstituted nucleosomal arrays were analyzed for their ability to undergo Mg^{2+} -dependent folding and oligomerization using analytical ultracentrifugation and differential centrifugation, respectively. Together, my results indicate that while CENP-A is a unique H3 histone variant with a nearly wholesale alteration of primary amino acid sequence in the N-terminal tail. CENP-A

has an altered interactions with a histone chaperone and is able to reconstitute nucleosomes and nucleosomal arrays with properties similar to canonical nucleosomes

3.2 Methods and Materials

3.2.1 Protein Expression and Purification – Major type histone H2A, H2B, H3 and H4 were expressed and purified as described (Dyer et al., 2004). Histone (H2A/H2B) dimers and (H3/H4) tetramers were renatured to complexes by combining equi-molar amounts in unfolding buffer (6M Gu-HCl, 20 mM Tris-HCl pH 7.5, 5 mM DTT) followed by extensive dialysis against refolding buffer (2M NaCl, 10 mM Tris-HCl pH 7.5, 1 mM EDTA). Histone complexes were then purified using size-exclusion chromatography on a Superdex S-200 column (GE Healthcare) (Dyer et al., 2004).

CENP-A was co-expressed with H4 from a bi-cistronic expression vector as described in (Black et al., 2004). The soluble CENP-A/H4 tetramer was purified by hydroxyapatite and SP-sepharose (cation exchange) chromatography (GE healthcare).

Recombinant His-yNap-1 (305p and wt) was purified by nickel affinity column. The His tag was cleaved with thrombin, followed with purification by ion-exchange as described in (McBryant et al., 2003).

3.2.2 DNA purification – The 147 bp palindromic α -sat DNA was purified as previously described (Dyer et al., 2004). The 208-12 5S rDNA used to prepare nucleosomal arrays was purified as previously described (Georgel et al., 1993; Schwarz and Hansen, 1994).

3.2.3 Binding affinity measurements. Fluorescence titrations were used to determine the binding affinity of 0.2 to 0.4 nM Alexa-546 NAP-1 to CENP-A in F buffer (300 mM NaCl, 0.5 mM EDTA, 1mM DTT and 20 mM Tris-HCL pH 7.5) using an AVIV

ATF105 spectrofluorometer. Labeled Nap-1 was added to both the sample and the reference cuvette, with non-labeled CENP-A/H4 histone complex added to the sample cuvette and buffer added to the reference. The ratio of the fluorescence signal from the sample cuvette to the reference cuvette was normalized to the maximum amount of signal change (12 % total change in signal) and was plotted as a function of protein concentration or final concentration. The K_d was determined by fitting equation 1 to the fluorescence change using Kaleidagraph software. Where *f.c.* equals fluorescent signal change, and $[P_t]$ equals total protein concentration

$$f.c. = \frac{f.c._{max} * [P_t]}{[P_t] * K_d} \quad \text{eq. 1}$$

3.2.4 Stoichiometry. Stoichiometries were determined by fluorescence titrations as above with the labeled protein concentration increased to >10-fold higher than the K_d . Singly labeled yNAP-1 (Alexa-546 fluorescent dye (Molecular Dynamics)) was added to reference and sample cuvettes with an initial concentration of 150 nM in 3mL clear cuvette. The (CENP-A/H4)₂ histone complex was titrated into both sample and reference cuvettes and incubated with stirring for 3 min. Twelve fluorescence emission measurements were taken for each titrated concentration at excitation and emission wavelengths of 553nm and 574nm respectively. Binding measurements were plotted as a function of protein titrated (CENP-A/H4)₂ to labeled protein (Nap-1) fluorescence change. Under these conditions, the protein ratio at which the fluorescence change plateaued indicates stoichiometry.

3.2.5 Salt Dialysis Reconstitution Nucleosomes were reconstituted as previously described (Dyer et al., 2004). Briefly, equal molar ratios of H2A - H2B dimers and H3 or CENP-A/H4 tetramers were mixed with 147 bp α -Sat DNA in TE buffer (10mM Tris-HCl, 0.25 mM EDTA, pH 7.5) containing 2.0 M KCl₂ and dialyzed using salt gradient dialysis into TE buffer (0 M KCl₂). Nucleosomes were heat shifted at 37° for 1

hour to uniformly position the octamer on the 147 bp DNA template. The nucleosomes were then purified from excess DNA and unbound protein using a Prep Cell Model 491 purification system (Bio-Rad) and analyzed by native – PAGE in 0.2 % TBE as described (Dyer et al., 2004).

Nucleosomal arrays were reconstituted as described (Hansen et al., 1991). Briefly, I reconstituted arrays by mixing equal molar ratios of histone H2A-H2B dimers and H3 or CENP-A/H4 tetramers with the 208-12 DNA template in TE buffer (10 mM Tris-HCl, .25 mM EDTA, pH 7.8) containing 2.0 M NaCl₂, followed by salt gradient dialysis to low salt TEN buffer (2.5 mM NaCl₂-TE) (Hansen et al., 1991).

3.2.6 EcoR1 template saturation analysis—Assays were performed as described (Tse and Hansen, 1997). Briefly, 1 µg of reconstituted nucleosomal arrays was digested with 10⁷ units of EcoR1 restriction enzyme for 2 hours at 21⁰C. Digested arrays were separated on a 1% agarose gel, stained with Ethidium Bromide and resolved using a Gel Logic 200 imager. The gel image was used for densitometry analysis of bands to determine the percentage of naked DNA using Scion software and calculated with the equation below.

$$\% \text{ Free DNA} = \frac{\text{Free DNA}}{((\text{Free DNA}) + (\text{NCP} \bullet 2.5))} \quad \text{eq. 2}$$

3.2.7 Nucleosome Crystallization –Nucleosomes with H3^{CATD} and CENP-A were crystallized by using salting in vapor diffusion at nucleosome concentrations ranging from 8-10 mg/ml with salt concentrations of either 34 mM KCl, 40 mM MnCl₂, 5 mM K-cacodylate or 33.75 mM KCl, 37.5 mM MnCl₂, 10 mM K-cacodylate. The crystals were soaked in 24% 2-methyl, 2,4-pentanediol (MPD) containing 5% trehalose (Luger et al., 1997). X-ray data were collected on a Rigaku RU-H3R rotating anode generator (1.54 Å Cu-Kα radiation) with osmic confocal multilayer optics system, R-axis IV⁺⁺ image plate detector and an X-stream cryo-cooling system.

3.2.8 Analytical Ultracentrifugation – Sedimentation velocity studies were carried out using a Beckman XL-A analytical ultracentrifuge using the absorbance optics. Samples were mixed to a final A_{260} of 0.6 - 0.8 and equilibrated to 20° C. for one hour prior to sedimentation. Nucleosomes were sedimented at 40-50,000 rpm and nucleosomal arrays were sedimented at 18-25,000 rpm. The radial increment used was 0.001 cm. Data was analyzed using the van Holde and Weischet method (Demeler and van Holde, 2004) to obtain the integral distribution of sedimentation coefficients ($G(s)$) using UltraScan v9.4. \bar{V} and ρ were calculated using Ultrascan. Second Moment analysis to determine the average sedimentation coefficient of nucleosome core particles was implemented within Ultrascan.

3.2.9 Folding of nucleosomal arrays- Nucleosomal arrays were diluted with TEN buffer to a final concentration of 1.8 mM $MgCl_2$ and a final A_{260} of 0.6 – 0.8. Sedimentation velocity experiments were carried out at 18,000 RPM for two hours with radial increments of 0.001cm. Data was analyzed using Van holde and Weischet method (Demeler and van Holde, 2004).

3.2.10 Atomic force microscopy- Reconstituted nucleosomal arrays were diluted to 60 ng/ml and applied to glutaraldehyde-APTES treated mica slides as previously described (Bash et al., 2003). Samples were imaged in air on an Asylum MFP-3D atomic force microscope in tapping mode with an AC240TS or AC160TS cantilever (Olympus). Images were analyzed using the MFP-3D Igor Pro software.

3.2.11 Oligomerization of nucleosomal arrays- Differential centrifugation was used as previously described (Gordon et al., 2005; Lu et al., 2006). Briefly, nucleosome arrays were diluted to an $A_{260} = 1.2$ with TEN buffer. Arrays were mixed with $MgCl_2$ -TEN buffer, incubated for five min. at room temperature then centrifuged in a benchtop microfuge at 13,000 RPM (~16,000 x g) for 5 min. The A_{260} of the supernatant was then measured in a Beckman DU 800 Spectrophotometer. Data is expressed as a

percentage of the total sample that remained in the supernatant as a function of $[\text{MgCl}_2]$. Results shown are the average of 3 independent assays.

3.3 Results

3.3.1 CENP-A/H4 interaction with nucleosome assembly protein – 1 (Nap-1)

The Nap1 family of histone chaperones bind H2A/H2B dimers, H3/H4 tetramers and histone variant complexes (Park and Luger, 2006). I have characterized the binding of the CENP-A/H4-Nap1 complex by native gel electrophoresis mobility shift assays (EMSA), gel filtration and sedimentation velocity and found a unique binding stoichiometry of the CENP-A/H4 histone complex to Nap1. Through these assays, I have been able to differentiate CENP-A from H3 containing histone complexes.

3.3.1.1 Histone complexes retain their tertiary structures at low salt

In order to compare the binding characteristics of the CENP-A/H4-Nap1 complex to other MT histone complexes, I purified renatured H2A/H2B dimers and H3/H4 tetramers by gel filtration chromatography. I also renatured a mutant of H3 in which histidine 113 has been changed to alanine (H3-H113A), together with wild type H4. This mutation disrupts the H3-H3 interface of the H3/H4 hetero-tetramer at the four-helix bundle. To confirm that H3-H113A forms a dimer with H4, but fails to form a $(\text{H3-H4})_2$ tetramer, I characterized the renatured histone complexes by gel filtration chromatography in 2 M NaCl. Elution volumes of the histone complexes were 88 mls for the H3-H113A/H4 complex, 90 mls for the H2A/H2B dimer and 80 mls for the H3/H4 tetramer (figure 3.2). The elution volume of the H3-H113A/H4 complex in 2 M NaCl was similar to the

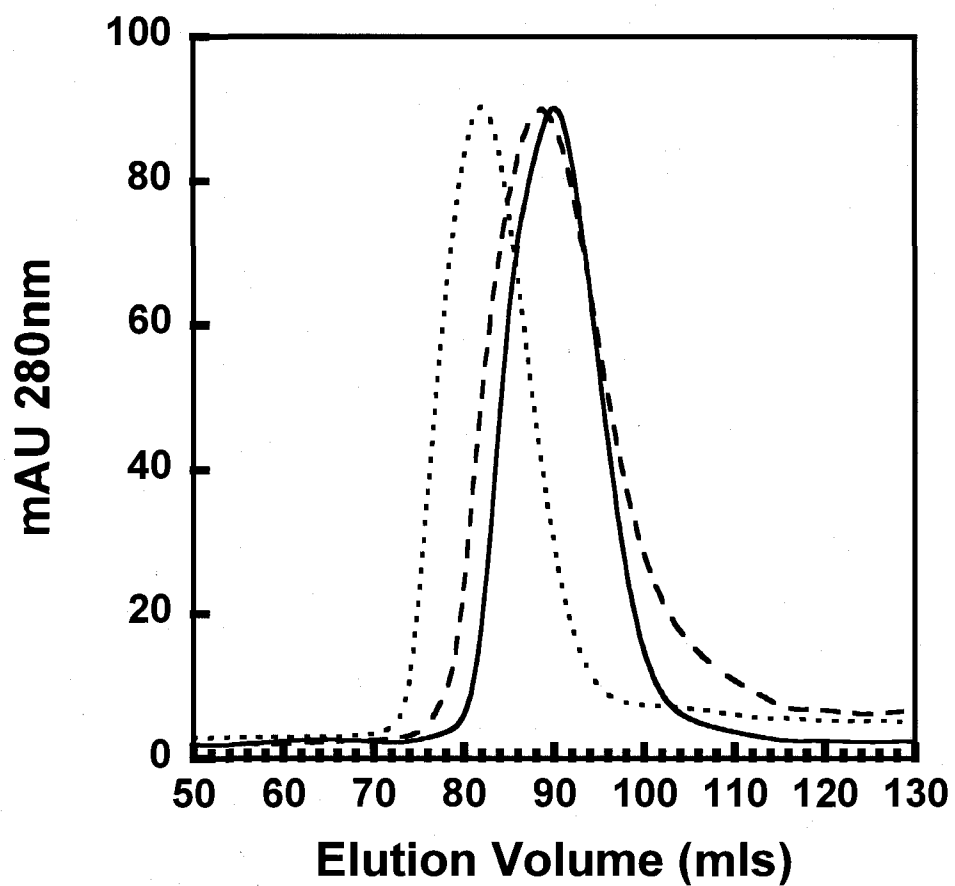


Figure 3.2 Gel filtration chromatographic analysis of histone complexes. Elution of H3/H4 tetramer (...), H3 (H113A)/H4 dimer (---), and H2A/H2B dimer (—). Histone complexes were purified using GE AKTA system over 130 mls of S200 superdex prepacked resin in a 16/60 column. UV absorbance was measured at 280 nm.

H2A/H2B dimer and indicates similar stokes radii, assuming the complexes are globular. The histone composition of each peak was confirmed by SDS-PAGE (data not shown). After dialyzing the histone complexes into buffer containing 100 mM NaCl, 10 mM Tris-Cl pH 7.5 and 1mM TCEP, I performed sedimentation velocity to confirm their oligomerization state under more physiological salt conditions. The sedimentation coefficient distributions were nearly identical for CENP-A/H4 and H3/H4 tetramers, with a midpoint of ~ 2.8 S (figure 3.3). The H2A/H2B dimer midpoint was ~ 1.9 S and the H3-H113A/H4 complex had a similar midpoint of ~2S (figure 3.3). These results indicate the histone complexes did not disassociate or aggregate at low salt and confirmed that H3-H113A forms a dimer when renatured with H4. About 25-30% of the histone complexes had a distinct tail lower S value in low salt (figure 3.3 0-30% of boundary fraction). This may be an indication that this fraction of the samples has disassociated into monomers and dimers, or exists in alternative conformations at low salt (Demeler et al., 1997). This type of microheterogeneity could also be caused by hydrodynamic non-ideality due to high protein concentrations and high surface-charge density.

3.3.1.2 CENP-A/H4-Nap1 complex has a different gel mobility than the H3/H4-Nap1 complex

Nap1 binding to major type H3/H4 tetramer and H2A/H2B dimer histone complexes have been previously described (McBryant et al., 2003). I was interested in characterizing the CENP-A/H4-Nap1 complex. For these studies I used a rationally designed mutant where amino acid 305 was mutated to a proline to prohibit Nap1 oligomerization (McBryant and Peersen, 2004; Park and Luger, 2006). I began by incubating varying amounts of Nap1 305P with a fixed amount of histone complex (H2A/H2B, CENP-A/H4, H3-H113A/H4 and H3/H4). The resulting complexes were

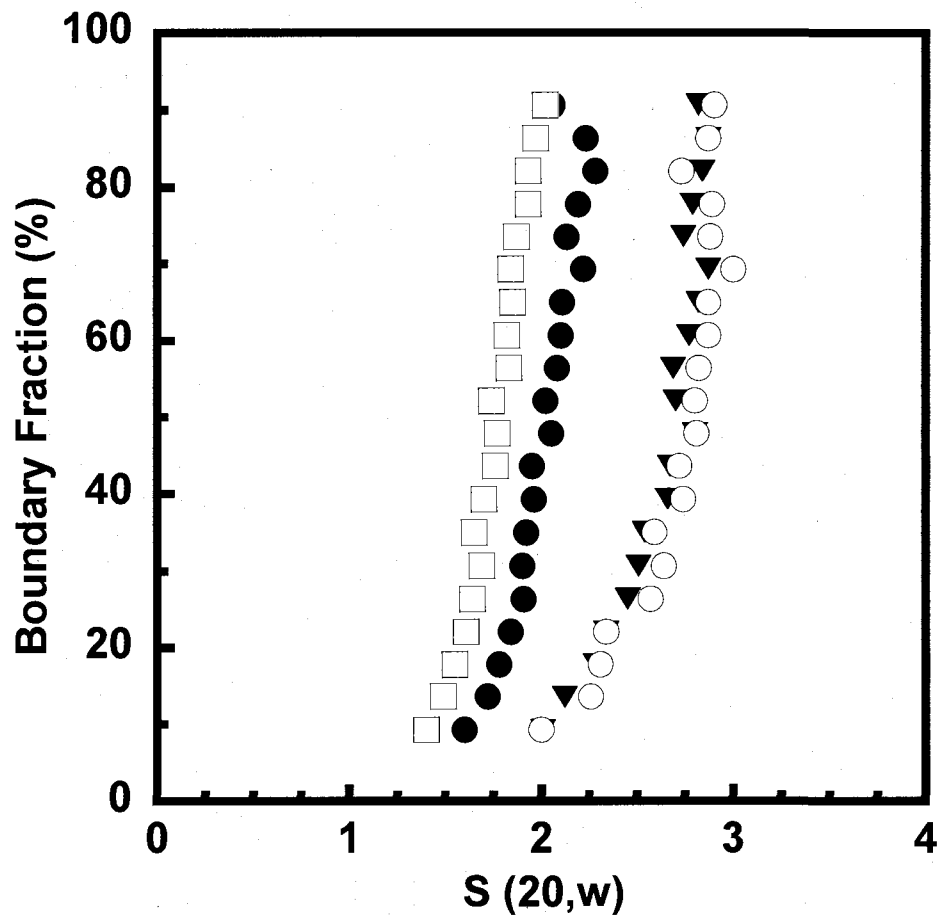


Figure 3.3 Analytical ultracentrifugation of histone complexes. Sedimentation coefficient distribution of histone complexes (H3/H4)₂ tetramer (▲), H2A/H2B dimer (●), H3 (H113A)/H4 (□) and (Cenp-A/H4)₂ tetramer (○) in 100 mM NaCl, 10 mM Tris-Cl pH 7.5, 1.0 mM TCEP. Samples were detected at 229 nm and sedimented at 50,000 rpm. The integral distribution of sedimentation coefficients (S) over the entire boundary (G(s)) is shown, corrected for water at 20°C ($S_{20,w}$).

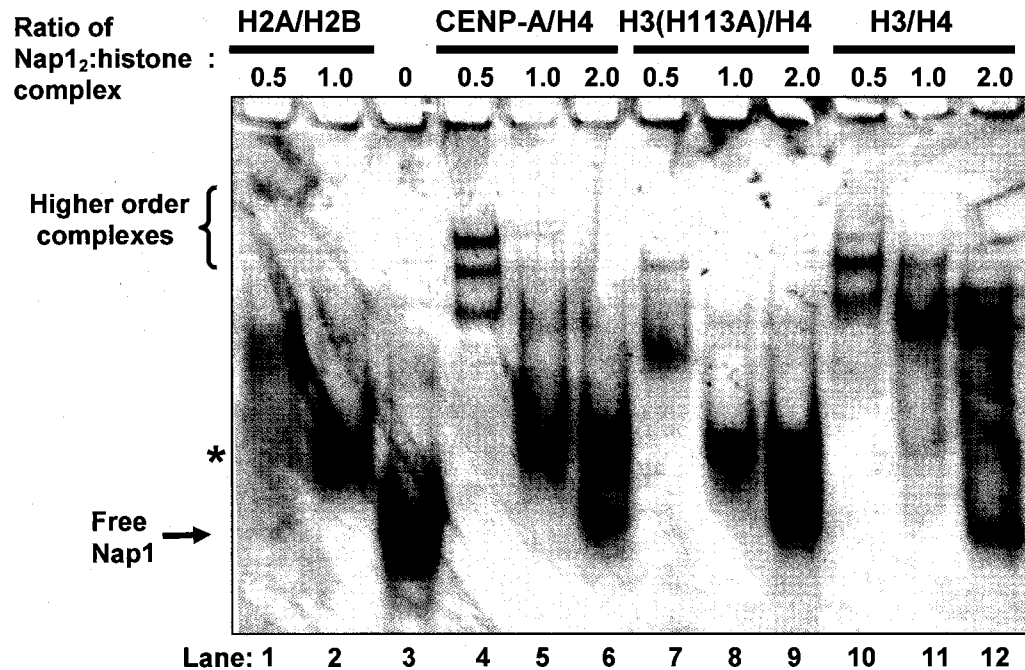


Figure 3.4 Nap:Histone EMSA. Nap-1 was titrated to histone complexes (H2A/H2B lanes 1 and 2, CENP-A/H4 lanes 4-5, H3-H113A/H4 lanes 7-9 and H3/H4 lanes 10-12) at molar ratios of Nap dimer to histone complex (r-value). (*) Indicates mobility of complex which was purified for further analysis (lanes 2, 5 and 8). Also noted are higher order complexes formed with a molar excess of histone to Nap was added. Shown are samples electrophoresed on a 5% Native-PAGE stained with coomassie blue.

resolved on a 5% native-PAGE (figure 3.4). I observed a decreased mobility of the protein bands as the ratio of histone complexes to Nap1 increased (figure 3.4). At a molar ratio of one histone complex (dimer or tetramer) per one Nap1 dimer, I observed a relatively homogenous band by native-PAGE (figure 3.4, (*) lanes 2, 5, 8 and 11). At molar ratios of 1:1 CENP-A/H4:Nap, the complex (figure 3.4 lane 5) had a similar mobility as the H2A/H2B-Nap complex (figure 3.4 lane 2) and as the H3-H113/H4:Nap1 complex (lane 8). The H3/H4 tetramer-Nap complex at a molar ratio of 1:1 produced a larger complex with a significantly lower mobility (lane 11). When an excess of Nap1 was added, I observed free Nap1 with a mobility similar to the mobility of Nap1 alone (figure 3.4, lane 4, 6, 9 and 12), indicating unbound Nap1. I did not observe free histone complexes, as histones do not run into the gel because of their highly basic charge. When I combined molar ratios of excess histone to Nap1, I observed large complexes which I attribute to non-specific binding at concentrations higher than the K_d (figure 3.4). Together these results suggest that Nap1 binds differently to CENP-A tetramers compared to MT H3/H4 tetramers.

3.3.1.3 Hydrodynamic analysis of purified histone:Nap1 complexes

To further analyze histone-Nap1 complexes, I analyzed complexes with molar ratios of 1 histone complex:1 Nap1 dimer by gel filtration chromatography. Peak fractions were determined by SDS and Native PAGE (data not shown). Based on their migration of SDS-PAGE, the pure homogeneous histone-Nap1 peaks were collected and concentrated. The resulting homogeneous preparations were subject to sedimentation velocity analysis. H2A/H2B and H3/H4:Nap1 complexes sedimented as a 5.5 S and 12-14 S species, respectively (figure 3.5). The H3-H113A/H4:Nap1 complex had a very similar sedimentation distribution as the H2A/H2B:Nap1 complex,

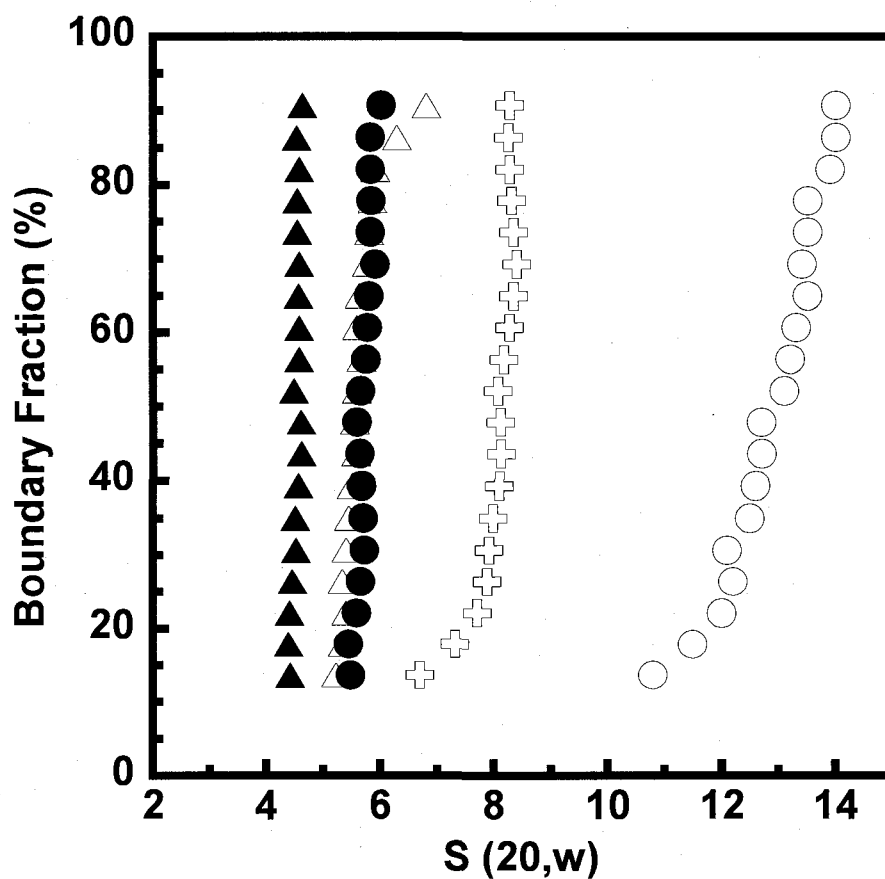


Figure 3.5 Analytical ultracentrifugation of Nap-1-histone complexes. Sedimentation coefficient distribution of Nap1 and histone complexes at molar ratios of (1:2) Nap1 305P dimer alone (▲), H2A/H2B:Nap1 (●), H3 (H113A)/H4:Nap1 (Δ), CENP-A/H4:Nap1 (⊕), and H3/H4:Nap1 (○) in 100 mM NaCl, 10 mM Tris-Cl pH 7.5, 1.0 mM TCEP. Scans were collected at 229 nm and sedimented at 50,000 rpm. The integral distribution of sedimentation coefficients (S) over the entire boundary ($G(s)$) is shown, corrected for water at 20°C ($S_{20,w}$).

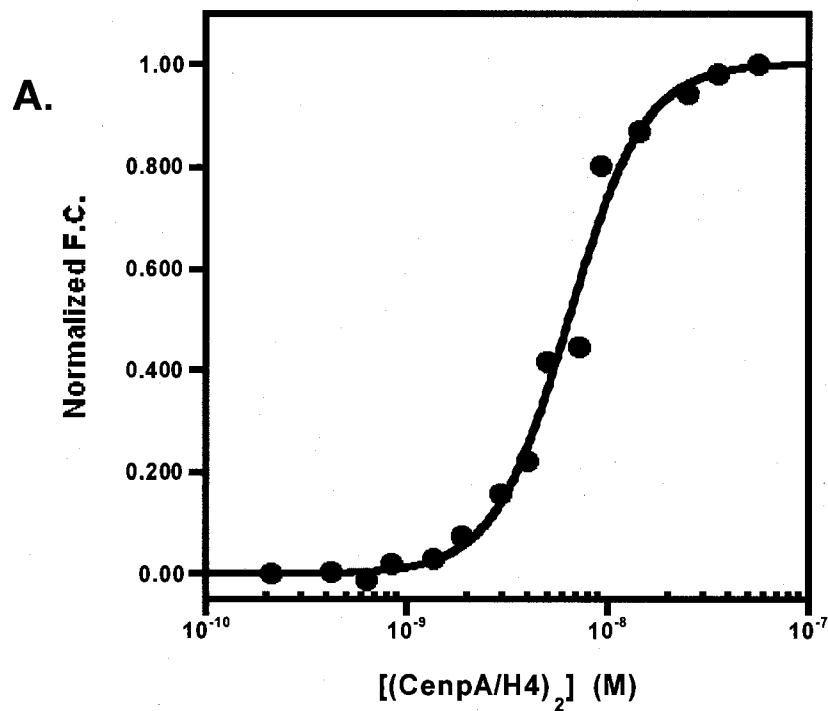
further confirming that the two complexes bind Nap1 in a similar stoichiometry. The CENP-A/H4:Nap1 complex, however, had a unique sedimentation distribution with a midpoint of 8 S (figure 3.5), even though the complexes H2A/H2B-Nap1, H3-H113A/H4-Nap1 and CENP-A/H4-Nap1) had the same gel mobility. These results show that the hydrodynamic shapes are different

between CENP-A-H4 and Nap1 but do not resolve the question of stoichiometries. The transition from 2S to 8S with the Nap-1 dimer is combined the 3S CENP-A/H4 tetramer initially suggests that two CENP-A tetramers bind one Nap1 dimer or two Nap1 dimers bind one CENP-A/H4 tetramer.

3.3.1.4 CENP-A/H4 binds Nap-1 as a dimer

To measure the stoichiometry and affinity of CENP-A/H4 to Nap1 I used fluorescently labeled Nap1. Three of the four cysteines were mutated to alanine to prevent the formation of multiple and heterogeneously labeled species. I then titrated CENP-A/H4 histone complexes into 3 nM of labeled Nap1. I observed a change in fluorescence emission signal, an indication of binding. When the fluorescence change (Eq.1 methods and materials) of Nap1 as a function of the histone concentration in log scale was plotted (figure 3.6.A), I was able to calculate the K_d and Hill coefficients to be 6.4 nM and 2.27, respectively. The affinity of CENP-A/H4 binding to NAP1 is similar to the major type H3/H4 complex of 9 nM (figure 3.6.B).

I hypothesized that the differences observed in EMSA and sedimentation velocity experiments between CENP-A/H4-Nap1 and H3/H4-Nap1 complexes are the result of a difference in stoichiometry between the CENP-A/H4 complex and Nap1. To test this hypothesis, I measured the stoichiometry by titrating CENP-A/H4 onto labeled Nap1 at 150 nM (more than 10 times greater than the K_d). The stoichiometry is equal to the



<u>Protein Titrated</u>	<u>[nM] K_d^{app}</u>	<u>Hill coefficient</u>	<u>Labeled protein</u>	<u>Ionic Strength (M)</u>	<u>pH</u>
H2A/H2B	7.8±0.4	<i>n.a.</i>	yNAP1(C414)	0.35	7.5
H3/H4	10.0±0.6	1.4±0.1	yNAP1(C414)	0.35	7.5
H3(H113A)/H4	16±0.7	1.3±0.1	yNAP1(C414)	0.35	7.5
CenpA/H4	6.4±0.4	2.2±0.3	yNAP1(C414)	0.35	7.5

Figure 3.6 Measurement of (CENP-A/H4)₂ binding to yNAP1. A. The representative data of normalized change in Nap-1 fluorescence as a function of [(CENP-A/H4)₂]. (0-5)×10⁻⁷ M (CENP-A/H4)₂ was titrated into buffer containing 4.0×10⁻⁹ M labeled yNap-1, K_d and Hill coefficients were calculated and fit to eq. 1. B. Results of the fit for histone complexes. Experiment courtesy of Greg Downing and Dr. Andy Andrews.

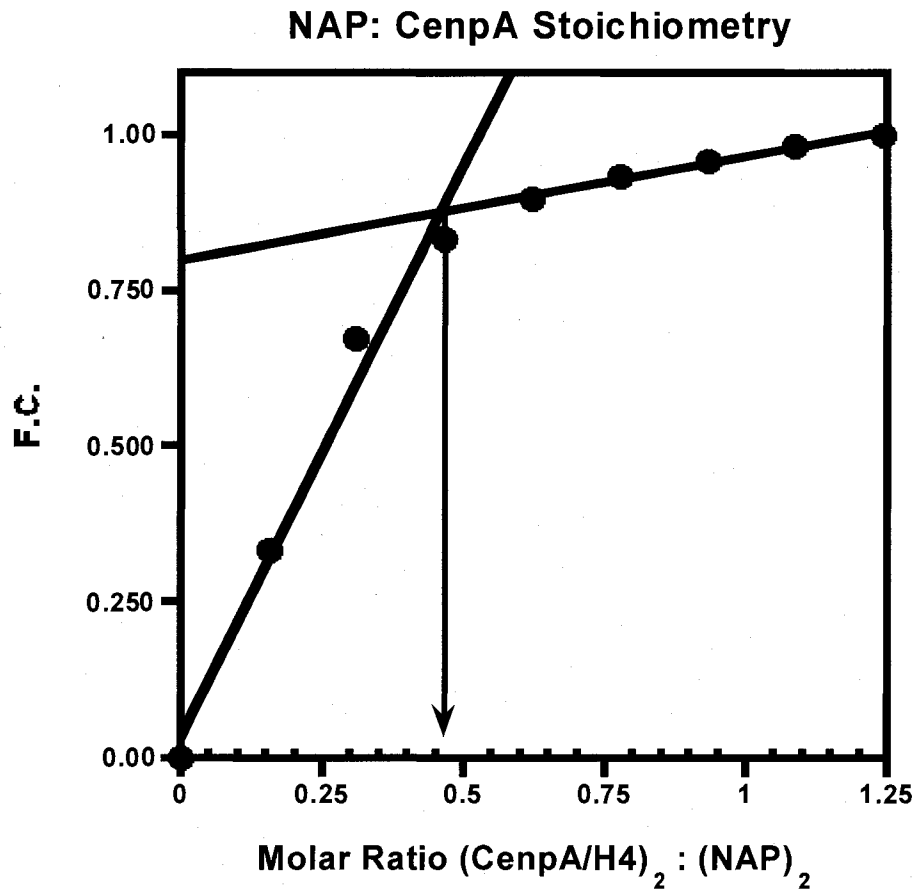


Figure 3.7 CENP-A tetramer: yNap-1 stoichiometry. Representative data of the binding stoichiometry measured by fluorescence change. The molar ratio at which there is no longer fluorescence change is the stoichiometry (arrow). This is measured to be around half a (CENP-A/H4)₂ tetramer (or one CENP-A/H4 dimer) binding each NAP-1 dimer. (experiment courtesy of Greg Downing and Dr. Andy Andrews).

concentration of CENP-A/H4 at which the fluorescence stops changing. This was determined to be 0.5 (CENP-A/H4)₂ tetramers per Nap1 dimer (or one CENP-A/H4 dimer per Nap1 dimer) (figure 3.7). This result is consistent with the gel shift experiments and strongly suggests that Nap1 interacts with a dimer of CENP-A/H4 or two Nap dimers bind to one CENP-A tetramer.

3.3.2 CENP-A mononucleosomes have similar nucleosome stability to MT H3 NCP

In attempt to resolve the recent discrepancies in literature regarding the composition of CENP-A containing nucleosomes, I have compared the properties of CENP-A containing nucleosomes to MT H3 nucleosomes (Camahort et al., 2007; Dalal et al., 2007; Mizuguchi et al., 2007). I reconstituted CENP-A (H2A, H2B, CENP-A, H4)₂ and MT nucleosomes (H2A, H2B, H3, H4)₂ on 147 bp DNA to obtain CENP-A and H3 containing nucleosome core particles (Dyer et al., 2004). Using native-PAGE I observed that reconstituted nucleosomes containing CENP-A and H3 have similar electrophoretic mobility and reposition identically to a central position on the 147 bp DNA upon heat shifting (figure 3.8.A). Purified nucleosomes were subjected to native and denaturing gel electrophoresis to determine the homogeneity and protein composition of the nucleosomes (figure 3.8.B and C). I found that both nucleosomes contained equivalent amounts of histones (H2A, H2B, CENP-A or H3 and H4).

I next applied sedimentation velocity to determine the size and shape of CENP-A nucleosomes, using MT H3 nucleosomes as controls. In 0 mM NaCl buffer, CENP-A and H3 containing nucleosomes had essentially identical sedimentation coefficient distributions with 10.85 (± 0.07) S_{avg} and 10.95 (± 0.21) S_{avg} respectively (figure 3.9.A). The S_{avg} values of CENP-A nucleosomes are the same as those previously obtained

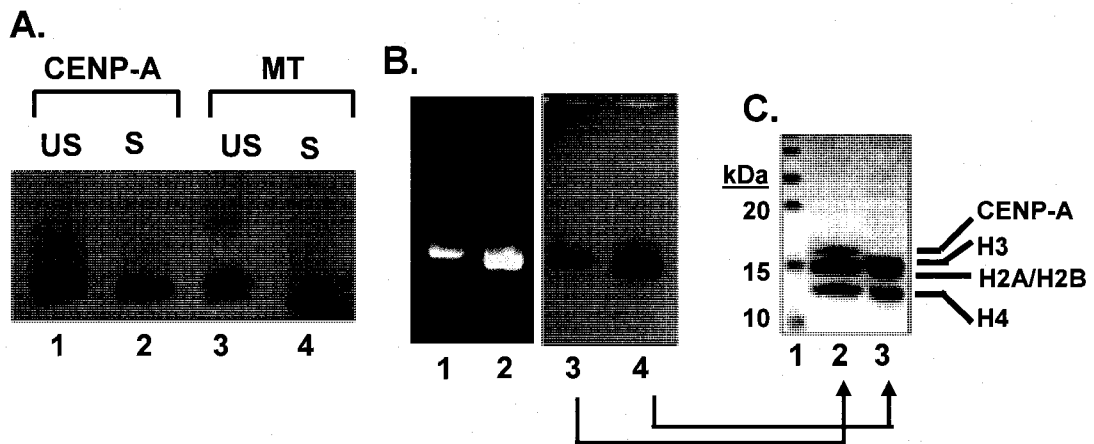


Figure 3.8.A. CENP-A and H3 Containing Nucleosome Reconstitution. Unshifted (US) (lanes 1,3) and shifted (S) (lanes 2,4) nucleosome core particles containing major type (MT) H3 and H3 variant CENP – A reconstituted with 147 bp α -Sat DNA. **B. PrepCell Purified Nucleosomes.** Nucleosome core particles containing major type H3 (lanes 2 and 4) and H3 variant CENP – A (lanes 1 and 3) reconstituted with 147 bp α -Sat DNA. Samples were run on a 5 % native – PAGE in 0.2 % TBE at 150 V for 1 hour and stained with ethidium bromide (left) and Imperial Protein Stain (Pierce) (right). **C. Protein Analysis of purified Nucleosome core particles.** After Prep Cell purification CENP – A (lane 2) and major type H3 (lane 3) containing nucleosomes were run on a 15 % SDS – PAGE at 180 V for 1 hour and stained with commassie blue. Lane 1 Precision plus (Bio-Rad) protein marker.

using endogenously purified nucleosome core particles (Ausio et al., 1984b; McGhee et al., 1980; Wilhelm and Wilhelm, 1980; Yager and van Holde, 1984). One aspect of nucleosome stability has been previously examined by measuring the sedimentation coefficient of the nucleosomes in buffers with increasing ionic strength (Ausio et al., 1984b; McGhee et al., 1980; Wilhelm and Wilhelm, 1980; Yager and van Holde, 1984). Incorporation of histone variants, like H2A.Z (Gautier et al., 2004) and H2A.bbd (Gautier et al., 2004), has been shown to decrease nucleosome stability. I used this approach to compare the average sedimentation coefficient of CENP-A nucleosomes to canonical nucleosomes in buffers containing 0 – 600 mM NaCl. With both nucleosomes, I observed a similar change in the sedimentation coefficient of 11.25 S – 9.25 S in buffer containing 0 – 600 mM NaCl (figure 3.9.B). As salt concentrations increase from 0 – 200 mM NaCl, the nucleosome shape is thought to transition from an oblate to a prolate shape (Czarnota and Ottensmeyer, 1996). From 100 – 200 mM NaCl the nucleosome has the same hydrodynamic shape as expected from the crystal structure (Czarnota and Ottensmeyer, 1996). Using second moment analysis (Demeler et al., 2000), I calculated average S values (S_{avg}) increase from 10.75 to 11.25 in buffer containing 0 mM NaCl - 50 mM NaCl (figure 3.9.B). At salt concentrations between 100 – 300 mM NaCl the ends of the 147 bp DNA begin to unravel from the histone octamer (Ausio et al., 1984b; Park et al., 2004; Yager and van Holde, 1984). From 300 – 600 mM NaCl the frictional coefficient of the nucleosome increases due to the release of the ends of the nucleosomal DNA (Czarnota and Ottensmeyer, 1996). I observed a nearly identical decrease in S – value from 10.75 to 9.75 when the NaCl concentration was increased from 300 – 600 mM NaCl for both nucleosomes. Sedimentation velocity of both CENP-A and MT nucleosomes measured from 0 – 600 mM NaCl showed that the salt based structural transitions are nearly identical (figure 3.9).

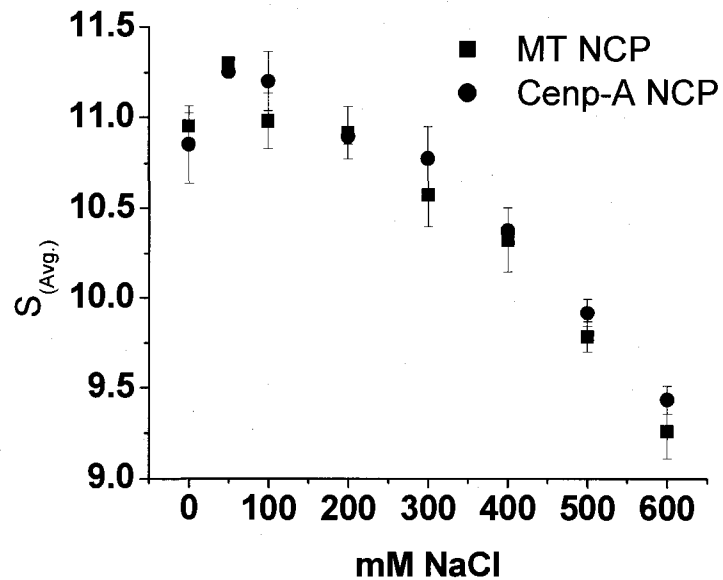


Figure 3.9 Nucleosome Stability. Ionic strength dependence of the sedimentation coefficient of reconstituted CENP – A containing nucleosome core particle (●) compared to reconstituted major type nucleosome core particle (■). The average sedimentation coefficient was measured in buffer containing 0 – 600 mM NaCl, 10 mM Tris-Cl pH 7.5, 1 mM EDTA. Runs were carried out at 30,000 RPM at 20⁰ C. and corrected for buffer viscosity. S_{Avg} values plotted are second moment analyses obtained using Ultra Scan version 9.0.

3.3.3 Reconstitution of fully saturated nucleosomal arrays contain a histone octamer with CENP-A

Because the H3 NTD plays a key role in chromatin condensation and because the N-terminal tail of CENP-A has only 16% homology with the MT H3 NTD, I reconstituted identically saturated nucleosomal arrays by combining an equal molar ratio of histones to DNA repeat. Because histone octamer saturation level can affect chromatin dynamics, I carefully determined the saturation level of these reconstituted arrays by analytical ultracentrifugation, atomic force microscopy, and EcoRI nuclease digestion (Fletcher and Hansen, 1995; Hansen et al., 1998; Schwarz et al., 1996; Tse and Hansen, 1997).

Sedimentation velocity of nucleosomal arrays in TEN buffer is used to determine the homogeneity octamer saturation of the DNA template. Using sedimentation velocity I obtained the integral sedimentation coefficient distribution ($G(s)$) of CENP-A and MT H3 containing nucleosome arrays in low salt TEN buffer (figure 3.10.A). The arrays have nearly identical $G(s)$ distribution. Thirty percent of the arrays have sedimentation coefficients lower than 27 S, indicating that they are slightly sub-saturated (≤ 11 nucleosomes / DNA template). Forty percent of the arrays have sedimentation coefficients ranging from 27 – 30 S, this is equivalent to a fully saturated nucleosomal array. Fully saturated arrays have an average of 12 nucleosomes present on the 208 – 12 DNA template (1 nucleosome per 208 bp repeat) (Hansen and Lohr, 1993).

I also used nuclease digestion to determine the percentage of unoccupied 5S DNA repeats in the samples. Digestion of the reconstituted templates with EcoRI results in a mixture of mono-nucleosomes and naked DNA which can be separated by agarose gel electrophoresis (figure 3.10.B) (Tse and Hansen, 1997). In figure 3.10.B lanes 1 and 2, digested arrays migrate as mononucleosomes (slow migrating band) and free

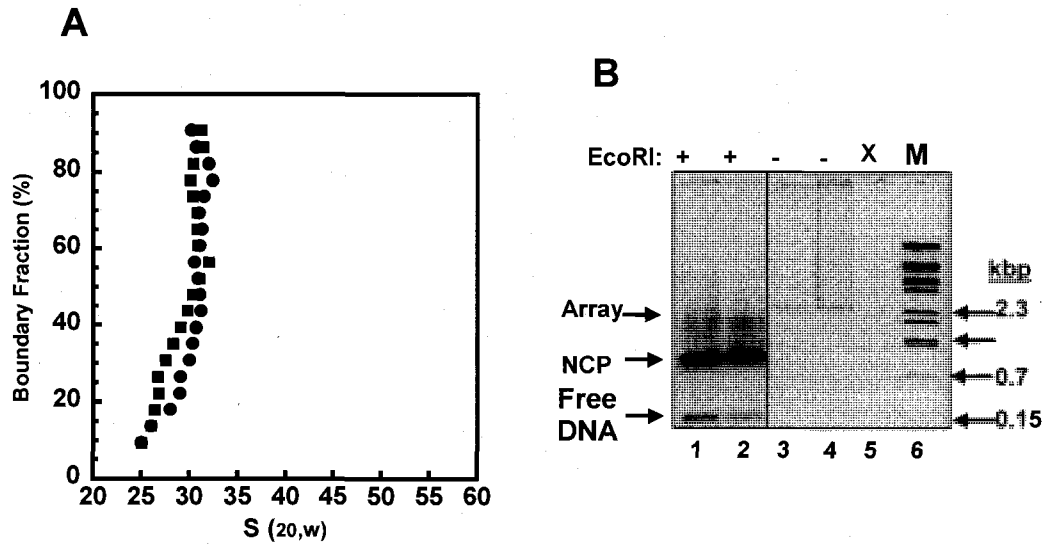


Figure 3.10.A Sedimentation velocity analysis of nucleosomal arrays. Reconstituted CENP – A (●) and major type human (■) 208-12 nucleosomal arrays in TEN buffer. Sedimentation Velocity experiments were carried out at 20,000 RPM, 20⁰C. and analyzed as described in methods and materials. The integral distribution of sedimentation coefficients (S) over the entire boundary (G(s)) is shown, corrected for water at 20⁰C ($S_{20,w}$). **B. EcoR1 Digestion Assay of nucleosomal arrays.** 1 μ g of reconstituted nucleosomal arrays (lanes 1 and 2) were digested with 10 units of EcoR1 for 24 hours at room temp. The digested arrays (lanes 3 and 4) were ran on a 1% agarose gel, stained with EtBr and visualized as described in methods and materials. The positions of the λ BstE-II marker [M (lane 6)] are shown at right. X indicates an empty lane (5).

DNA (faster migrating band). After staining with ethidium bromide, I measured the band intensity of the nucleosome and free DNA bands and determined the percentage of free DNA, taking into consideration that the ethidium bromide intercalation is decreased in nucleosomal DNA (Fletcher et al., 1994; Hansen et al., 1999). These assays showed that the CENP-A arrays contained 6% free 208 bp repeat while the MT contained 5%. Both species contain an average of 12 (± 1) nucleosomes per 208 – 12 DNA template.

To visualize the topography of the reconstituted arrays, I utilized atomic force microscopy (AFM) in air in the tapping mode (figure 3.11). In figure 3.11 individual nucleosomes can be visualized on the 208x12 DNA template as the “beads-on-a-string” structure. Amplitude analysis of individual arrays indicates equal height of about 1 nM for both CENP-A and MT H3 nucleosomes on the arrays (figure 3.11 C and D). This suggests both arrays have the ability to form nucleosomal arrays in which each nucleosome contains an octamer of histones.

The results from sedimentation velocity, nuclease digestion and AFM analyses demonstrate that the nucleosomal arrays were, on average, fully saturated with 12 nucleosomes per template and exist in an extended conformation at low salt as expected. These reconstituted arrays were next used to study how CENP-A might influence the formation of higher order chromatin structures.

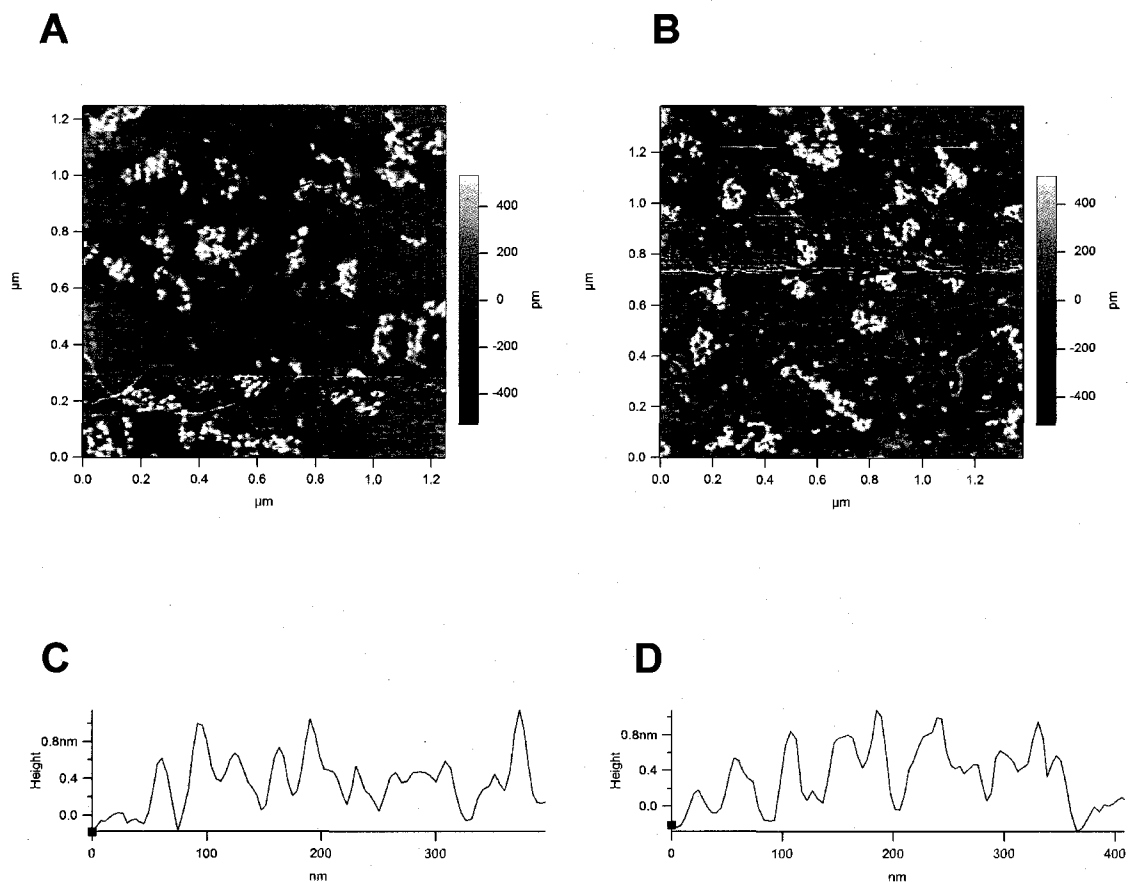


Figure 3.11 Atomic Force Microscopy of Nucleosomal Arrays – Tapping mode (in air) images of MT H3 (A) and CENP-A (B) containing nucleosomal arrays diluted to 60 ng/ml and applied to APTES-glutaraldehyde treated mica slides. Amplitude images of nucleosomal arrays traced (red/blue dot) of MT H3 (C) and CENP-A (D) containing arrays.

3.3.4 Nucleosomal arrays containing CENP-A have similar folding characteristics as major type H3 arrays

Centromeric chromatin containing CENP-A is polarly positioned on the outsides of the metaphase aligned chromosome (Blower et al., 2002) and is a distinct domain that it is classified as neither heterchromatin nor euchromatin (Sullivan and Karpen, 2004). Therefore, I was interested in determining whether the incorporation of CENP-A into nucleosomal arrays might cause a difference in the intra-nucleosomal array interactions. This could affect the centromeric chromatin structure, and result in distinct centromeric chromatin. The H3 NTD contributes to chromatin folding (Kan et al., 2007). The composition and length of MT H3 and CENP-A NTDs are dramatically different (figure 3.1) thus I hypothesize that the CENP-A arrays would fold under different salt concentrations. To study the folding of CENP-A nucleosomal arrays, I incubated arrays with 1.8 mM MgCl₂ and used sedimentation velocity to determine the sedimentation coefficient distribution of the folded arrays (figure 3.13). Both species were able to form the maximally folded 55S structure, and 40% of the arrays sedimented between from 40 – 55 S. The 40% that were able to fold is representative of the 40% of arrays that were fully saturated (27 – 30S) (figure 3.10). The sedimentation coefficient distributions closely superimposed, suggesting that formation of higher order chromatin structures were essentially identical (figure 3.12). The least saturated (30%) of the arrays were unable to fold at this concentration of MgCl₂ and did not sediment larger than 30 S. Regardless, the transition from the 29S “beads-on-a-string” nucleosomal array to the maximally folded 55S array is identical despite the differences in the composition and length of the CENP-A and MT NTDs.

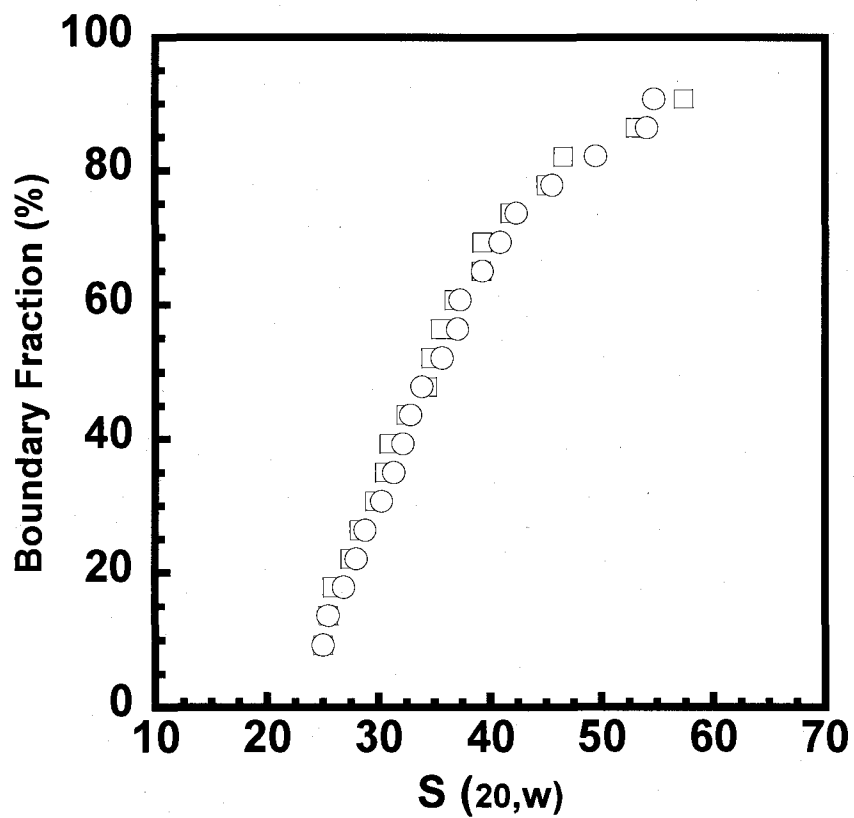


Figure 3.12 CENP-A nucleosomal array folding CENP-A (○) and MT H3 (□) 208-12 nucleosomal arrays in 1.8 mM MgCl₂-TEN buffer. Sedimentation Velocity experiments were carried out at 15,000 RPM, 20⁰ C. and analyzed as described in methods and materials. The diffusion corrected integral distribution of sedimentation coefficients corrected for water at 20⁰ C (S_{20,w}) is shown.

3.3.5 CENP – A and major type H3 containing nucleosomal arrays make similar inter-nucleosomal interactions

Nucleosome array oligomerization is a reversible and cooperative process that requires higher Mg^{2+} concentrations (> 2.0 mM $MgCl_2$) (Lu et al., 2006; Schwarz and Hansen, 1994). Characterization of nucleosomal array oligomerization was first observed under low speed sedimentation velocity experiments (Schwarz et al., 1996) and has subsequently been assayed by differential centrifugation (Fan et al., 2002; Hansen, 2002; Hansen and Lohr, 1993; Hansen et al., 1991; Pollard et al., 1999; Schwarz et al., 1996; Schwarz and Hansen, 1994; Tse et al., 1998b). After the addition of $MgCl_2$, differential centrifugation separates oligomerized arrays from soluble non-oligomerized arrays. I used this oligomerization assay to investigate if the NTD amino acid differences between CENP-A and H3 affect the long-range inter-nucleosomal array interactions. Figure 3.13 shows a plot of the fraction of soluble CENP-A and mH3 containing arrays as a function of $[MgCl_2]$. The formation of associated oligonucleosomal arrays is indicated by the loss of percent absorbance of the supernatant from the exposure to $MgCl_2$. Both nucleosomal arrays had the classical, cooperative oligomerization behavior seen previously (Fletcher and Hansen, 1996; Schwarz et al., 1996). In our experiments both nucleosomal arrays began to oligomerize at 2.0 mM $MgCl_2$ and were complete by 6.0 mM $MgCl_2$ (figure 3.13). These results indicate that CENP-A and MT H3 have similar ability to oligomerize, and together suggest that arrays of CENP-A containing nucleosomes are able to form higher-order chromatin complexes despite a nearly wholesale alteration of primary amino acid sequence in the CENP-A NTD.

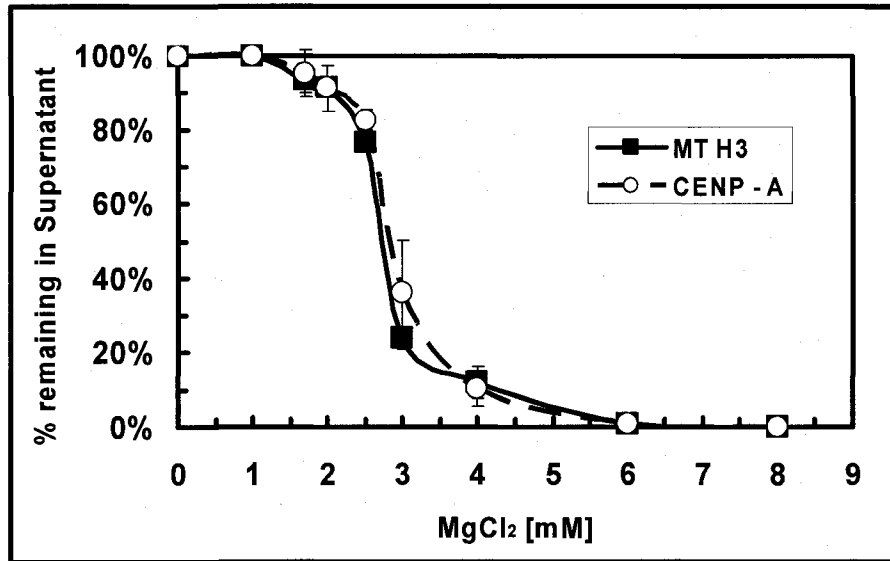


Figure 3.13 Mg²⁺-dependent oligomerization of nucleosomal arrays. Equally saturated nucleosomal arrays were incubated with the indicated concentration of MgCl₂ and assayed for oligomerization (see methods and materials). Shown is the % total A₂₆₀ that remained in the supernatant after micro-centrifugation as a function of MgCl₂.

3.4 Discussion

The centromere is a multi-factorial chromatin epicenter controlled and modulated by multiple trans and cis acting elements. The role of CENP-A in forming and /or maintaining centromeric chromatin is poorly understood. Here I have compared the functions of CENP-A to major type H3 *in vitro*, using biochemical and biophysical approaches.

3.4.1 The histone chaperone Nap-1 has a unique binding to the CENP-A/H4 complex

Histone chaperones bind histones in both the cytoplasm and nucleus and deposit or relocate histones to chromatin. Previous experiments have elegantly shown that the histone chaperone Asf1 can bind (English et al., 2006) and load (Tagami et al., 2004) H3/H4 onto DNA as a dimer *in vivo*. I was interested in the properties that differentiate CENP-A from major type H3 and used EMSA, sedimentation velocity and fluorescence studies to observe CENP-A/H4-Nap1 complexes with distinct size, shape and stoichiometry, as compared with H3/H4-Nap1 complexes. The electrophoretic gel mobility of the CENP-A/H4-Nap1 complex was similar to the H2A/H2B-Nap1 and the H3-H113A/H4-Nap1 complexes (figure 3.4), which suggests that the mass and charge is similar for the three complexes. This was perplexing, noting that alone CENP-A/H4 form tetramers and H2A/H2B and H3-H113A/H4 form dimers. Sedimentation velocity experiments showed that the CENP-A/H4-Nap1 complex has a unique sedimentation coefficient distribution compared to the H2A/H2B-Nap1 and the H3-H113A/H4-Nap1 complexes (figure 3.5). Because the S is proportional to the Mass (M) divided by the frictional coefficient (f), and the overall mass of the two types of H3 (15273 Da.) and

CENP-A (15859 Da.) are similar, a difference in f will change the S value. These data indicate that the CENP-A/H4-Nap1 complex either has a smaller frictional coefficient or larger mass than the histone dimer-Nap1 complexes.

Recent findings suggest the presence of a CENP-A^{CID} as a "hemisome" (Dalal et al., 2007). Also, the structure of the histone chaperone Asf1 has been solved bound to the H3/H4 dimer (English et al., 2006). I have shown that the CENP-A/H4 complex binds Nap1 as a dimer with a cooperative Hill coefficient, unlike the H3/H4 tetramer which binds Nap1 as a heterotetramer non-cooperatively (figure 3.7). Thus, I hypothesize that CENP-A/H4 could load on to DNA as a dimer, rather than the canonical (H3/H4)₂ tetramer. This may be one way to distinguish the CENP-A/H4 complex from the H3/H4 complex *in vivo*. During DNA replication, bulk chromatin segregate as a H3-H4 tetramer (Jackson, 1988). However, studies have shown a population of H3-H4 to be distributed in newly synthesized DNA as a dimer (Tagami et al., 2004). This raises the possibility that specific regions of the genome could have different segregation mechanisms. One model of how CENP-A could be maintained at the centromere would involve a transient hemisome containing one copy of each histone (H2A, H2B, CENP-A and H4) during early mitosis, which would remain on the parental strand DNA while the other nucleosome half would assemble on newly replicated DNA to mark proper centromeric location on the DNA. In late mitosis/ early G1 phase the hemisomes containing CENP-A could be recognized by CENP-A/H4-chaperone complexes to deposit newly transcribed H2A/H2B and CENP-A/H4 dimers onto CENP-A half nucleosomes to form the octameric (CENP-A, H4, H2A, H2B)₂ nucleosome during late mitosis and/or G1 phase. This ultimately would form centromeric chromatin containing an octamer of histones (H2A, H2B, CENP-A and H4) (see model in figure 3.14). Alternatively, half of the octameric CENP-A nucleosomes could associate with the daughter strand of DNA and the other half with the parent strand, to maintain

centromeric chromatin. These models are among many and more data is required to substantiate them.

3.4.2 CENP-A nucleosomes have similar ionic strength stability

The results above and the previously published results with show the inability of CENP-A to form histone octamers at elevated ionic strength (Black et al., 2004), I investigated the effect of CENP-A on the structure and stability of the nucleosome. I attribute the decreased electrophoretic gel mobility of CENP-A nucleosomes to be the result of its more basic pI (figure 3.8); CENP-A has a calculated pI of 11.7, 0.6 units higher than H3. Another explanation could be an alternate nucleosome shape. However, sedimentation velocity showed similar hydrodynamic shape suggesting that the overall size and shape of the CENP-A and MT NCPs are similar (figure 3.9).

I investigated the structural transitions of CENP-A nucleosomes by analyzing the sedimentation distribution in response to changes in ionic strength. CENP-A nucleosomes had similar hydrodynamic transitions as nucleosomes containing MT histones, indicating that CENP-A forms stable nucleosomes. I was unable to obtain diffraction data from the CENP-A nucleosomes (discussed in future directions and figure 3.15), I suspect This was caused by the incorporation of CENP-A which prohibited nucleosomes from obtaining uniform crystal packing.

3.4.3 Nucleosomal arrays containing CENP-A have the similar ability to oligomerize nucleosomal arrays as arrays containing major type mouse H3.

It has been shown that CENP-A is present at centromeric chromatin with a distinct pattern in post translational modifications and unique architecture (Sullivan and Karpen, 2004). Incorporation of CENP-A results in a unique chromatin architecture.

Therefore I have directly compared the chromatin condensation properties of CENP-A and MT H3 containing nucleosomal arrays. I show that CENP-A is unable to differentiate chromatin structural transitions from MT H3 containing nucleosomal arrays. These studies suggest that the difference in centromeric chromatin may be influenced by trans acting factors like centromere binding proteins and/or the post-translational modification code.

Karpen *et al* defined centromeric chromatin as neither heterochromatin nor euchromatin, based on the lack of similar post-translational modification (Sullivan and Karpen, 2004). The N-terminal primary amino acid sequence of CENP-A and major type H3 are highly divergent, with only 15% homology. Major type H3 is 135 amino acids long while the H3 variant CENP-A is 140 amino acids long. H3 has been shown to be post-translationally modified by acetylation, methylation and phosphorylation on 16 N-terminal residues, while phosphorylation at Ser 9 is the only PTM that has been identified on CENP-A. (Hake and Allis, 2006). Only six of the 37 residues within the N-terminal tail of CENP-A are conserved with major type H3, indicating that CENP-A nucleosomes will unlikely have the same set of post – translational modifications on the N-terminal tail. Therefore, a unique set of PTMs could differentiate CENP-A containing chromatin.

The CENP-A Targeting Domain (CATD) contains the Loop-1 (L-1) and α -helix-2 (α -2) structured regions (figure 3.1 and figure 3.15.C) and is required to localize nucleosomes to the centromere (Black et al., 2004). Interestingly, the amino acid H3-K79 within the L-1 loop lies on the surface of the nucleosome core and makes crystal packing contacts with adjacent nucleosomes (figure 3.1) (Luger et al., 1997). H3-K79 has been shown to be methylated by Disrupter of Telomeric silencing (Dot1) *in vivo* and is believed to be involved with heterochromatin formation (Lacoste et al., 2002; Ng et al., 2002; Park et al., 2002; van Leeuwen et al., 2002). The L-1 loop of CENP-A

have 2 more amino acids than MT H3, thus I propose that the position of H3-K79 could be shifted in CENP-A nucleosomes thereby changing the surface chemistry of this region. This may either affect the contact point of nucleosome cores and/or alter the recognition of CENP-A binding factors.

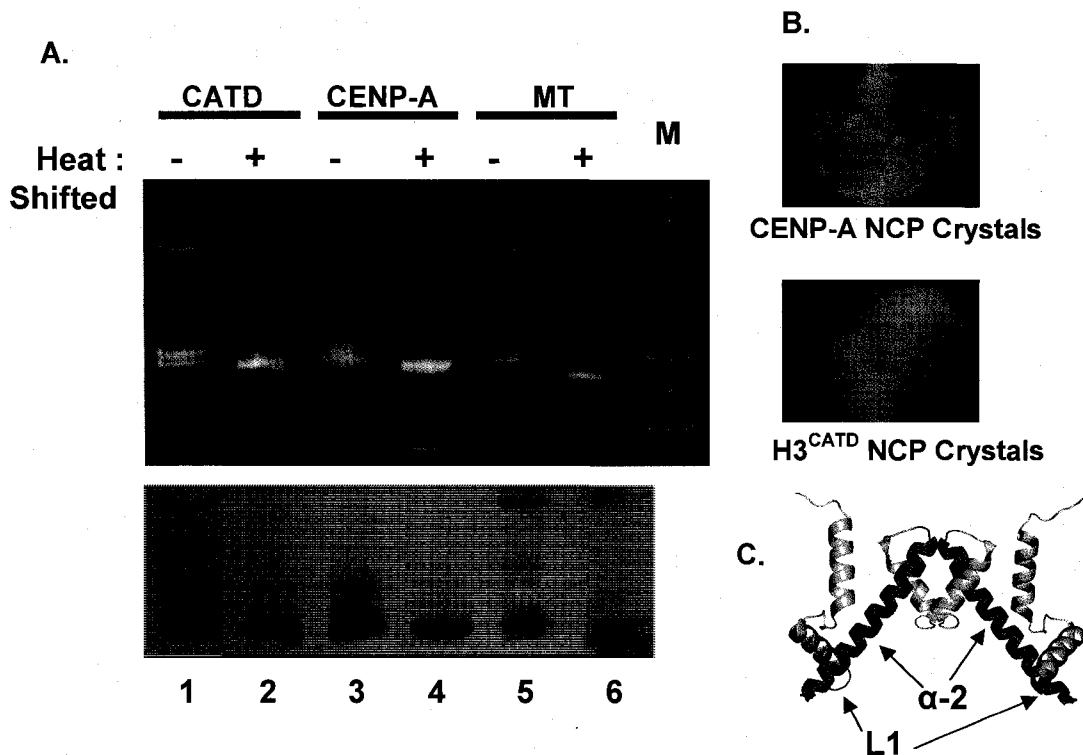
Numerous additional centromeric proteins have been identified. Specifically proteins CENP-B, -C, -H, -M, -M, -T and -U were purified using a TAP-tagged CENP-A nucleosome and together are called the Nucleosome Associated Complex (NAC) (Foltz et al., 2006; Okada et al., 2006). Centromere proteins CENP-I, -K, -L, -O, -P, -Q, -R and -S are not associated directly with purified CENP-A nucleosomes and are categorized by the term CENP-A distal (CAD) (Foltz et al., 2006; Okada et al., 2006). Components of the NAC and CAD are constitutively associated with the vertebrate centromere, suggesting they could play a role in the separate pathway of CENP-A deposition and maintenance.

I have presented a way in which CENP-A could maintain the presence on centromeric chromatin. Also, I have shown that CENP-A can form chromatin with canonical like salt structural transitions. I hypothesize that the pathway to differentiate CENP-A containing chromatin involves more than just the H3 variant. Together, with a difference in chaperone binding, post-translational modifications and the divergent NTDs, all may play a role in distinguishing centromeric chromatin.

3.5 Future Directions

3.5.1 Crystallization attempts of nucleosomes containing CENP-A

I attempted to obtain a high resolution molecular structure of the CENP-A containing nucleosome by crystallizing the CENP-A nucleosome and a nucleosome containing a histone chimera of the loop-1 (L-1) and α -helix-2 (α -2) regions of CENP-A substituted



3.15.CENP-A nucleosome crystallization. A. H3^{CATD}/ CENP-A/ major type nucleosome reconstitution. Nucleosome core particles containing H3^{CATD} (lanes 1 and 2), CENP – A (lane 3 and 4) and major type H3 (lane 5 and 6) histone octamers reconstituted with 147 bp α -Sat DNA. Nucleosomes were heat shifted (+) for 1 hour at 37⁰C (lanes 2, 4 and 6). Samples were electrophoresed on a 5 % native – PAGE in 0.2 % TBE at 150 V for 1 hour and stained with Et Br (top) and Imperial Protein Stain (Pierce) (bottom). **B. Nucleosome Crystallization** CENP-A (top) and H3^{CATD} (bottom) nucleosome crystals formed in sitting drop trays by vapor diffusion. **C.** Pymol representation of Cenp-A Targeting Domain (CATD) residues 78-115 (pink), MT H3 residues (light blue).

into the major type histone H3. The L-1 and α -2 regions of CENP-A are sufficient to target nucleosomes to the centromere and maintain proper chromosome segregation (Black et al., 2004). This region of CENP-A has been identified as the CENP-A Targeting Domain (CATD). I reconstituted nucleosomes containing CENP-A and H3^{CATD} (figure 3.10.A) and purified NCPs using Prep Cell gel chromatography (data not shown). I was able to crystallize nucleosomes containing CENP-A and the H3^{CATD} chimera, although under different salt concentrations as the MT nucleosome crystallization (figure 3.B). CENP-A nucleosomes formed crystals with a flat fragile morphology while H3^{CATD} nucleosome crystals were larger and had similar morphology as MT nucleosome crystals. However, neither of nucleosome diffracted at the home-source x-ray generator (data not shown). To crystallize CENP-A nucleosomes larger screens must be used to obtain crystals which diffract.

Chapter 4

The Effect of Histone H3-K56 Acetylation on the Nucleosome and Chromatin Structure

Abstract

In this chapter I have addressed the hypothesis that acetylation of H3 K56 disrupts chromatin higher order structure via alterations in the protein-DNA interactions in the nucleosome core. My data indicate that acetylation of the core of the nucleosome affects the nucleosome structure and disrupts nucleosomal array condensation.

4.1 Introduction

Post-translational modifications (PTM) of histones modulate chromatin architecture and alter recruitment of chromatin binding proteins, which ultimately affects cellular processes, including gene transcription, DNA repair, and DNA replication (Goldberg et al., 2007; Morris et al., 2007; Taverna et al., 2007). In general, H3-K56Ac is found in chromatin regions which are thought to have a chromatin structure, which has accessible DNA relative to bulk chromatin. Acetylation of K56 (H3-K56Ac) enhances gene expression (Xu et al., 2005), DNA repair, and is found on newly synthesized histones which are deposited onto newly replicated DNA (Masumoto et al., 2005). There are two symmetry related H3 K56 residues located on the α -N helix near the entry and exit sites of nucleosomal DNA (figure 4.1) and this amino acid is conserved from yeast to humans. To maintain heterochromatin in chromosome foci such as telomeres, the acetyl group is removed from H3-K56Ac by the hst3 and hst4 histone deacetylases (HDAC) of the Sir complex (Celic et al., 2006; Xu et al., 2007). Acetylation of the histone tails have been shown to inhibit intramolecular folding of nucleosomal arrays which results in increase gene transcription (Shogren-Knaak et al., 2006; Tse et al., 1998a; Tse et al., 1998b; Wang and Hayes, 2008). Yet the affect of acetylation within the core of the nucleosome is poorly investigated.

In yeast, the histone acetyltransferase (HAT) Rtt109 is the only enzyme which acetylates H3-K56 (Han et al., 2007). It has structural homology to the metazoan HAT p300/CBP (Tang et al., 2008). Rtt109 co-purifies with (Krogan et al., 2006) and is stabilized (Fillingham et al., 2008) by the histone chaperone Vps75. Vps75 is a H3-H4 chaperone of the Nap1 family (Selth and Svejstrup, 2007).

Here I have used recombinant Rtt109-Vps75 to acetylate H3 at residue 56 *in vitro* to study the effect of this modification on nucleosome and chromatin structure. I have

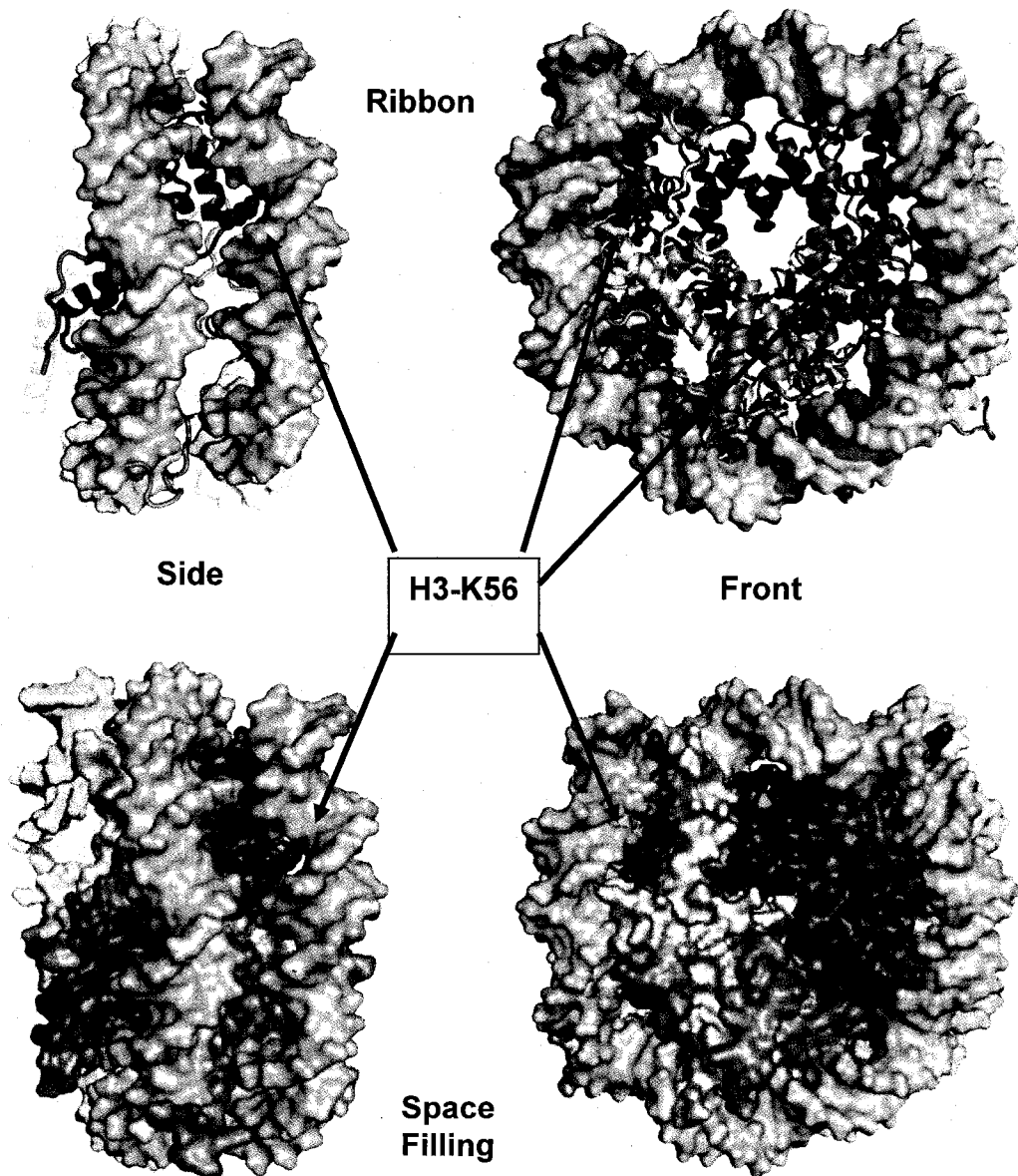


Figure 4.1 Location of H3-K56 in the nucleosome. Arrows point to the location of H3-K56 (magenta). H3-K56 makes one of the many water mediated hydrogen bonds in the nucleosome core. Nucleosome core particle pdb entry 1AOI rendered in Pymol. H4 (green), H3 (blue), H2A (yellow), H2B (red).

reconstituted nucleosomes and nucleosomal arrays with histones octamers containing H3-K56Q, -K56E and H3 acetylated on K56. I observed hydrodynamic differences when H3-K56Ac and H3-K56Q containing nucleosomes were subject to analytical ultracentrifugation in increased levels of NaCl, which I speculate is a result of changes in the nucleosome structure. I have also demonstrated that H3-K56Ac and H3-K56Q arrays require higher concentration of $MgCl_2$ to make inter and intra nucleosomal array interactions. I propose that the role of H3-K56 acetylation is to inhibit chromatin condensation by disrupting the protein-DNA interaction between H3-K56 and the DNA phosphate backbone. Thus, these small changes in the nucleosome structure result in alteration of the intramolecular nucleosomal array folding and oligomerization, which could play a role in euchromatic regions.

4.2 Methods and Materials

4.2.1 Histone mutagenesis – I used an adopted quickchange mutagenesis (Stratagene) method to create H3-K56Q and H3-K56E point-mutants (Kirsch and Joly, 1998; Wang and Malcolm, 1999).

4.2.2 Protein expression and purification – Histone protein expression and purification was performed as described previously (Dyer et al., 2004).

6xHis-Vps75 and GST-Rtt109 were over-expressed and purified from C+ RK and RP pLysS E. coli strains. GST-Rtt109 was purified using glutathione agarose (Qiagen) followed by S200 size exclusion chromatography in 500 mM NaCl, 10 mM Tris-Cl pH 7.5, 1 mM EDTA to remove DNA contamination. 6xHis-Vps75 was purified using standard nickel affinity procedures (Qiagen) and dialyzed into 100 mM NaCl, 10 mM Tris-Cl pH 7.5, 1 mM EDTA. Purification yielded 5 mgs/L of 6xHis-Vps75 and 2 mgs/L of GST-Rtt109.

4.2.3 DNA purification – The 147 bp palindromic α -sat DNA was purified as previously described (Dyer et al., 2004). The 208-12 5S rDNA used to prepare nucleosomal arrays was purified as previously described (Georgel et al., 1993; Schwarz and Hansen, 1994).

4.2.4 Gel Electrophoresis – Native-5% PAGE were electrophoresed in 0.2 X TBE as previously described (Dyer et al., 2004). 5% acetic acid/ 6 M urea/ 15% 60%:0.4% acrylamide:bisacrylamide gel electrophoresis (AU-PAGE) were prepared and run as previously described (Shechter et al., 2007). Gels were pre-run for 12 hours at 150V prior to loading. Samples were mixed with 2x loading buffer (6M Urea, 0.02 % pyronin Y (w/v), 5% glacial acetic acid (v/v) and 12.5 mg/ml protamine sulfate), electrophoresed at 150V for three hours, and stained with commassie blue.

4.2.5 Acetylation Reactions – GST-Rtt109 (HAT), histone chaperone His-Vps75 and the substrates H3 (dissolved in 100 mM NaCl, 10 mM Tris-Cl pH 7.5, 1 mM DTT) or renatured (H3/H4)₂ tetramers (in 100 mM NaCl, 10 mM Tris-Cl pH 7.5, 1 mM DTT) were mixed at various ratios in reaction buffer (RB) containing 100 mM NaCl, 10 mM Tris-Cl pH 7.5, 1 mM DTT. An aliquot from the reaction was frozen with liquid nitrogen and stored at -80^o C for use as a non-acetylated control for AU-PAGE. Under our experimental conditions, I found specific acetylation to H3-K56 by combining 0.5 μ M Rtt109, 25 μ M Vps75 and 25 μ M H3 and 500 μ M of AcCoA (freshly dissolved in water) in RB and incubated for 1-2 hours at 21^oC in a 50 ml siliconized Erlenmeyer flask. Reactions were quenched by flash freezing with liquid nitrogen. Samples were analyzed by mass spectrometry and AU-PAGE and western blot analysis to determine the efficiency of acetylation.

To purify H3-K56ac from the acetylation reaction, I added de-ionized urea to the thawed acetylation reaction to a final concentration of 6 M + RB (purification buffer (PB) in order to dissociate the complex and quench the acetylation reaction. The

reaction was mixed with two mls of SP-sepharose fast flow previously incubated in PB (Pharmacia) and rotated overnight at 4°C. The slurry was decanted into an empty 20 ml 1x10 cm column and the flow-through was collected. The resin was washed with PB + 250 mM NaCl, eluted with PB + 500 mM NaCl and PB + 1 M NaCl the fractions collected were analyzed on a 15% SDS-PAGE and visualized by commassie blue staining. The purified H3-K56ac fractions were pooled and dialyzed against water and 5 mM β -MeEtOH 3x over 18 hours at 4°C. To determine the mass of the product, an aliquot was removed for mass spectrometry analysis. The dialyzed H3-K56Ac was then lyophilized for long term storage.

4.2.6 Mass Spectrometry – 1 ul of purified sample was mixed with 1 ul of Sinapinic acid (10 mg/ml in 50% ACN, 0.1% TFA). The mixture is spotted on the MALDI target and allowed to air dry. The sample is analyzed by an Ultraflex-TOF/TOF mass spectrometer (Bruker Daltonics, Billerica, MA) in positive ion, linear mode using a 25 kV accelerating voltage. External calibration is done using an 8 peptide calibration mixture on a spot adjacent to the sample. The raw data is processed using the SNAP algorithm in the FlexAnalysis software (version 3.0, Bruker Daltonics). An average peak list is generated using a signal-to-noise threshold of 6 for MS spectra.

4.2.7 Reconstitution of Nucleosomes and Nucleosomal Arrays - Nucleosomes were reconstituted as previously described (Dyer et al., 2004). Briefly, equal molar ratios of Histone octamers containing H3-K56Q, H3-K56E or H3-K56Ac were mixed with 147 bp α -Sat DNA in TE buffer (10mM Tris-HCl, 0.25 mM EDTA, pH 7.5) containing 2.0 M KCl₂. and dialyzed using salt gradient dialysis into TE buffer (0 M KCl₂). Nucleosomes were heat shifted at 37° for 1 hour to uniformly position the octamer on the 147 bp DNA template. The nucleosomes were then purified from excess DNA and unbound protein using a Prep Cell Model 491 purification system

(Bio-Rad) and analyzed by native – PAGE in 0.2 % TBE as described (Dyer et al., 2004).

Nucleosomal arrays were reconstituted as described (Hansen et al., 1991). Briefly, equal molar ratios of histone octamers containing H2A, H2B, H4 and either H3-K56Q, H3-K56E or H3-K56Ac were mixed with the 208-12 DNA template in TE buffer (10 mM Tris-HCl, 0.25 mM EDTA, pH 7.8) containing 2.0 M NaCl₂, followed by extensive salt gradient dialysis to low salt TEN buffer (2.5 mM NaCl₂-TE) (Hansen et al., 1991).

4.2.8 EcoR1 template saturation analysis - Assays were performed as described (Tse and Hansen, 1997). Briefly, 1 µg of reconstituted nucleosomal arrays was digested with 10 units of EcoR1 restriction enzyme for 24 hours at 21^o C. Digested arrays were separated on a 1% agarose gel, stained with Ethidium Bromide and resolved using a Gel Logic 200 imager. The gel image was used for densitometry analysis of bands to determine the percentage of free DNA using Scion software and calculated using:

$$\% \text{ Free DNA} = \frac{\text{Free DNA}}{((\text{Free DNA}) + (\text{NCP} \bullet 2.5))} \quad \text{eq. 2}$$

4.2.9 Nucleosome Crystallization – Nucleosomes containing H3-K56Q, H3-K56E and H3-K56Ac were crystallized by using salting in vapor diffusion at nucleosome concentrations ranging from 8-10 mg/ml and solution conditions of 36 mM KCl, 40 mM MnCl₂, 5 mM K-cacodylate and 36 mM KCl, 42 mM MnCl₂, 5 mM K-cacodylate. The crystals were soaked in 24% 2-methyl, 2,4-pentanediol (MPD), 5% trehalose, 40.0 mM KCl, 37.0 mM MnCl₂ 5.0 mM K-Cacodylate, pH 6.0 (Luger et al., 1997). X-ray data was collected from the Advanced Light Source (beam line 422) at Lawrence Berkley laboratories (University of California–Berkley). The data was processed with Denzo and Scalepack. PDB entry 1KX5 (147 bp MT xenopus NCP) was used as a search model for molecular replacement. Molecular replacement and further refinement was

done with CNS (Brunger, 2007). Coot was used for model building (Emsley and Cowtan, 2004).

4.2.10 Analytical Ultracentrifugation – Sedimentation velocity studies were carried out using a Beckman XL-A analytical ultracentrifuge using the absorbance optics. Samples were mixed to a final A_{260} of 0.6 - 0.8 and equilibrated at 20° C. for one hour prior to sedimentation. Nucleosomes were sedimented at 40-50,000 rpm and nucleosomal arrays were sedimented at 18-25,000 rpm. The radial increment used was 0.003 cm. Data was analyzed using improved method of van Holde and Weischet (Demeler and van Holde, 2004) to obtain the integral distribution of sedimentation coefficients ($G(s)$) using UltraScan v9.4 for windows. \bar{V} and ρ were calculated using Ultrascan. Second Moment analysis, used to determine the average sedimentation coefficient of nucleosome core particles, was implemented within Ultrascan.

4.2.11 Folding of nucleosomal arrays- Nucleosomal arrays were diluted with TEN buffer to a final concentration of 2.0 mM $MgCl_2$ and a final A_{260} of 0.6 – 0.8. Sedimentation velocity experiments were carried out at 18,000 RPM for 2 hours with radial increments of 0.001cm Data was analyzed using improved method of van Holde and Weischet (Demeler and van Holde, 2004) to obtain the integral distribution of sedimentation coefficients ($G(s)$) using UltraScan v9.4 for windows.

4.2.12 Oligomerization of nucleosomal arrays- Differential centrifugation was used as previously described (Gordon et al., 2005; Lu et al., 2006). Briefly, nucleosome arrays were diluted to an $A_{260} = 1.2$ with TEN buffer. Arrays were mixed with $MgCl_2$ -TEN buffer, incubated for five minutes at room temperature and then centrifuged in a bench-top microfuge at 13,000 RPM (~16,000 x g) for 5 min. The A_{260} of the supernatant was then measured in a Beckman DU 800 Spectrophotometer. Data is

expressed as a percentage of the total sample that remained in the supernatant as a function of MgCl_2 .

4.3 Results

4.3.1 Optimization of large scale specific acetylation of histone H3 at lysine 56 *in vitro*

To reconstitute nucleosomes and nucleosomal arrays with acetylated H3-K56, I optimized the large scale acetylation of H3 by Rtt109 *in vitro*. Rtt109 is inefficient at acetylating H3-K56 within the nucleosome complex (Han et al., 2007). Therefore, I acetylated the H3 monomer and H3 in complex with H4 (H3/H4)₂ using recombinant Gst-Rtt109 along with His-Vps75 (figure 4.2.A). I varied the amount of enzyme (Rtt109), histone chaperone (Vps75), substrate (H3 alone or (H3/H4)₂), and time to achieve specific acetylation, then analyzed the amount of acetylation using AU-PAGE, western blot and mass spectroscopy.

I began using renatured (H3/H4)₂ tetramers as a substrate and found that specific acetylation of H3-K56 by Rtt109 was dependent on the presence of the histone chaperone Vps75, consistent with earlier results (ref). AU-PAGE was used as a measurement of global acetylation and also confirmed that H4 was not acetylated by Rtt109 (figure 4.2.B). Western blotting with H3-K56Ac specific antibodies confirmed that the residue K56 is acetylated (figure 4.2.C). These small scale reactions were

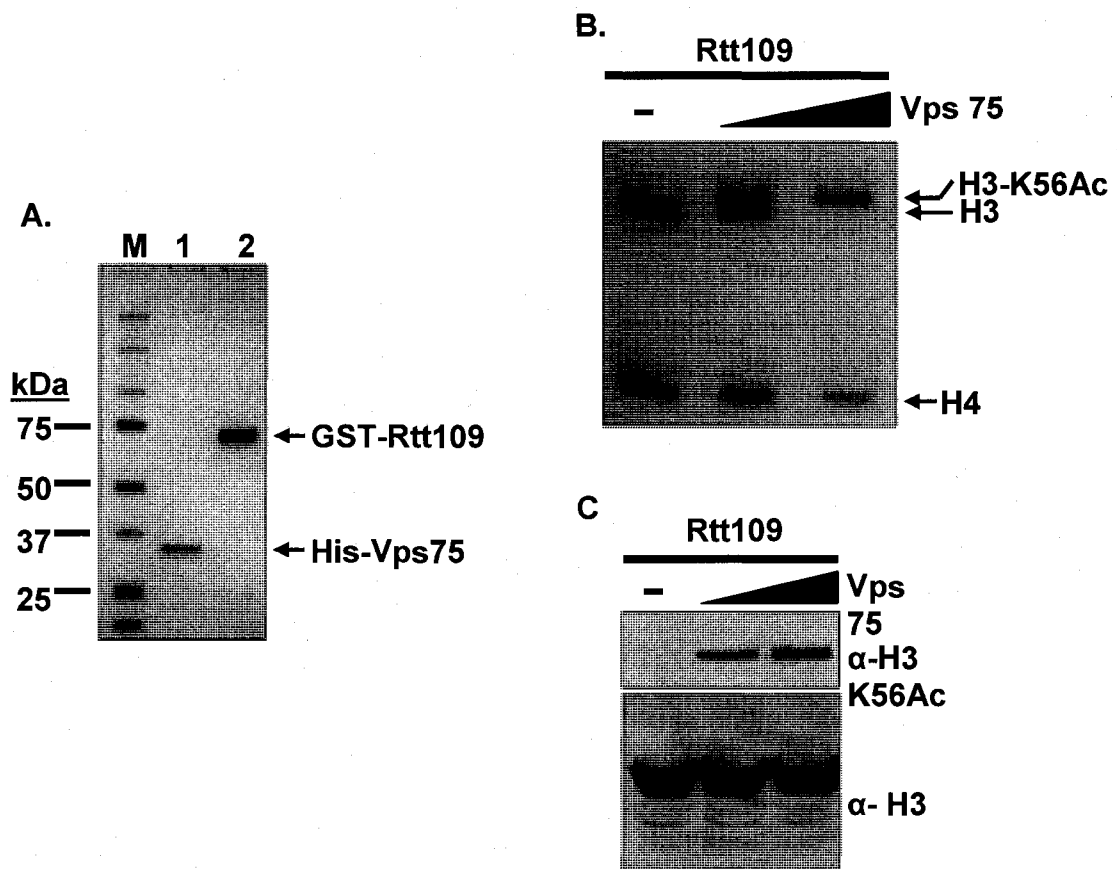


Figure 4.2 Rtt109 in vitro acetylation of H3-K56 in the context of the (H3-H4)₂ tetramer. **A.** Purified histone chaperone (VPS75) and HAT (RTT109) proteins. 3 ug of purified 6xHis tagged VPS75 (lane 1) and GST tagged Rtt109 (lane 2) run on a 10% SDS-PAGE stained with coomassie blue. Samples from the acetylation reaction were electrophoresed on an (B) AU-PAGE or (C) SDS-PAGE for western blotting. In the reaction H3/H4 and Rtt109 remained constant at 25 and 0.5 μ M, respectively, the Vps75 concentration was increased from 0 – 25 μ M.. **B.** Samples were mixed with 2x AU-PAGE running buffer then electrophoresed for 3 hours at 200 V and stained with coomassie blue. **C.** Samples from the reaction were mixed with 2x SDS-PAGE running buffer and electrophoresed a 15% SDS-PAGE. Bands were then transferred to nitrocellulose paper and probed for α -K56ac (top) and α -H3 (bottom). Figure C is courtesy of Dr. Y. J. Park.

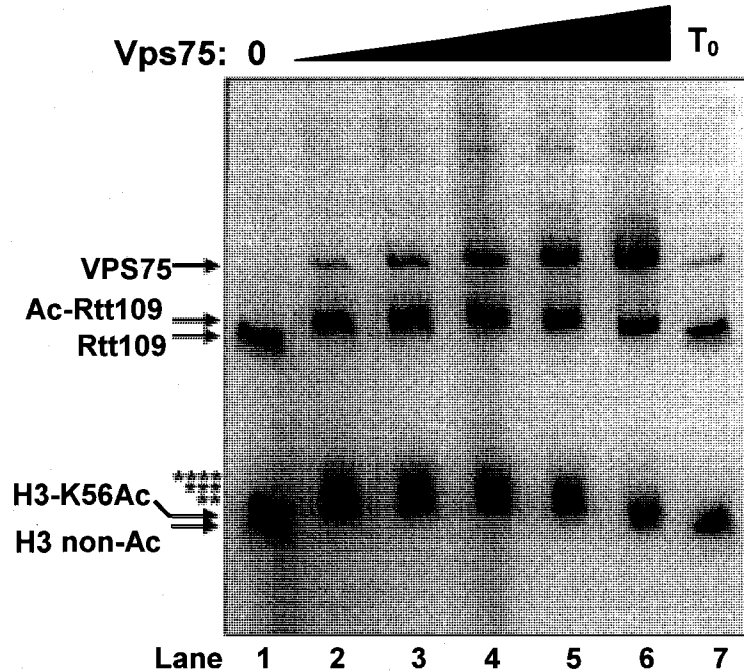


Figure 4.3 Vps75 contribution to the specific acetylation of H3-K56 by Rtt109. AU-PAGE of acetylation reaction containing 0.5 μ M Rtt109, 0-25 μ M Vps75, 25 μ M xenopus H3 in buffer containing 100 mM NaCl, 10 mM Tris-Cl pH 7.5, 1 mM EDTA, 1 mM AcCoA incubated for 1 hour at 21^oC. Lane 1 contains Rtt109 and H3 but is absent of Vps75. Lanes 2-6 contain Rtt109, H3 and 0.5-50 μ M Vps75. Lane 7 is an unacetylated control and contains Rtt109, H3 and 25 μ M Vps75 the reaction was stopped by freezing in liquid nitrogen at time 0. Vps75, Rtt109 and acetylated Rtt109, and H3 species are indicated left of gel. (**-****) indicate acetylation sites other than H3-K56.

carried out in 20 μ l reactions containing 25 μ M of (H3-H4)₂ tetramer, 0.5 μ M of Rtt109 and 0-25 μ M of Vps75. In many circumstances, I observed by AU-PAGE non-specific hyper- or hypo-acetylation of H3 i) when the Vps75 concentration was lower than H3 (figure 4.2.B, 4.2.C and 4.3 lane 1) ii) when the reaction contained more than a 1:50 molar ratio of Rtt109 to H3 (data not shown), and iii) when the reaction proceeded for more than two hours (data not shown) even when other conditions were optimized. I next attempted to acetylate and purify H3 from a large scale (mg amounts) reaction *in vitro*. Using the (H3-H4)₂ tetramer as a substrate could complicate the purification of H3 from H4 with ion-exchange chromatography. My objective was to purify H3-K56Ac alone, which would allow me to combine with H2A, H2B and H4 to renature histone octamers. Therefore, I used histone H3 as a substrate. Consistent with results using the (H3-H4)₂ tetramer as a substrate, specificity of H3-K56 acetylation increased as the concentration of Vps75 increased to equal molar with the H3 concentration (figure 4.3.B and C and 4.4.A). To acetylate 10 mgs of H3 at Lys-56 I combined 25 μ M of H3, 25 μ M of Vps75 and 0.5 μ M of Rtt109 in a total volume of 20 mls of RB for two hours at 21^oC (figure 4.5.A). The addition of 25 μ M of H3 into RB containing 0.5 μ M Rtt109 and 25 μ M Vps75 caused aggregation (not observed with (H3-H4)₂ as the substrate) decreasing the yield of H3-K56ac from the reaction. A small fraction of the aggregate persisted after the addition of 6 M urea to the completed acetylation reaction. I separated the aggregate from the mixture by centrifugation at 15k r.p.m. in a benchtop centrifuge. I analyzed the pellet by SDS-PAGE, which determined that it contained H3 and His-Vps75 (data not shown). I attempted to purify the H3 from His-Vps75 by Ni-chelate chromatography but the aggregate did not bind to the Ni resin. The apparently irreversible aggregation we observed may be an indication of non-physiological stoichiometries between H3, Vps75 and Rtt109 in these buffer conditions.

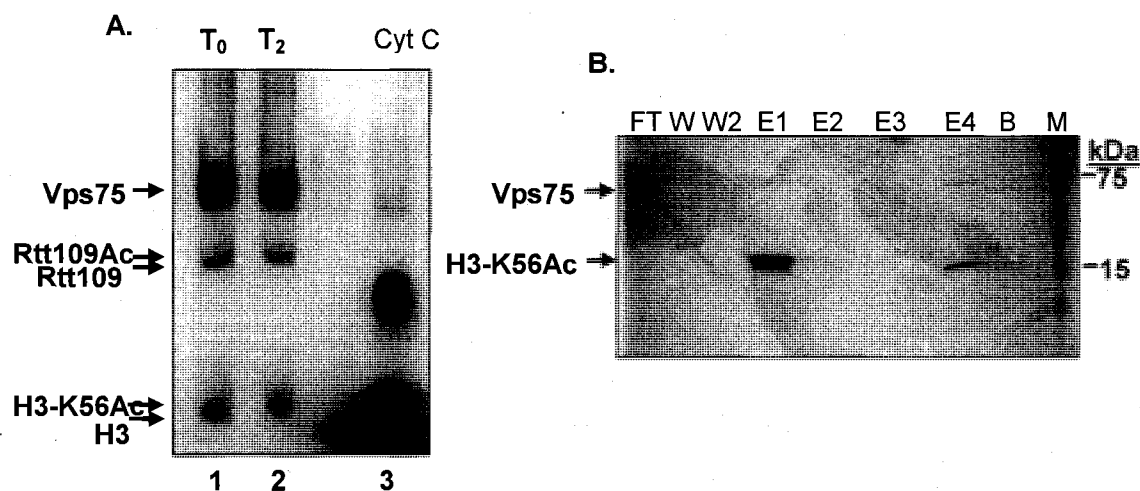


Figure 4.4.A. Large scale acetylation and purification of H3-K56Ac. H3 was acetylated at lysine 56 by Rtt109-Vps75. 10 mgs of H3 was mixed at 25 μ M with a molar ratio of 50:50:1 H3:Vps75:Rtt109 in buffer (100 mM NaCl, 10 mM Tris-Cl pH 7.5 and 1 mM DTT). 20 μ l of the reactions from T₀ (lane 1) T₂ (lane 2) was mixed with 2x AU-PAGE running buffer and electrophoresed on this AU-PAGE. The gel was pre-run for 12 hours at 150 V then samples were loaded and electrophoresed for 3 hours at 200 V. **B.** Ion exchange purification of *in vitro* acetylated H3 under denaturing conditions. The denatured mixture was incubated with SP-Sepharose FF ion exchange resin overnight at 4°C. The histone was eluted by step-wise salt titration, the purified fractions were analyzed by 15% SDS-PAGE and stained with coomassie blue. Flow through (FT) and washes (W1 and W2) contained Rtt109 and Vps75 at salt concentrations 100-250 mM NaCl. I was able to elute pure fractions of H3-K56Ac (E1 and E2) at 500 mM NaCl. There was also a population of aggregated H3-K56ac and Vps75 which remained on the resin until 1 M NaCl (E4). Fractions E1 and E2 were combined and dialyzed into water and lyophilized for long term storage.

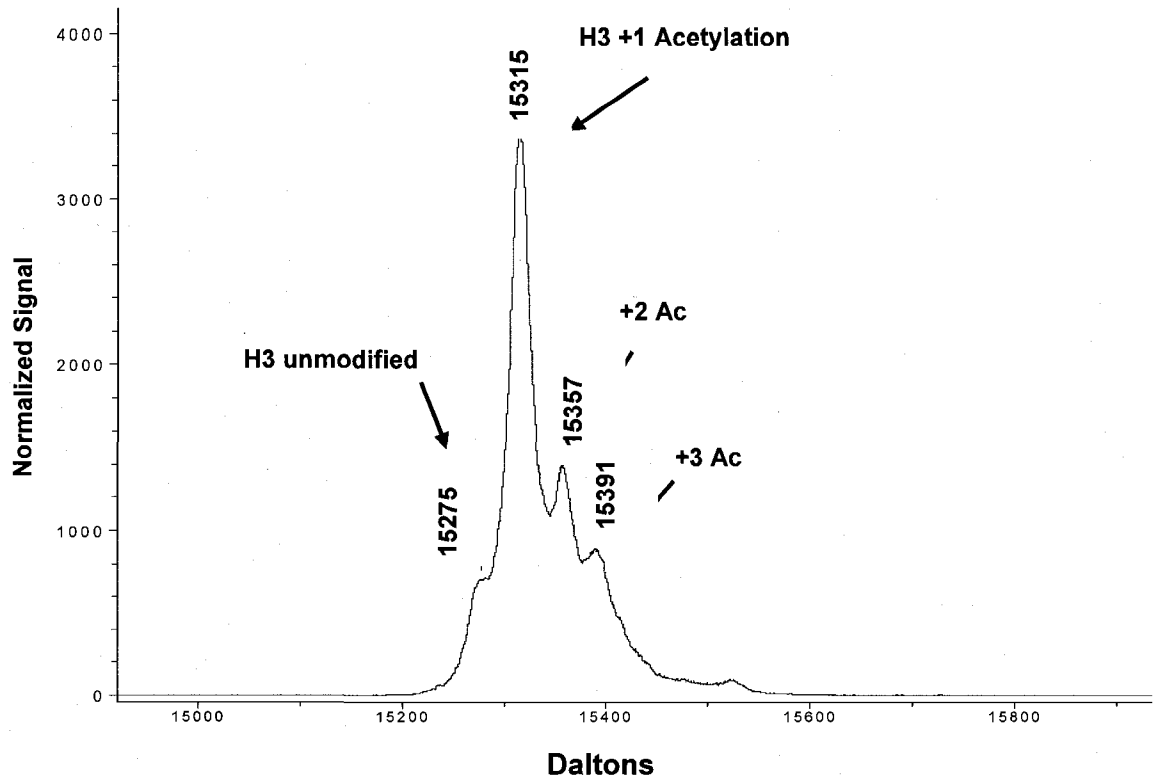


Figure 4.5 Mass Spectrometry of Acetylated H3 An aliquot of purified fractions was analyzed by mass spectrometry to determine molecular weight distributions of purified histone. 10 pMoles of purified sample was analyzed by an Ultraflex-TOF/TOF mass spectrometer in positive ion, linear mode. The molecular weight of unmodified H3 is 15273 Da. the molecular weight of an acetyl group is 45 Da.

Under denaturing conditions, I purified H3-K56ac by ion-exchange chromatography; this also stopped the reaction from non-specific acetylation (see methods and materials). The purified fractions were analyzed by SDS-PAGE (figure 4.4.B). Purified H3-K56ac was dialyzed into water and analyzed by mass spectrometry (figure 4.5), and lyophilized for long-term storage. I have demonstrated a large-scale acetylation of H3 at lysine 56.

4.3.2 Histone octamers containing H3-K56Ac and point mutants H3-K56E and H3-K56Q are able to reconstitute nucleosomes

It has been proposed that H3-K56 acetylation disrupts the nucleosome structure (Ozdemir et al., 2006; Xu et al., 2005). I reconstituted nucleosomes containing H3-K56Ac to study the crystal structure and hydrodynamic characteristic properties of nucleosomes. I began by combining H3-K56ac with histones H2A, H2B and H4 to renature histone octamers. K-Q mutations have been used to mimic the constitutive acetylation in yeast (Recht et al., 2006; Schneider et al., 2006) and in nucleosomal array model systems (Wang and Hayes, 2008) to elucidate the function of acetylation. Acetylation of lysine residues removes the positive charge; therefore, I made two different point mutations to major type *Xenopus* histone H3 lysine 56 to either a glutamine (H3-K56Q) or glutamate (H3-K56E). These point mutants were used as controls for the examination of the effects acetylation may have on nucleosome structure and chromatin condensation. Glutamate changes the positively charged lysine to negative. The glutamine substitution changes lysine to an uncharged polar sidechain resembling the physiochemical properties of acetylation.

H3-K56Ac and mutant histones H3-K56Q and H3-K56E were renatured into octamers by mixing with stoichiometric amounts of H2A, H2B, and H4 in denaturing

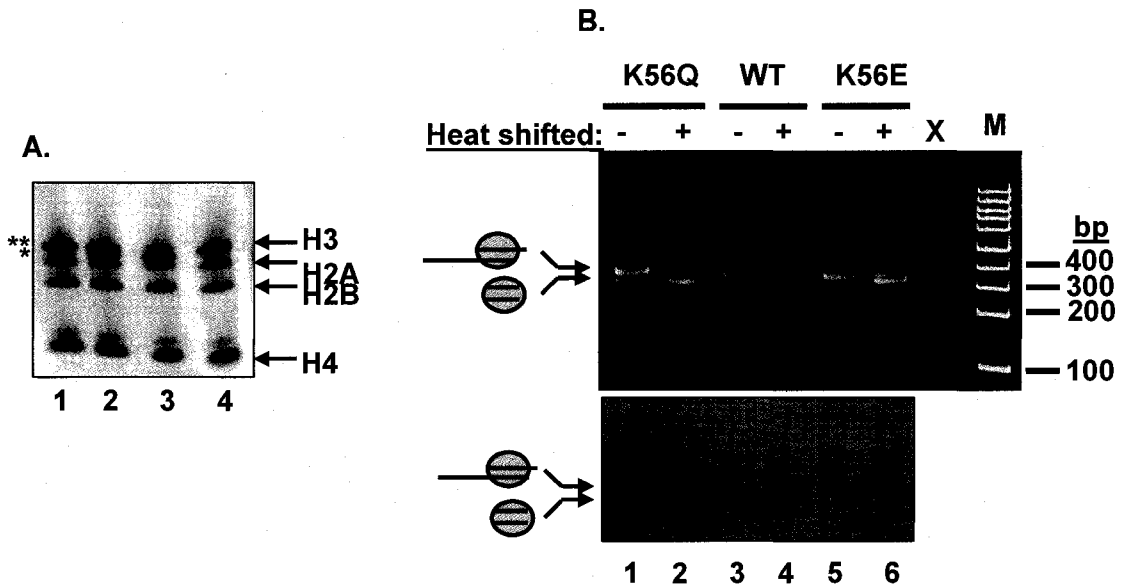


Figure 4.6.A. Mutation in H3 changes electrophoretic mobility 4 μ g of refolded histone octamers containing mutations to histone H3 K56Q (lane 1), K56Q with WT H3 (lane 2), WT (lane 3) and K56E (lane 4) were loaded and electrophoresed on an AU-PAGE stained with coomassie blue. (*) indicates MT H3 and (**) indicates H3-K56Q and H3-K56E mobility. **B.** Reconstituted nucleosomes containing H3-K56 mutations have similar ability to heat shift. Nucleosome core particles containing H3 K56Q (lanes 1 and 2), WT H3 (lane 3 and 4) and H3 K56E (lane 5 and 6) reconstituted with 147 bp α -Sat DNA. Nucleosomes were heat shifted (+) for 1 hour at 370C (lanes 2,4 and 6). Samples were run on a 5 % native – PAGE in 0.2 % TBE at 150 V for 1 hour and stained with Et Br (top) and Imperial Protein Stain (Pierce) (bottom). M indicates 100 bp marker.

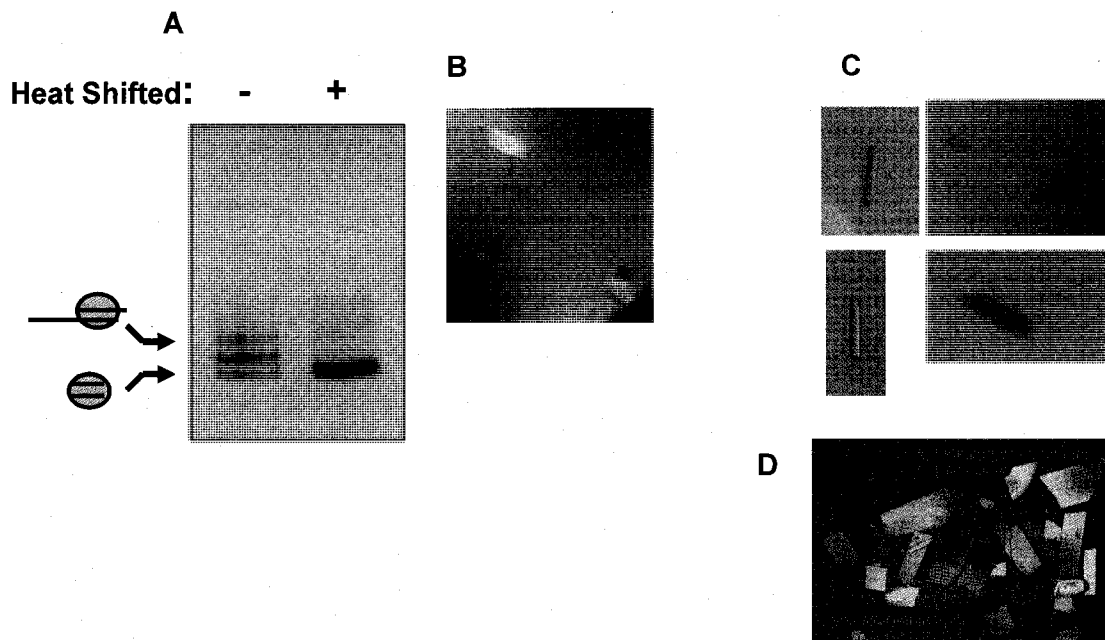


Figure 4.7 Nucleosome crystallization. **A.** 5% Native-PAGE of reconstituted nucleosomes containing in vitro acetylated H3-K56 unshifted (-) and heat shifted for 1 hour at 37°C (+). **B.** H3-K56Ac nucleosome crystals. **C.** H3-K56Q nucleosome crystals. **D.** H3-K56E nucleosome crystals. Summary of data collection statistics in appendix.

conditions and thoroughly dialyzed into renaturing buffer. Histone octamers were purified on an S200 size exclusion column; the mono-disperse elution profile was identical to wt octamer (data not shown) indicating that the point mutation did not affect the size or distribution of the histone octamer. This is not surprising, as H3-56 is located on the outside of the histone octamer. AU-PAGE is a sensitive measurement of protein charge and size, and was next used to analyze the mutant octamers. Figure 4.6.A shows how the loss of one positively charged lysine residue decreased the mobility of H3.

Using these renatured octamers, I reconstituted mononucleosomes using the 147 bp α -satellite palindromic DNA (figure 4.6.B and 4.7.A) (Dyer et al., 2004). These nucleosomes were able to heat shift to a central position on the 147 bp DNA and had similar electrophoretic mobility as the MT nucleosome, indicating that H3-K56Ac does not inhibit nucleosome formation.

4.3.3 Analysis to whether H3-K56Ac affects the nucleosomes crystal structure

To investigate whether the acetylation of K56 affects nucleosome structure, I crystallized nucleosomes containing H3-K56ac (figure 4.7). The nucleosomes crystallized under similar conditions to that of wild type *xenopus* NCPs (Luger et al., 1997). However, H3-K56ac did not diffract to a resolution better than 5Å. I also crystallized nucleosomes containing either H3-K56E or H3-K56Q, which allowed me to solve the structures using molecular replacement to a resolution of 3.1 and 3.5 Å, respectively (Table shown in appendix).

In the crystal structures of H3-K56Q and-K56E NCPs, the DNA path at the entry and exit site of the nucleosome was not significantly altered by the substitution of Q or E for the positively charged K (figure 4.8.A). While the phosphate backbone was clearly

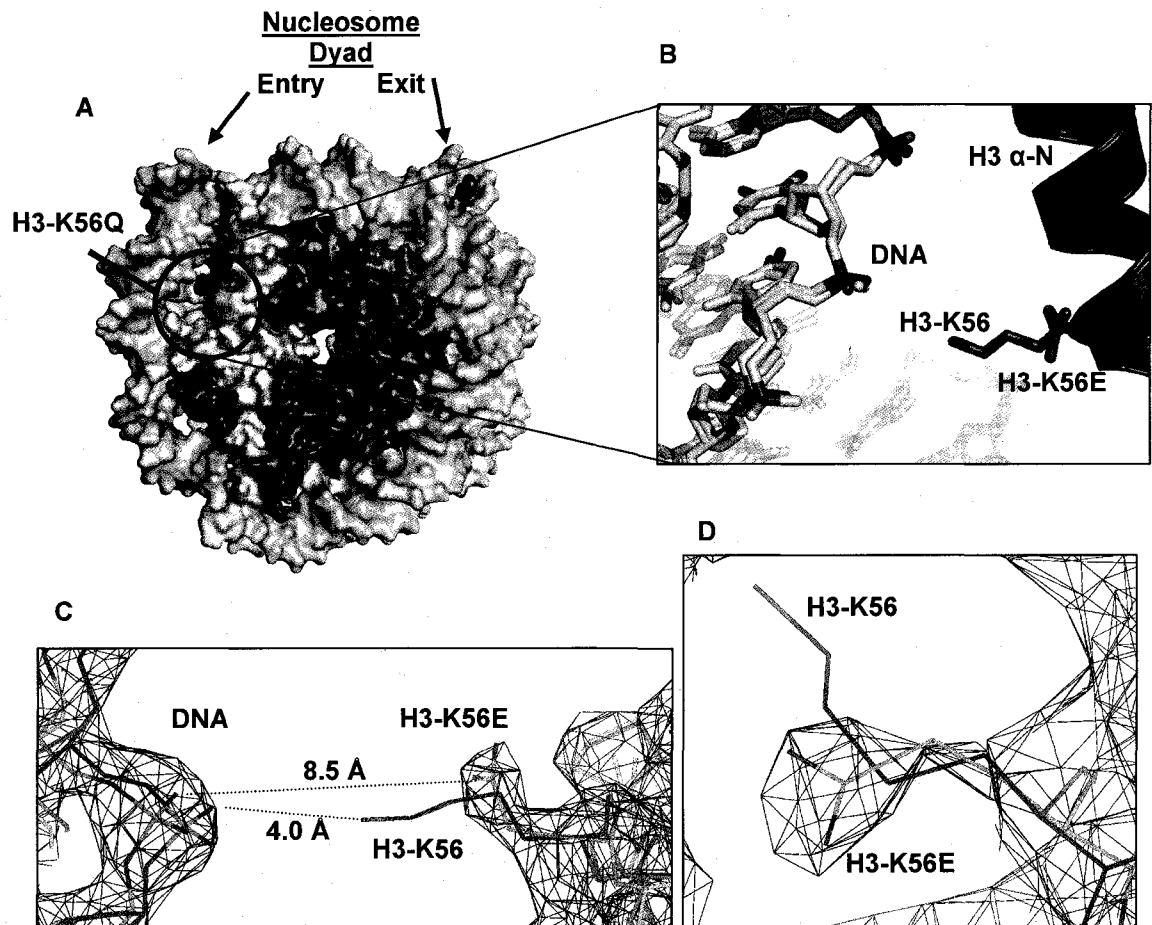


Figure 4.8 Crystal structure of nucleosome containing H3-K56E. **A.** Location of H3-K56Q (pink) in the nucleosome (surface representation). Histones H2A, H2B, H3 and H4 shown in light yellow, red, blue and green, respectively, DNA shown in grey. **B.** H3-K56E has a different conformation than H3-K56. Structure of H3-K56E nucleosome superimposed with WT nucleosome (ribbon diagram). Shown with DNA (grey) phosphates (red w/ grey) MT and (solid red) H3-K56E. **C.** H3-K56Q mutation increases the distance from DNA. Fo-Fc maps generated in CNS contoured to 2.0σ , displayed in coot. Indicates the difference in distance from side chain to DNA (green backbone WT, yellow backbone H3-K56E). **D.** Composite omit maps generated in CNS with residues H3-50-60 omitted in the model.

visible in the electron density maps (figure 4.8.C and D), I observed a small difference in the path of the modeled DNA (figure 4.8). Although, at this resolution I suspect that this difference is not significant. These data suggest that these mutations H3-K56E or H3-K56Q do not disrupt the global structure of nucleosomes as shown by a rmsd of .3478 Å for H3-K56E compared to PDB entry 1KX5. Due to the low resolution H3-K56Q, I was unable to determine side chain conformations and therefore did not calculate the rmsd differences.

In MT nucleosomes, H3-K56 makes water mediated hydrogen bonds with the phosphate backbone. In mutant nucleosomes the H3-K56E side chain is clearly visible in the electron density generated in omit maps (figure 4.8.D). The mutant glutamic acid relocates the side chain of H3-K56 away from the DNA and towards the solvent. This could decrease the protein-DNA stability at the entry and exit of the nucleosome.

4.3.4 H3-K56 contributes to nucleosome stability

In attempt to resolve the recent claims in the literature regarding stability of the H3-K56Ac containing nucleosomes, I used sedimentation velocity to analyze the salt-dependent structural transitions of nucleosomes containing H3-K56ac, H3-K56Q and non-modified nucleosomes (MT). Major type nucleosome core particles are stable over a wide range of NaCl concentrations and undergo conformational changes between 0 – 700 mM NaCl (Ausio et al., 1984b; McGhee et al., 1980; Park et al., 2004; Wilhelm and Wilhelm, 1980; Yager and van Holde, 1984). Above 750 mM NaCl, histones begin to disassociate from the DNA (Yager et al., 1989; Yager and van Holde, 1984). I have used nucleosomes containing (H2A, H2B, H4, H3-K56Ac or H3-K56Q)₂

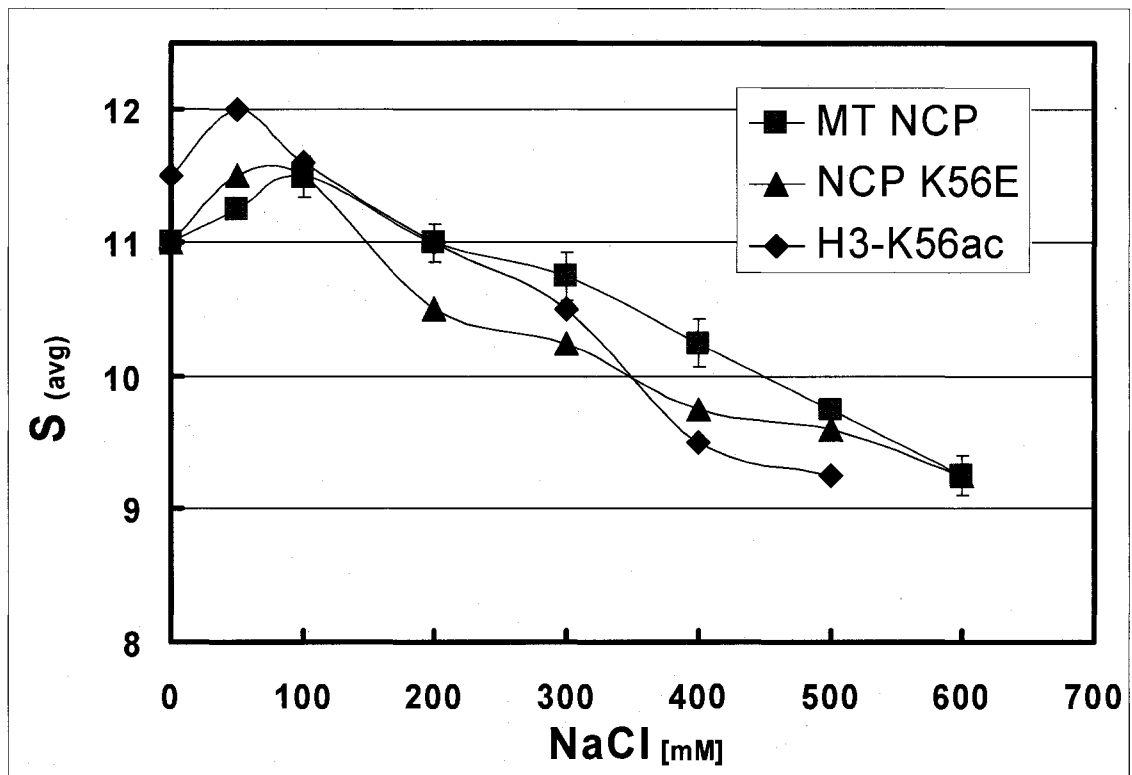


Figure 4.9 H3-K56 contributes to the nucleosome stability in salt. Ionic strength dependence of the reconstituted NCP containing major type histones (MT) (red ■) compared to reconstituted NCP with point mutation H3 K56Q (black ▲) which mimics acetylation and nucleosomes containing in vitro acetylated H3-K56 (blue ◆). The buffer used was 0-600 mM NaCl, 10 mM Tris-Cl pH 7.5, 1 mM EDTA. Runs were carried out at 50,000 RPM at 20° and corrected for buffer viscosity. Second moment analysis was obtained using Ultra Scan version 9.4.

and (H2A, H2B, H3, H4)₂ with 147 bp DNA to study the hydrodynamic properties using sedimentation velocity in increasing ionic strength.

Nucleosomes were incubated with 0 – 600 mM NaCl, sedimented and analyzed using the UltraScan software package to calculate the average sedimentation coefficient. I observed different salt-dependent hydrodynamic properties with nucleosomes containing H3-K56ac, H3-K56Q and MT nucleosomes.

From 0-100 mM NaCl H3-K56Ac NCPs had a 0.5 larger sedimentation coefficient than MT and H3-K56Q NCPs (figure 4.9). At 100 mM NaCl, the S values for H3-K56Ac, H3-K56Q and MT NCP intersect at 11S. From 100 – 200 mM NaCl, the nucleosome has the same hydrodynamic shape as expected from the crystal structure (Czarnota and Ottensmeyer, 1996). As the NaCl concentration is increased from 300-600 H3-K56Ac and H3-K56Q, nucleosomes have lower average S-values (figure 4.9). From 300 – 600 mM NaCl, the frictional coefficient of the nucleosome increases, likely due to the unraveling the ends of the nucleosomal DNA (Czarnota and Ottensmeyer, 1996; Park et al., 2004). These data sets indicate a small difference in salt-dependent structural transitions of nucleosomes containing K56Ac. I have also observed that the point mutation H3-K56Q does not identically replicate the H3-K56Ac-NCP hydrodynamic transitions in elevated NaCl. However, the point mutation from K to Q and the acetylation of H3-K56 both change the hydrodynamic structure of the nucleosome core particle. I suspect this the difference in sedimentation may be due to a change in the nucleosome structure causing a change in frictional coefficients, although I did not observe a decrease in the stability of the acetylated nucleosome.

4.3.5 H3-K56Ac disrupts chromatin condensation

It has been speculated that acetylation of H3-K56 enhances accessibility to DNA by either inhibiting chromatin condensation or facilitating recognition by nucleosome remodeling enzymes (Ozdemir et al., 2006; Xu et al., 2005). I propose that acetylation of K56 may affect gene transcription and DNA repair by altering the chromatin structure via small changes in the structure of the nucleosome core. I have demonstrated that acetylation affects the frictional coefficient of the nucleosome core particle from 0-600 mM NaCl which may be caused by a change in the hydrodynamic nucleosome structure. To test this hypothesis, I reconstituted nucleosomal arrays with recombinant histones (containing H2A, H2B, H4 and either in vitro acetylated H3-K56, H3-K56Q or non-modified H3) on the 208x12 5S DNA model template to analyze the Mg^{++} dependent nucleosomal array condensation. To determine whether the nucleosome template was equally saturated, I used sedimentation velocity and EcoR1 digestion.

Sedimentation velocity of nucleosomal arrays in TEN buffer is used to determine the homogeneity and octamer saturation of the DNA template (Demeler et al., 1997; Fletcher et al., 1994; Hansen et al., 1991). Using sedimentation velocity, I obtained the integral sedimentation coefficient distribution (Gs) of H3-K56Q, H3-K56Ac and MT H3 containing nucleosome arrays in low salt TEN buffer (figure 2.10). The sedimentation velocity of nucleosomal arrays containing non-acetylated and acetylated H3-K56 and H3-K56Q histones produced similar sedimentation coefficient distributions (figure 4.10). I obtained distributions with values ranging from 22-30S with midpoints of 25S for H3-K56ac, 26S for H3-K56Q and 25S for MT H3 arrays, which is equivalent to an average of 10.5 ± 2 nucleosomes per 208-12 DNA template.

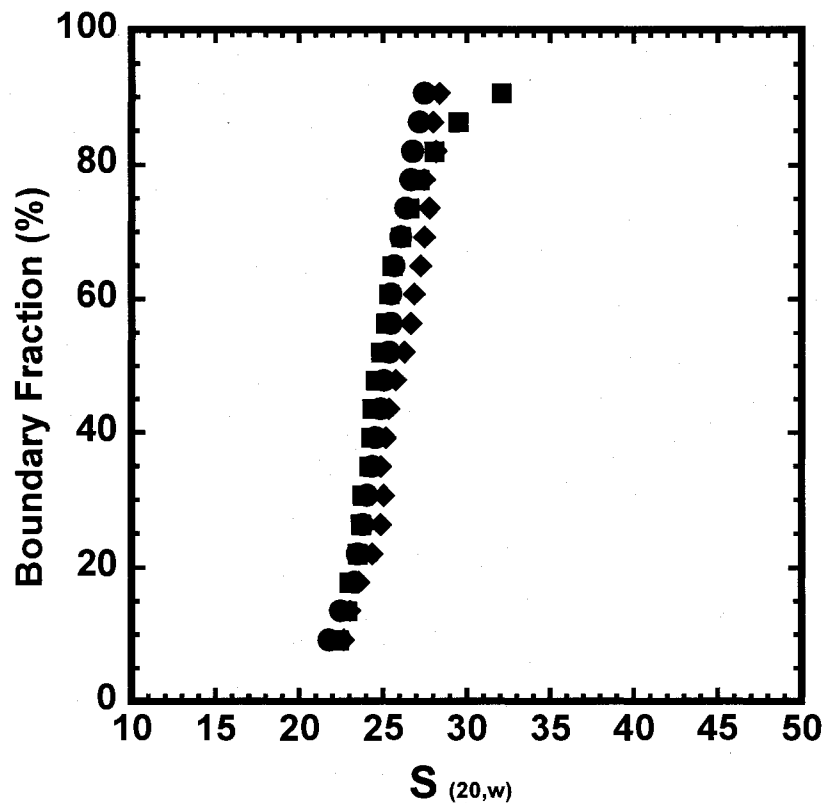


Figure 4.10 Sedimentation velocity analysis of nucleosomal arrays in TEN buffer. Reconstituted 208-12 nucleosomal arrays containing unmodified xenopus (●) xenopus H3-K56Q (■) and H3-K56Ac (◆) histone octamers in TEN buffer. Sedimentation velocity experiments were carried out at 20,000 RPM, 20° C. and analyzed as described in methods and materials. Shown is the diffusion corrected integral distribution of S corrected for water at 20° C. ($S_{20,w}$) is shown.

Digestion with EcoRI cleaves the array into twelve 197 bp fragments. Digested arrays migrate as either free DNA or nucleosomal DNA. The gel band density is measured to determine the percentage of non-occupied 208 bp repeat. I determined the percentage of DNA to be 14.2% for H3-K56Ac, 13.8% for H3-K56Q and 13.2% for non-modified arrays. Twelve and a half percent of free DNA repeats is equivalent to an average of 10.5 nucleosomes per 208-12 template. Sedimentation velocity and EcoRI digestion results together suggest that H3-K56Ac, H3-K56Q and WT H3 containing arrays are equally saturated with an average of 10.5 nucleosomes per 208-12 template. Therefore, I was able to compare these nucleosomal arrays in chromatin condensation assays, and any changes I observe will be due to the altered histones rather than different saturation levels.

I assayed nucleosomal array oligomerization, which mimics inter-chromatin fiber interactions in cellular chromatin (Hansen, 2002; Lu et al., 2006; Schwarz et al., 1996), by measuring the amount of monomeric arrays as a function of $MgCl_2$ concentration (figure 4.11). When compared to unmodified arrays, H3-K56 acetylated arrays and H3-K56Q arrays require more $MgCl_2$ for inter-nucleosomal array oligomerization. Arrays containing H3-K56Ac require ~ 0.5 mM more $MgCl_2$ to induce inter-nucleosomal array oligomerization. The non-modified arrays begin to form non-soluble oligomers at 1.75 mM while arrays containing H3-K56Ac begin to oligomerize at 2.25 mM $MgCl_2$. The point at which 50% of the arrays are oligomerized (Mg^{50}) is 2.3 mM for non-modified and 2.8 mM and 2.75 mM for H3-K56Ac and H3-K56Q arrays, respectively (figure 4.10). Thus, acetylation of H3-K56 slightly inhibits inter-nucleosomal array oligomerization.

Upon titration of $MgCl_2$, nucleosomal arrays transition from a “beads-on-a-string” array to folded arrays in which nucleosomes make short range intra – nucleosomal array interactions through protein-DNA and protein-protein interactions mediated by

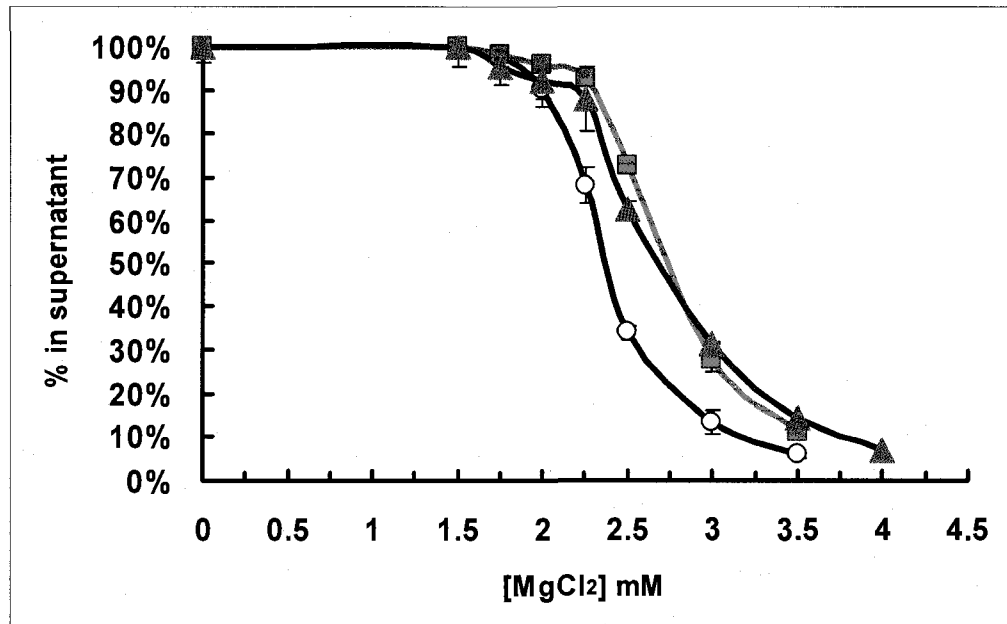


Figure 4.11 Acetylation of H3-K56 inhibits the Mg^{+2} -dependent oligomerization of nucleosomal arrays. Nucleosomal arrays containing WT *xenopus* (○), H3-K56Q (■), and H3-K56Ac (Δ) were incubated with the indicated concentration of $MgCl_2$ and assayed for oligomerization (see methods and materials). Shown is the % total A_{260} that remained in the supernatant after micro-centrifugation as a function of $MgCl_2$.

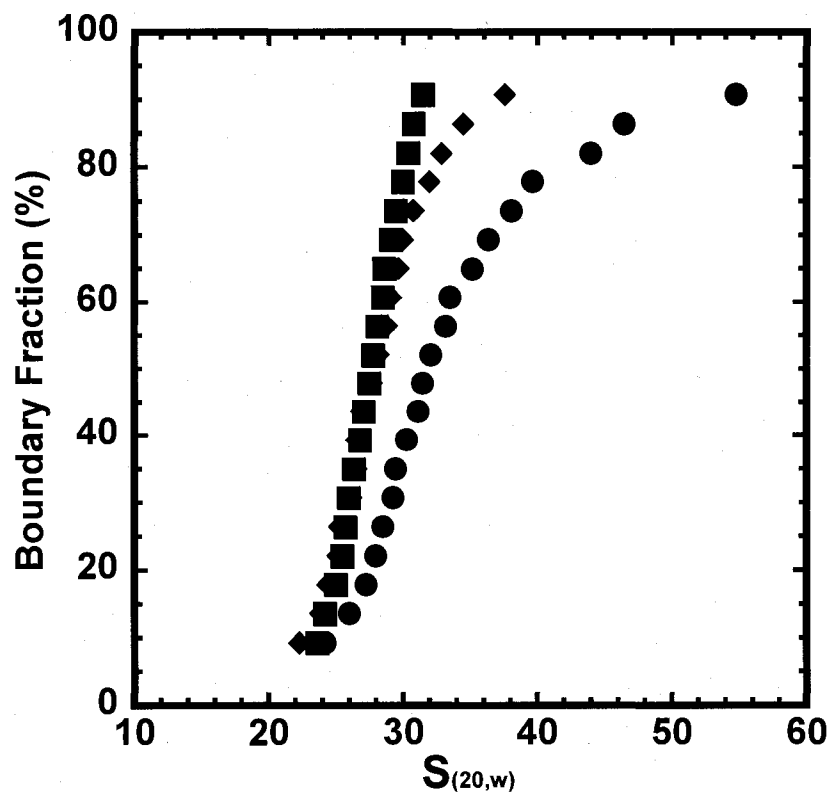


Figure 4.12 H3-K56Ac inhibits intra-nucleosomal array folding Non-modified xenopus (●) and xenopus containing H3-K56Ac (■) and H3-K56Q (◆) 208-12 nucleosomal arrays in 1.0 mM MgCl₂-TEN and 1.5 mM MgCl₂-TEN buffer. Sedimentation Velocity experiments were carried out at 15,000 RPM, 20^o C. and analyzed as described in methods and materials. Shown is the diffusion corrected integral distribution of sedimentation coefficients corrected for water at 20^o C ($S_{(20,w)}$).

the histone NTDs (Kan et al., 2007; Schwarz and Hansen, 1994). The nucleosomal array transition to the moderately folded and fully folded structures have sedimentation coefficients of 40S and 55S, respectively (Schwarz and Hansen, 1994). This experiment reproduces reversible transitions that are seen when endogenous chromatin purified from living cells is similarly treated (Fletcher and Hansen, 1996). I used sedimentation velocity to assay the transition from the unfolded 'beads-on-a-string' array to the maximally folded 55S nucleosomal array (figure 4.12). I incubated nucleosomal arrays containing the acetylated H3-K56, H3-K56Q and non-acetylated arrays with 1.0 mM MgCl₂ and measured the sedimentation. A substantial proportion of the non-acetylated arrays sedimented between 40-55S (figure 4.12), which is indicative of a mixture of moderately folded (40S) and maximally folded (55S) nucleosomal arrays. Arrays containing H3-K56Ac and H3-K56Q were unable to achieve the 55S structure in 1.0 mM MgCl₂. Together these data sets demonstrate that acetylation of H3-K56 disrupts intra-nucleosomal array folding and oligomerization.

4.4 Discussion

These data suggest that acetylation of H3-K56 may slightly affect the nucleosome structure and inhibit both oligomerization and folding of nucleosomal arrays. I postulate that acetylation of H3-K56 may disrupt the protein-DNA interaction of the nucleosome and cause an inhibition nucleosomal array condensation. Such a mechanism could play a role in euchromatin formation and enable DNA accessibility to cellular mechanisms such as histone exchange, transcription and DNA damage/repair.

4.4.1 Large scale *in vitro* acetylation of H3-K56

The physical interaction between Rtt109 and Vps75 is unknown. However *in vivo* one function of Vps75 may be to stabilize Rtt109 (Fillingham et al., 2008). The HAT, Rtt109, is barely catalytically active on its own, but is dependent on the histone chaperone Vps75 to target specific acetylation to H3-K56 (figure 4.3 and 4.4). However, Asf1 can substitute for Vps75 in the acetylation reaction *in vivo* (Driscoll et al., 2007; Fillingham et al., 2008; Han et al., 2007; Tsubota et al., 2007) and *in vitro* (data not shown). This may be caused by the histone chaperone binds H3 alone or the (H3-H4)₂ complex and presents H3 to Rtt109 for specific acetylation.

Rtt109 along with Gcn5 have been shown to be involved with the acetylation of H3-K9 (Fillingham et al., 2008). Although further experiments are necessary to confirm which residues are acetylated after H3-K56 by Rtt109 *in vitro*, from our analyses I estimate that a majority of the purified sample is homogeneously acetylated at K56. Therefore, our observations with nucleosomes and nucleosomal arrays are mainly the result of H3-K56 acetylation.

4.4.2 H3-K56 contributes to the stability of the nucleosome

Thus far there have been no direct analyses regarding the effect of H3-K56 acetylation on nucleosome structure. I applied x-ray crystallography and sedimentation velocity techniques to compare the nucleosome structure and stability of reconstituted nucleosomes containing K56Ac and K56Q. H3-K56Ac NCP crystallized under conditions similar to WT *Xenopus* nucleosomes. However, the crystals were brittle, did not contain substantial volume and had poor x-ray diffraction (5Å). Reconstituted H3-K56Ac NCPs were able to heat shift to a central position and, as

observed using sedimentation velocity, from homogenous samples. I suspect the poor diffraction quality could be due to the highly dynamic ends of the nucleosomal DNA which may inhibit the intra-nucleosome base stacking necessary to nucleate uniform NCP crystal packing (Davey et al., 2002; Luger et al., 1997). The poor diffraction quality could also be due to the inhibitory chromatin condensation effect of H3-K56 acetylation. The nucleosomes-nucleosome interactions, which nucleate the crystal packing, could have been similarly inhibited as the chromatin condensation shown with nucleosomal arrays.

Nucleosome crystals containing point mutations H3-K56E and H3-K56Q diffracted to 3.1 Å. Using electron density maps made with omitted H3 residues 50-60 clearly showed the side chain of H3-K56E. There is a lot of area for alternate side chain conformations and post-translational modifications at this location. This indicates that the modification to H3-K56 could spatially exist without perturbing the DNA path. I did not observe a significant difference in the position of the DNA. This also demonstrates that the mutation and the acetylation of H3-K56 do not inhibit the formation of the nucleosome. However, the similarities of the mutant nucleosomes to WT nucleosomes could be the result of nucleosome purification in a conformation compatible for nucleating the crystal lattice. Base stacking of adjacent nucleosomes is critical for nucleosome crystallization (Luger et al., 1997). Therefore, if the ends of the nucleosomal DNA are in a dynamic on/off state crystallization could catch the nucleosomes in the conformation similar to MT nucleosome crystals. However, I did observe differences in the hydrodynamic transitions of nucleosomes containing H3-K56Q and H3-K56Ac.

I investigated the structural transitions of nucleosomes containing H3-K56Ac and H3-K56Q by analyzing the sedimentation distribution in response to changes in ionic strength. H3-K56Q was used to simulate the effects of a constitutively acetylated

residue. H3-K56Ac causes a greater change in nucleosome structural transitions than H3-K56Q, both relative to the MT nucleosomes. My data suggest that acetylation of H3-K56 may influence the dynamics of the protein-DNA interactions at the entry and exit of the nucleosome resulting in smaller S-values in buffer containing NaCl concentrations > 200 mM NaCl. One explanation may be that altered protein-DNA interaction at the entry and exit point of the nucleosome cause the DNA ends to unravel from the histone octamer. The sedimentation coefficient ($S_{20,w}$) is proportional to the Mass (M) divided by the frictional coefficient (f). Therefore, if the ends of the DNA unravel from the nucleosome the $S_{20,w}$ would theoretically decrease. This may be one of the reasons for the altered sedimentation coefficients of H3-K56Ac nucleosomes from 300- 500 mM NaCl.

Nucleosome dynamics have been quantitatively examined using kinetic studies which measure nuclease accessibility to nucleosomal DNA (Polach and Widom, 1999). The highest accessibility is found at the ends of the nucleosomal DNA and is thought to be the result of transient DNA 'breathing' and not nucleosome sliding (Anderson et al., 2002). Acetylation of H3-K56 could alter the equilibrium to more exposed DNA at the ends of nucleosomal DNA, but direct measurements are necessary to test this hypothesis.

4.4.3 Acetylation of the nucleosome core disrupts nucleosomal array condensation

It has been proposed that acetylated H3-K56 affects chromatin structure by enabling DNA to be more accessible to transcription factors, DNA damage/repair and chromatin remodelers (Ozdemir et al., 2006; Williams et al., 2008; Xu et al., 2005; Xu et al.,

2007). I have reconstituted nucleosome arrays containing H3-K56Ac and H3-K56Q to investigate the role histone acetylation within the nucleosome core has on chromatin condensation. I have demonstrated that H3-K56Ac inhibits chromatin condensation. In our assays, nucleosomal arrays containing H3-K56Ac and H3-K56Q required more $MgCl_2$ to make intra-nucleosomal and inter-nucleosomal array interactions. H3-K56ac and H3-K56Q nucleosomal arrays are only able to form the moderately folded conformation under the same conditions in which WT arrays were able to form the maximally folded 55S structure (figure 4.11). This indicates chromatin containing the H3-K56Ac may shift the equilibrium toward the unfolded chromatin state.

H3-K56 lies ~ 10 bp from the entry and exit sites of nucleosomal DNA. I predict that a disruption of the protein-DNA interaction at this site could increase the nucleosome linker DNA length. EM studies with arrays containing a nucleosome repeat length of 207 bp have ~11 nucleosomes per 11 nm with ~35 nm diameter, while a 217 bp NRL contain ~ 17 nucleosomes per 11 nm and a folded diameter of ~45 nm (Robinson et al., 2006). Thus I hypothesize that the release of the ends of the DNA in H3-K56Ac and H3-K56Q chromatin may increase the linker DNA length and result in chromatin which is resistant to form the '30 nm' fiber.

The angle at which the DNA enters and exits the DNA is critical for the formation of the compacted folded chromatin fiber (Robinson and Rhodes, 2006). Another hypothesis to how H3-K56Ac may inhibit chromatin condensation is by altering the angle at which the DNA enters and exits the nucleosome. To test directly test these hypothesizes, site nuclease digestion would directly examine the amount of DNA which is protected by H3-K56Ac nucleosomes.

Even though I have shown that H3-56Ac inhibits chromatin condensation, I do not rule out that acetylation of H3-K56 may also enhance recognition by nucleosome binding proteins (such as Swi/Snf and Sir2) which actively alter the chromatin packing.

Such enzymes could bind to the area of the modification (α -N) or the released DNA, which would lead to either the nucleosome repositioning (Swi/Snf) in euchromatin or the removal of acetylation at H3-K56ac in heterochromatin foci by HDACs (Sir2).

4.5 Future Directions

The preparation of crystallization-quantities of enzymatically modified NCP has not been reported in the literature, thus this result is novel and a significant contribution towards our goal of investigating the structure and function of nucleosomes with a post-translational modifications within the core.

Sedimentation velocity analysis does not directly measure the release of the DNA ends. I was only able to measure the overall shape of the nucleosome core particle. To directly examine the effects of H3-K56Q, H3-K56E and H3-K56Ac on the nucleosome dynamics methods developed by the Widom lab could be used (Polach and Widom, 1995). Another method could use FRET to directly measure the rate at which the DNA ends disassociate from the nucleosome with labeled DNA and histone .

It also would also be interesting to determine if acetylation of H3-K56 would reduce the affinity of Vps75 and/or Rtt109 to the histone. If this were so, then this could aid in reducing the non-specific acetylation of lysine residues in H3.

Table 4.1 Summary of crystallography data

Data collection	H3-K56E	H3-K56Q
Space group	P212121	P212121
Unit Cell	106.04, 109.56, 181.35 90.00, 90.00, 90.00	105.56, 109.54, 180.65 90.00, 90.00, 90.00
resolution	40.0-2.9	40.0-3.0
Mosaicity	1.17	0.69
Total number of reflections	282924	308860
Number of unique reflections	47390	42705
Average redundancy	5.97	7.23
% completeness	99.7	100.0
Rmerge	0.103	0.192
Reduced ChiSquared	0.98	0.99
Output <l/sigl>	9.0	6.0
Refinement		
refinement resolution:	40.0 - 3.0 A	40.0 - 3.5 A
theoretical total number of reflections in resolution range	82288 (100.0 %)	51011 (100.0 %)
number of reflections rejected	0 (0.0 %)	0 (0.0 %)
total number of reflections used	81011 (98.4 %)	50165 (98.3 %)
number of reflections in working set	77023 (93.6 %)	47701 (93.5 %)
number of reflections in test set	3988 (4.8 %)	2464 (4.8 %)
Rfree	0.2997	0.3593
Rworking	0.2287	0.2711
rmsd bonds	0.007031	0.008602
rmsd angles	1.12210	1.31416

Appendix- Closing remarks

This work as demonstrated that histones with a large amount of primary sequence variation can maintain a conserved function, although, single post-translational modifications can affect chromatin condensation. We observed similarities in chromatin function when comparing the centromeric H3 variant CENP-A to major type H3, even with a lack of sequence conservation. On the other hand, we demonstrated how a single post-translational modification (PTM) to Lysine-56 on histone H3 and histone orthologs can differ in chromatin condensation properties. Together, these studies suggest that subtle variations in histone sequence or posttranslational modifications may result in differences in chromatin higher order structure. Further studies are needed to determine if histones with PTMs and histone variants have different protein-protein interactions such as histone chaperones or histone modifying enzymes. Differences in binding could lead to functional differentiation such as localization of histones to chromatin foci such as centromeres and/or areas of active gene transcription.

References

- Anderson, J.D., Thastrom, A. and Widom, J. (2002) Spontaneous access of proteins to buried nucleosomal DNA target sites occurs via a mechanism that is distinct from nucleosome translocation. *Mol Cell Biol*, **22**, 7147-7157.
- Annunziato, A.T. and Hansen, J.C. (2000) Role of histone acetylation in the assembly and modulation of chromatin structures. *Gene Expr*, **9**, 37-61.
- Ausio, J., Borochoy, N., Seger, D. and Eisenberg, H. (1984a) Interaction of chromatin with NaCl and MgCl₂. Solubility and binding studies, transition to and characterization of the higher-order structure. *J Mol Biol*, **177**, 373-398.
- Ausio, J., Seger, D. and Eisenberg, H. (1984b) Nucleosome core particle stability and conformational change. Effect of temperature, particle and NaCl concentrations, and crosslinking of histone H3 sulfhydryl groups. *J Mol Biol*, **176**, 77-104.
- Bash, R., Wang, H., Yodh, J., Hager, G., Lindsay, S.M. and Lohr, D. (2003) Nucleosomal arrays can be salt-reconstituted on a single-copy MMTV promoter DNA template: their properties differ in several ways from those of comparable 5S concatameric arrays. *Biochemistry*, **42**, 4681-4690.
- Bednar, J., Horowitz, R.A., Dubochet, J. and Woodcock, C.L. (1995) Chromatin conformation and salt-induced compaction: three-dimensional structural information from cryoelectron microscopy. *J Cell Biol*, **131**, 1365-1376.
- Black, B.E., Brock, M.A., Bedard, S., Woods, V.L., Jr. and Cleveland, D.W. (2007) An epigenetic mark generated by the incorporation of CENP-A into centromeric nucleosomes. *Proc Natl Acad Sci U S A*, **104**, 5008-5013.
- Black, B.E., Foltz, D.R., Chakravarthy, S., Luger, K., Woods, V.L., Jr. and Cleveland, D.W. (2004) Structural determinants for generating centromeric chromatin. *Nature*, **430**, 578-582.
- Blower, M.D. and Karpen, G.H. (2001) The role of *Drosophila* CID in kinetochore formation, cell-cycle progression and heterochromatin interactions. *Nat Cell Biol*, **3**, 730-739.

- Blower, M.D., Sullivan, B.A. and Karpen, G.H. (2002) Conserved organization of centromeric chromatin in flies and humans. *Dev Cell*, **2**, 319-330.
- Brunger, A.T. (2007) Version 1.2 of the Crystallography and NMR system. *Nat Protoc*, **2**, 2728-2733.
- Butler, P.J. and Thomas, J.O. (1980) Changes in chromatin folding in solution. *J Mol Biol*, **140**, 505-529.
- Camahort, R., Li, B., Florens, L., Swanson, S.K., Washburn, M.P. and Gerton, J.L. (2007) Scm3 is essential to recruit the histone h3 variant cse4 to centromeres and to maintain a functional kinetochore. *Mol Cell*, **26**, 853-865.
- Cameron, I.L., Hunter, K.E. and Smith, N.K. (1988) Fluctuation in the intracellular concentration of Na⁺ and Cl⁻ but not of K⁺ or Mg²⁺ at mitosis of the first cell cycle in fertilized sea urchin eggs. *Cell Biol Int Rep*, **12**, 951-958.
- Carroll, C.W. and Straight, A.F. (2007) Centromeric chromatin gets loaded. *J Cell Biol*, **176**, 735-736.
- Carruthers, L.M. and Hansen, J.C. (2000) The core histone N termini function independently of linker histones during chromatin condensation. *J Biol Chem*, **275**, 37285-37290.
- Carruthers, L.M., Schirf, V.R., Demeler, B. and Hansen, J.C. (2000) Sedimentation velocity analysis of macromolecular assemblies. *Methods Enzymol*, **321**, 66-80.
- Celic, I., Masumoto, H., Griffith, W.P., Meluh, P., Cotter, R.J., Boeke, J.D. and Verreault, A. (2006) The sirtuins hst3 and Hst4p preserve genome integrity by controlling histone h3 lysine 56 deacetylation. *Curr Biol*, **16**, 1280-1289.
- Chakravarthy, S., Park, Y.J., Chodaparambil, J., Edayathumangalam, R.S. and Luger, K. (2005) Structure and dynamic properties of nucleosome core particles. *FEBS Lett*, **579**, 895-898.
- Chodaparambil, J.V., Barbera, A.J., Lu, X., Kaye, K.M., Hansen, J.C. and Luger, K. (2007) A charged and contoured surface on the nucleosome regulates chromatin compaction. *Nat Struct Mol Biol*, **14**, 1105-1107.
- Czarnota, G.J. and Ottensmeyer, F.P. (1996) Structural states of the nucleosome. *J Biol Chem*, **271**, 3677-3683.

- Daban, J.R. (2003) High concentration of DNA in condensed chromatin. *Biochem Cell Biol*, **81**, 91-99.
- Dalal, Y., Wang, H., Lindsay, S. and Henikoff, S. (2007) Tetrameric structure of centromeric nucleosomes in interphase *Drosophila* cells. *PLoS Biol*, **5**, e218.
- Davey, C.A., Sargent, D.F., Luger, K., Maeder, A.W. and Richmond, T.J. (2002) Solvent mediated interactions in the structure of the nucleosome core particle at 1.9 Å resolution. *J Mol Biol*, **319**, 1097-1113.
- Davie, J.R. (1982) Two-dimensional gel systems for rapid histone analysis for use in minislab polyacrylamide gel electrophoresis. *Anal Biochem*, **120**, 276-281.
- Davie, J.R. and Saunders, C.A. (1981) Chemical composition of nucleosomes among domains of calf thymus chromatin differing in micrococcal nuclease accessibility and solubility properties. *J Biol Chem*, **256**, 12574-12580.
- De Koning, L., Corpet, A., Haber, J.E. and Almouzni, G. (2007) Histone chaperones: an escort network regulating histone traffic. *Nat Struct Mol Biol*, **14**, 997-1007.
- Demeler, B., Behlke, J. and Ristau, O. (2000) Molecular parameters from sedimentation velocity experiments: whole boundary fitting using approximate and numerical solutions of Lamm equation. *Methods Enzymol*, **321**, 38-66.
- Demeler, B., Saber, H. and Hansen, J.C. (1997) Identification and interpretation of complexity in sedimentation velocity boundaries. *Biophys J*, **72**, 397-407.
- Demeler, B. and van Holde, K.E. (2004) Sedimentation velocity analysis of highly heterogeneous systems. *Anal Biochem*, **335**, 279-288.
- Driscoll, R., Hudson, A. and Jackson, S.P. (2007) Yeast Rtt109 promotes genome stability by acetylating histone H3 on lysine 56. *Science*, **315**, 649-652.
- Dunn, K.L. and Davie, J.R. (2005) Stimulation of the Ras-MAPK pathway leads to independent phosphorylation of histone H3 on serine 10 and 28. *Oncogene*, **24**, 3492-3502.
- Dyer, P.N., Edayathumangalam, R.S., White, C.L., Bao, Y., Chakravarthy, S., Muthurajan, U.M. and Luger, K. (2004) Reconstitution of nucleosome core particles from recombinant histones and DNA. *Methods Enzymol*, **375**, 23-44.

- Earnshaw, W.C. and Migeon, B.R. (1985) Three related centromere proteins are absent from the inactive centromere of a stable isodicentric chromosome. *Chromosoma*, **92**, 290-296.
- Eitoku, M., Sato, L., Senda, T. and Horikoshi, M. (2008) Histone chaperones: 30 years from isolation to elucidation of the mechanisms of nucleosome assembly and disassembly. *Cell Mol Life Sci*, **65**, 414-444.
- Emsley, P. and Cowtan, K. (2004) Coot: model-building tools for molecular graphics. *Acta Crystallogr D Biol Crystallogr*, **60**, 2126-2132.
- English, C.M., Adkins, M.W., Carson, J.J., Churchill, M.E. and Tyler, J.K. (2006) Structural basis for the histone chaperone activity of Asf1. *Cell*, **127**, 495-508.
- Fan, J.Y., Gordon, F., Luger, K., Hansen, J.C. and Tremethick, D.J. (2002) The essential histone variant H2A.Z regulates the equilibrium between different chromatin conformational states. *Nat Struct Biol*, **9**, 172-176.
- Felsenfeld, G. and McGhee, J.D. (1986) Structure of the 30 nm chromatin fiber. *Cell*, **44**, 375-377.
- Fernandez-Segura, E. and Warley, A. (2008) Electron probe X-ray microanalysis for the study of cell physiology. *Methods Cell Biol*, **88**, 19-43.
- Fillingham, J., Recht, J., Silva, A.C., Suter, B., Emili, A., Stagljar, I., Krogan, N.J., Allis, C.D., Keogh, M.C. and Greenblatt, J.F. (2008) Chaperone control of the activity and specificity of the histone H3 acetyltransferase Rtt109. *Mol Cell Biol*, **28**, 4342-4353.
- Fletcher, T.M. and Hansen, J.C. (1995) Core histone tail domains mediate oligonucleosome folding and nucleosomal DNA organization through distinct molecular mechanisms. *J Biol Chem*, **270**, 25359-25362.
- Fletcher, T.M. and Hansen, J.C. (1996) The nucleosomal array: structure/function relationships. *Crit Rev Eukaryot Gene Expr*, **6**, 149-188.
- Fletcher, T.M., Krishnan, U., Serwer, P. and Hansen, J.C. (1994) Quantitative agarose gel electrophoresis of chromatin: nucleosome-dependent changes in charge, sharp, and deformability at low ionic strength. *Biochemistry*, **33**, 2226-2233.

- Foltz, D.R., Jansen, L.E., Black, B.E., Bailey, A.O., Yates, J.R., 3rd and Cleveland, D.W. (2006) The human CENP-A centromeric nucleosome-associated complex. *Nat Cell Biol*, **8**, 458-469.
- Freidkin, I. and Katcoff, D.J. (2001) Specific distribution of the *Saccharomyces cerevisiae* linker histone homolog HHO1p in the chromatin. *Nucleic Acids Res*, **29**, 4043-4051.
- Furuyama, T., Dalal, Y. and Henikoff, S. (2006) Chaperone-mediated assembly of centromeric chromatin in vitro. *Proc Natl Acad Sci U S A*, **103**, 6172-6177.
- Garcia-Ramirez, M., Dong, F. and Ausio, J. (1992) Role of the histone "tails" in the folding of oligonucleosomes depleted of histone H1. *J Biol Chem*, **267**, 19587-19595.
- Garcia-Ramirez, M., Leuba, S.H. and Ausio, J. (1990) One-step fractionation method for isolating H1 histones from chromatin under non-denaturing conditions. *Protein Expr Purif*, **1**, 40-44.
- Gautier, T., Abbott, D.W., Molla, A., Verdel, A., Ausio, J. and Dimitrov, S. (2004) Histone variant H2ABbd confers lower stability to the nucleosome. *EMBO Rep*, **5**, 715-720.
- Georgel, P., Demeler, B., Terpening, C., Paule, M.R. and van Holde, K.E. (1993) Binding of the RNA polymerase I transcription complex to its promoter can modify positioning of downstream nucleosomes assembled in vitro. *J Biol Chem*, **268**, 1947-1954.
- Goldberg, A.D., Allis, C.D. and Bernstein, E. (2007) Epigenetics: a landscape takes shape. *Cell*, **128**, 635-638.
- Gordon, F., Luger, K. and Hansen, J.C. (2005) The core histone N-terminal tail domains function independently and additively during salt-dependent oligomerization of nucleosomal arrays. *J Biol Chem*, **280**, 33701-33706.
- Hake, S.B. and Allis, C.D. (2006) Histone H3 variants and their potential role in indexing mammalian genomes: the "H3 barcode hypothesis". *Proc Natl Acad Sci U S A*, **103**, 6428-6435.
- Han, J., Zhou, H., Li, Z., Xu, R.M. and Zhang, Z. (2007) The Rtt109-Vps75 histone acetyltransferase complex acetylates non-nucleosomal histone H3. *J Biol Chem*, **282**, 14158-14164.

- Hansen, J.C. (2002) Conformational dynamics of the chromatin fiber in solution: determinants, mechanisms, and functions. *Annu Rev Biophys Biomol Struct*, **31**, 361-392.
- Hansen, J.C., Ausio, J., Stanik, V.H. and van Holde, K.E. (1989) Homogeneous reconstituted oligonucleosomes, evidence for salt-dependent folding in the absence of histone H1. *Biochemistry*, **28**, 9129-9136.
- Hansen, J.C., Fletcher, T.M. and Kreider, J.I. (1999) Quantitative analysis of chromatin higher-order organization using agarose gel electrophoresis. *Methods Mol Biol*, **119**, 113-125.
- Hansen, J.C., Kreider, J.I., Demeler, B. and Fletcher, T.M. (1997) Analytical ultracentrifugation and agarose gel electrophoresis as tools for studying chromatin folding in solution. *Methods*, **12**, 62-72.
- Hansen, J.C. and Lohr, D. (1993) Assembly and structural properties of subsaturated chromatin arrays. *J Biol Chem*, **268**, 5840-5848.
- Hansen, J.C., Tse, C. and Wolffe, A.P. (1998) Structure and function of the core histone N-termini: more than meets the eye. *Biochemistry*, **37**, 17637-17641.
- Hansen, J.C. and Turgeon, C.L. (1999) Analytical ultracentrifugation of chromatin. *Methods Mol Biol*, **119**, 127-141.
- Hansen, J.C., van Holde, K.E. and Lohr, D. (1991) The mechanism of nucleosome assembly onto oligomers of the sea urchin 5 S DNA positioning sequence. *J Biol Chem*, **266**, 4276-4282.
- Jackson, V. (1988) Deposition of newly synthesized histones: hybrid nucleosomes are not tandemly arranged on daughter DNA strands. *Biochemistry*, **27**, 2109-2120.
- Jansen, L.E., Black, B.E., Foltz, D.R. and Cleveland, D.W. (2007) Propagation of centromeric chromatin requires exit from mitosis. *J Cell Biol*, **176**, 795-805.
- Kan, P.Y., Lu, X., Hansen, J.C. and Hayes, J.J. (2007) The H3 tail domain participates in multiple interactions during folding and self-association of nucleosome arrays. *Mol Cell Biol*, **27**, 2084-2091.

- Kerrigan, L.A. and Kadonaga, J.T. (1992) Periodic binding of individual core histones to DNA: inadvertent purification of the core histone H2B as a putative enhancer-binding factor. *Nucleic Acids Res*, **20**, 6673-6680.
- Kirsch, R.D. and Joly, E. (1998) An improved PCR-mutagenesis strategy for two-site mutagenesis or sequence swapping between related genes. *Nucleic Acids Res*, **26**, 1848-1850.
- Krogan, N.J., Cagney, G., Yu, H., Zhong, G., Guo, X., Ignatchenko, A., Li, J., Pu, S., Datta, N., Tikuisis, A.P., Punna, T., Peregrin-Alvarez, J.M., Shales, M., Zhang, X., Davey, M., Robinson, M.D., Paccanaro, A., Bray, J.E., Sheung, A., Beattie, B., Richards, D.P., Canadien, V., Lalev, A., Mena, F., Wong, P., Starostine, A., Canete, M.M., Vlasblom, J., Wu, S., Orsi, C., Collins, S.R., Chandran, S., Haw, R., Rilstone, J.J., Gandi, K., Thompson, N.J., Musso, G., St Onge, P., Ghanny, S., Lam, M.H., Butland, G., Altaf-Ul, A.M., Kanaya, S., Shilatifard, A., O'Shea, E., Weissman, J.S., Ingles, C.J., Hughes, T.R., Parkinson, J., Gerstein, M., Wodak, S.J., Emili, A. and Greenblatt, J.F. (2006) Global landscape of protein complexes in the yeast *Saccharomyces cerevisiae*. *Nature*, **440**, 637-643.
- Lacoste, N., Utley, R.T., Hunter, J.M., Poirier, G.G. and Cote, J. (2002) Disruptor of telomeric silencing-1 is a chromatin-specific histone H3 methyltransferase. *J Biol Chem*, **277**, 30421-30424.
- Laybourn, P.J. and Kadonaga, J.T. (1991) Role of nucleosomal cores and histone H1 in regulation of transcription by RNA polymerase II. *Science*, **254**, 238-245.
- Lowary, P.T. and Widom, J. (1998) New DNA sequence rules for high affinity binding to histone octamer and sequence-directed nucleosome positioning. *J Mol Biol*, **276**, 19-42.
- Lu, X. and Hansen, J.C. (2004) Identification of specific functional subdomains within the linker histone H10 C-terminal domain. *J Biol Chem*, **279**, 8701-8707.
- Lu, X., Klonoski, J.M., Resch, M.G. and Hansen, J.C. (2006) In vitro chromatin self-association and its relevance to genome architecture. *Biochem Cell Biol*, **84**, 411-417.
- Luger, K. (2006) Dynamic nucleosomes. *Chromosome Res*, **14**, 5-16.
- Luger, K. and Hansen, J.C. (2005) Nucleosome and chromatin fiber dynamics. *Curr Opin Struct Biol*, **15**, 188-196.

- Luger, K., Mader, A.W., Richmond, R.K., Sargent, D.F. and Richmond, T.J. (1997) Crystal structure of the nucleosome core particle at 2.8 Å resolution. *Nature*, **389**, 251-260.
- Lusser, A. and Kadonaga, J.T. (2004) Strategies for the reconstitution of chromatin. *Nat Methods*, **1**, 19-26.
- Masumoto, H., Hawke, D., Kobayashi, R. and Verreault, A. (2005) A role for cell-cycle-regulated histone H3 lysine 56 acetylation in the DNA damage response. *Nature*, **436**, 294-298.
- McBryant, S.J., Park, Y.J., Abernathy, S.M., Laybourn, P.J., Nyborg, J.K. and Luger, K. (2003) Preferential binding of the histone (H3-H4)₂ tetramer by NAP1 is mediated by the amino-terminal histone tails. *J Biol Chem*, **278**, 44574-44583.
- McBryant, S.J. and Peersen, O.B. (2004) Self-association of the yeast nucleosome assembly protein 1. *Biochemistry*, **43**, 10592-10599.
- McGhee, J.D., Felsenfeld, G. and Eisenberg, H. (1980) Nucleosome structure and conformational changes. *Biophys J*, **32**, 261-270.
- Mizuguchi, G., Xiao, H., Wisniewski, J., Smith, M.M. and Wu, C. (2007) Nonhistone Scm3 and histones CenH3-H4 assemble the core of centromere-specific nucleosomes. *Cell*, **129**, 1153-1164.
- Morris, S.A., Rao, B., Garcia, B.A., Hake, S.B., Diaz, R.L., Shabanowitz, J., Hunt, D.F., Allis, C.D., Lieb, J.D. and Strahl, B.D. (2007) Identification of histone H3 lysine 36 acetylation as a highly conserved histone modification. *J Biol Chem*, **282**, 7632-7640.
- Ng, H.H., Xu, R.M., Zhang, Y. and Struhl, K. (2002) Ubiquitination of histone H2B by Rad6 is required for efficient Dot1-mediated methylation of histone H3 lysine 79. *J Biol Chem*, **277**, 34655-34657.
- Okada, M., Cheeseman, I.M., Hori, T., Okawa, K., McLeod, I.X., Yates, J.R., 3rd, Desai, A. and Fukagawa, T. (2006) The CENP-H-I complex is required for the efficient incorporation of newly synthesized CENP-A into centromeres. *Nat Cell Biol*, **8**, 446-457.
- Ozdemir, A., Masumoto, H., Fitzjohn, P., Verreault, A. and Logie, C. (2006) Histone H3 lysine 56 acetylation: a new twist in the chromosome cycle. *Cell Cycle*, **5**, 2602-2608.

- Palmer, D.K., O'Day, K., Wener, M.H., Andrews, B.S. and Margolis, R.L. (1987) A 17-kD centromere protein (CENP-A) copurifies with nucleosome core particles and with histones. *J Cell Biol*, **104**, 805-815.
- Park, J.H., Cosgrove, M.S., Youngman, E., Wolberger, C. and Boeke, J.D. (2002) A core nucleosome surface crucial for transcriptional silencing. *Nat Genet*, **32**, 273-279.
- Park, Y.J., Dyer, P.N., Tremethick, D.J. and Luger, K. (2004) A new fluorescence resonance energy transfer approach demonstrates that the histone variant H2AZ stabilizes the histone octamer within the nucleosome. *J Biol Chem*, **279**, 24274-24282.
- Park, Y.J. and Luger, K. (2006) Structure and function of nucleosome assembly proteins. *Biochem Cell Biol*, **84**, 549-558.
- Peterson, C.L. and Laniel, M.A. (2004) Histones and histone modifications. *Curr Biol*, **14**, R546-551.
- Polach, K.J. and Widom, J. (1995) Mechanism of protein access to specific DNA sequences in chromatin: a dynamic equilibrium model for gene regulation. *J Mol Biol*, **254**, 130-149.
- Polach, K.J. and Widom, J. (1999) Restriction enzymes as probes of nucleosome stability and dynamics. *Methods Enzymol*, **304**, 278-298.
- Pollard, K.J., Samuels, M.L., Crowley, K.A., Hansen, J.C. and Peterson, C.L. (1999) Functional interaction between GCN5 and polyamines: a new role for core histone acetylation. *Embo J*, **18**, 5622-5633.
- Recht, J., Tsubota, T., Tanny, J.C., Diaz, R.L., Berger, J.M., Zhang, X., Garcia, B.A., Shabanowitz, J., Burlingame, A.L., Hunt, D.F., Kaufman, P.D. and Allis, C.D. (2006) Histone chaperone Asf1 is required for histone H3 lysine 56 acetylation, a modification associated with S phase in mitosis and meiosis. *Proc Natl Acad Sci U S A*, **103**, 6988-6993.
- Regnier, V., Novelli, J., Fukagawa, T., Vagnarelli, P. and Brown, W. (2003) Characterization of chicken CENP-A and comparative sequence analysis of vertebrate centromere-specific histone H3-like proteins. *Gene*, **316**, 39-46.

- Robinson, P.J., Fairall, L., Huynh, V.A. and Rhodes, D. (2006) EM measurements define the dimensions of the "30-nm" chromatin fiber: evidence for a compact, interdigitated structure. *Proc Natl Acad Sci U S A*, **103**, 6506-6511.
- Robinson, P.J. and Rhodes, D. (2006) Structure of the '30 nm' chromatin fibre: a key role for the linker histone. *Curr Opin Struct Biol*, **16**, 336-343.
- Sanders, M.M. (1978) Fractionation of nucleosomes by salt elution from micrococcal nuclease-digested nuclei. *J Cell Biol*, **79**, 97-109.
- Sanders, M.M. and Hsu, J.T. (1977) Fractionation of purified nucleosomes on the basis of aggregation properties. *Biochemistry*, **16**, 1690-1695.
- Schalch, T., Duda, S., Sargent, D.F. and Richmond, T.J. (2005) X-ray structure of a tetranucleosome and its implications for the chromatin fibre. *Nature*, **436**, 138-141.
- Schneider, J., Bajwa, P., Johnson, F.C., Bhaumik, S.R. and Shilatifard, A. (2006) Rtt109 is required for proper H3K56 acetylation: a chromatin mark associated with the elongating RNA polymerase II. *J Biol Chem*, **281**, 37270-37274.
- Schwarz, P.M., Felthouser, A., Fletcher, T.M. and Hansen, J.C. (1996) Reversible oligonucleosome self-association: dependence on divalent cations and core histone tail domains. *Biochemistry*, **35**, 4009-4015.
- Schwarz, P.M. and Hansen, J.C. (1994) Formation and stability of higher order chromatin structures. Contributions of the histone octamer. *J Biol Chem*, **269**, 16284-16289.
- Selth, L. and Svejstrup, J.Q. (2007) Vps75, a new yeast member of the NAP histone chaperone family. *J Biol Chem*, **282**, 12358-12362.
- Shechter, D., Dormann, H.L., Allis, C.D. and Hake, S.B. (2007) Extraction, purification and analysis of histones. *Nat Protoc*, **2**, 1445-1457.
- Shogren-Knaak, M., Ishii, H., Sun, J.M., Pazin, M.J., Davie, J.R. and Peterson, C.L. (2006) Histone H4-K16 acetylation controls chromatin structure and protein interactions. *Science*, **311**, 844-847.
- Simpson, R.T., Thoma, F. and Brubaker, J.M. (1985) Chromatin reconstituted from tandemly repeated cloned DNA fragments and core histones: a model system for study of higher order structure. *Cell*, **42**, 799-808.

Song, J.S., Liu, X., Liu, X.S. and He, X. (2008) A high-resolution map of nucleosome positioning on a fission yeast centromere. *Genome Res.*

Stoler, S., Keith, K.C., Curnick, K.E. and Fitzgerald-Hayes, M. (1995) A mutation in CSE4, an essential gene encoding a novel chromatin-associated protein in yeast, causes chromosome nondisjunction and cell cycle arrest at mitosis. *Genes Dev*, **9**, 573-586.

Sullivan, B.A., Blower, M.D. and Karpen, G.H. (2001) Determining centromere identity: cyclical stories and forking paths. *Nat Rev Genet*, **2**, 584-596.

Sullivan, B.A. and Karpen, G.H. (2004) Centromeric chromatin exhibits a histone modification pattern that is distinct from both euchromatin and heterochromatin. *Nat Struct Mol Biol*, **11**, 1076-1083.

Suto, R.K., Clarkson, M.J., Tremethick, D.J. and Luger, K. (2000) Crystal structure of a nucleosome core particle containing the variant histone H2A.Z. *Nat Struct Biol*, **7**, 1121-1124.

Tagami, H., Ray-Gallet, D., Almouzni, G. and Nakatani, Y. (2004) Histone H3.1 and H3.3 complexes mediate nucleosome assembly pathways dependent or independent of DNA synthesis. *Cell*, **116**, 51-61.

Tang, Y., Holbert, M.A., Wurtele, H., Meeth, K., Rocha, W., Gharib, M., Jiang, E., Thibault, P., Verrault, A., Cole, P.A. and Marmorstein, R. (2008) Fungal Rtt109 histone acetyltransferase is an unexpected structural homolog of metazoan p300/CBP. *Nat Struct Mol Biol*, **15**, 738-745.

Taverna, S.D., Li, H., Ruthenburg, A.J., Allis, C.D. and Patel, D.J. (2007) How chromatin-binding modules interpret histone modifications: lessons from professional pocket pickers. *Nat Struct Mol Biol*, **14**, 1025-1040.

Thoma, F., Koller, T. and Klug, A. (1979) Involvement of histone H1 in the organization of the nucleosome and of the salt-dependent superstructures of chromatin. *J Cell Biol*, **83**, 403-427.

Thomas, C.A., Jr. (1971) The genetic organization of chromosomes. *Annu Rev Genet*, **5**, 237-256.

Tse, C., Georgieva, E.I., Ruiz-Garcia, A.B., Sendra, R. and Hansen, J.C. (1998a) Gcn5p, a transcription-related histone acetyltransferase, acetylates nucleosomes

- and folded nucleosomal arrays in the absence of other protein subunits. *J Biol Chem*, **273**, 32388-32392.
- Tse, C. and Hansen, J.C. (1997) Hybrid trypsinized nucleosomal arrays: identification of multiple functional roles of the H2A/H2B and H3/H4 N-termini in chromatin fiber compaction. *Biochemistry*, **36**, 11381-11388.
- Tse, C., Sera, T., Wolffe, A.P. and Hansen, J.C. (1998b) Disruption of higher-order folding by core histone acetylation dramatically enhances transcription of nucleosomal arrays by RNA polymerase III. *Mol Cell Biol*, **18**, 4629-4638.
- Tsubota, T., Berndsen, C.E., Erkmann, J.A., Smith, C.L., Yang, L., Freitas, M.A., Denu, J.M. and Kaufman, P.D. (2007) Histone H3-K56 acetylation is catalyzed by histone chaperone-dependent complexes. *Mol Cell*, **25**, 703-712.
- van Holde, K. and Yager, T. (2003) Models for chromatin remodeling: a critical comparison. *Biochem Cell Biol*, **81**, 169-172.
- Van Holde, K.E. (1989) *Chromatin*. Springer-Verlag, New York.
- van Leeuwen, F., Gafken, P.R. and Gottschling, D.E. (2002) Dot1p modulates silencing in yeast by methylation of the nucleosome core. *Cell*, **109**, 745-756.
- Wang, W. and Malcolm, B.A. (1999) Two-stage PCR protocol allowing introduction of multiple mutations, deletions and insertions using QuikChange Site-Directed Mutagenesis. *Biotechniques*, **26**, 680-682.
- Wang, X. and Hayes, J.J. (2008) Acetylation mimics within individual core histone tail domains indicate distinct roles in regulating the stability of higher-order chromatin structure. *Mol Cell Biol*, **28**, 227-236.
- White, C.L., Suto, R.K. and Luger, K. (2001) Structure of the yeast nucleosome core particle reveals fundamental changes in internucleosome interactions. *Embo J*, **20**, 5207-5218.
- Wilhelm, M.L. and Wilhelm, F.X. (1980) Conformation of nucleosome core particles and chromatin in high salt concentration. *Biochemistry*, **19**, 4327-4331.
- Williams, S.K., Truong, D. and Tyler, J.K. (2008) Acetylation in the globular core of histone H3 on lysine-56 promotes chromatin disassembly during transcriptional activation. *Proc Natl Acad Sci U S A*, **105**, 9000-9005.

- Wolffe, A. (1998) *Chromatin : structure and function*. Academic Press, San Diego.
- Woodcock, C.L. (2006) Chromatin architecture. *Curr Opin Struct Biol*, **16**, 213-220.
- Woodcock, C.L., Frado, L.L. and Rattner, J.B. (1984) The higher-order structure of chromatin: evidence for a helical ribbon arrangement. *J Cell Biol*, **99**, 42-52.
- Woodcock, C.L. and Horowitz, R.A. (1998) Electron microscopic imaging of chromatin with nucleosome resolution. *Methods Cell Biol*, **53**, 167-186.
- Woodcock, C.L., Skoultchi, A.I. and Fan, Y. (2006) Role of linker histone in chromatin structure and function: H1 stoichiometry and nucleosome repeat length. *Chromosome Res*, **14**, 17-25.
- Xu, F., Zhang, K. and Grunstein, M. (2005) Acetylation in histone H3 globular domain regulates gene expression in yeast. *Cell*, **121**, 375-385.
- Xu, F., Zhang, Q., Zhang, K., Xie, W. and Grunstein, M. (2007) Sir2 deacetylates histone H3 lysine 56 to regulate telomeric heterochromatin structure in yeast. *Mol Cell*, **27**, 890-900.
- Yager, T.D., McMurray, C.T. and van Holde, K.E. (1989) Salt-induced release of DNA from nucleosome core particles. *Biochemistry*, **28**, 2271-2281.
- Yager, T.D. and van Holde, K.E. (1984) Dynamics and equilibria of nucleosomes at elevated ionic strength. *J Biol Chem*, **259**, 4212-4222.
- Yoda, K., Ando, S., Morishita, S., Houmura, K., Hashimoto, K., Takeyasu, K. and Okazaki, T. (2000) Human centromere protein A (CENP-A) can replace histone H3 in nucleosome reconstitution in vitro. *Proc Natl Acad Sci U S A*, **97**, 7266-7271.
- Zhang, D.E. and Nelson, D.A. (1988) Histone acetylation in chicken erythrocytes. Rates of deacetylation in immature and mature red blood cells. *Biochem J*, **250**, 241-245.
- Zinkowski, R.P., Meyne, J. and Brinkley, B.R. (1991) The centromere-kinetochore complex: a repeat subunit model. *J Cell Biol*, **113**, 1091-1110.